



National Library of Canada

Bibliothèque nationale du Canada

CANADIAN THESES ON MICROFICHE

THÈSES CANADIENNES SUR MICROFICHE

NAME OF AUTHOR/NOM DE L'AUTEUR Alan G. Whitney

TITLE OF THESIS/TITRE DE LA THÈSE Nuclear Magnetic Resonance Measurements of Some Species Adsorbed on Zinc Oxide.

UNIVERSITY/UNIVERSITÉ Simon Fraser University, Burnaby 2, B.C.

DEGREE FOR WHICH THESIS WAS PRESENTED/ GRADE POUR LEQUEL CETTE THÈSE FUT PRÉSENTÉE Ph.D.

YEAR THIS DEGREE CONFERRED/ANNÉE D'OBTENTION DE CE GRADE 1975

NAME OF SUPERVISOR/NOM DU DIRECTEUR DE THÈSE Dr. Ian D. Gay

Permission is hereby granted to the NATIONAL LIBRARY OF CANADA to microfilm this thesis and to lend or sell copies of the film.

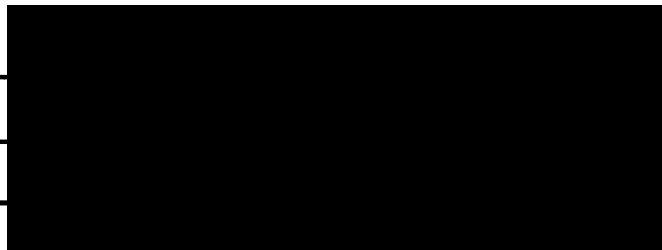
The author reserves other publication rights, and neither the thesis nor extensive extracts from it may be printed or otherwise reproduced without the author's written permission.

L'autorisation est, par la présente, accordée à la BIBLIOTHÈQUE NATIONALE DU CANADA de microfilmer cette thèse et de prêter ou de vendre des exemplaires du film.

L'auteur se réserve les autres droits de publication; ni la thèse ni de longs extraits de celle-ci ne doivent être imprimés ou autrement reproduits sans l'autorisation écrite de l'auteur.

DATED/DATE January 20 1975 SIGNED/SIGNÉ _____

PERMANENT ADDRESS/RÉSIDENCE FIXE



Nuclear Magnetic Resonance Measurements of
Some Species Adsorbed on Zinc Oxide

by

Alan Gordon Whitney

B.Ed. University of Alberta, 1965

A THESIS SUBMITTED IN PARTIAL FULFILLMENT OF
THE REQUIREMENTS FOR THE DEGREE OF
DOCTOR OF PHILOSOPHY

in the Department

of

Chemistry

© ALAN GORDON WHITNEY

SIMON FRASER UNIVERSITY

January 1975

All rights Reserved. This Thesis may not be
reproduced in whole or in part, by photocopy
or other means, without permission of the author.

APPROVAL

Name: Alan G. Whitney

Degree: Doctor of Philosophy

Title of Thesis: Nuclear Magnetic Resonance Measurements
of Some Species Adsorbed on Zinc Oxide

Examining Committee

Chairman: Dr. T. N. Bell

Dr. Ian D. Gay

Senior Supervisor

Dr. F. J. Wells

Dr. D. Sutton

Dr. D. Crozier

Dr. H. A. Resing

U.S. Naval Research Lab

External Examiner

Date Approved: _____

PARTIAL COPYRIGHT LICENSE

I hereby grant to Simon Fraser University the right to lend my thesis or dissertation (the title of which is shown below) to users of the Simon Fraser University Library, and to make partial or single copies only for such users or in response to a request from the library of any other university, or other educational institution, on its own behalf or for one of its users. I further agree that permission for multiple copying of this thesis for scholarly purposes may be granted by me or the Dean of Graduate Studies. It is understood that copying or publication of this thesis for financial gain shall not be allowed without my written permission.

Title of Thesis/Dissertation:

Nuclear Magnetic Resonance Measurements of Some Species Adsorbed on
Zinc Oxide.

Author:

(signature)

Alan G. Whitney

(name)

January 20, 1975.

(date)

ABSTRACT

Nuclear Magnetic Resonance and Relaxation measurements have been made of ethylene, propene, some fluorine derivatives of ethylene, some light saturated hydrocarbons, and tetra methyl silane, all adsorbed on zinc oxide. The major emphasis of the study is on the ethylene /zinc oxide system.

Chemical shift measurements were made utilizing a Varian XL- 100 Nuclear Magnetic Resonance Spectrometer operating at 100 MHz, and a modified NMR Specialties spectrometer operating at 15MHz. For ethylene such measurements were made at coverages from .2 to 1 monolayer. It was found that the protons of the adsorbed ethylene experience a downfield shift on adsorption, the shift being coverage dependent. It is argued that this shift and the resonance curve are consistent with donation of electrons to the surface, that the species remains olefinic in character, i.e. is pi-bonded to the surface, and that the adsorption site is most likely a zinc atom.

Studies of propene at coverages above .3 of a monolayer showed similar downfield shifts for the olefin protons while the methyl protons experienced a smaller downfield shift. Evidence of other workers for a more strongly bound propene species at low coverages (below .3 monolayers) is supported in that no resonance could be

observed presumably because of a short T_2 due to the species being relatively immobile, despite a comparatively high population.

Proton chemical shifts measured for species considered to be physisorbed on the surface such as ethane, propane, butane, pentane, and tetra methyl silane, were found to be only slightly downfield from the free species. This small shift is explained as a Van der Waals effect.

Fluorine NMR studies of fluorine derivatives of ethylene adsorbed on zinc oxide showed rather remarkable upfield shifts on adsorption, behavior markedly different than the ethylene case. A ^{13}C spectrum was also obtained for ethylene on a ZnO pellet. The spectra showed a downfield shift and the J-J coupling was resolved. The coverage for this measurement was however very high, so that the system was predominately physisorbed ethylene.

A model capable of interpreting relaxation due to molecular motion of adsorbed species was constructed along the lines of earlier work, but utilizing the Wigner Rotational Matrices for coordinate transformation. This model enables one to calculate all of the spectral densities at any frequency, and thus a theoretical relaxation time for a particular motion and relaxation mechanism.

Extensive relaxation measurements were made on the

ethylene/ZnO system. Application of the model derived reproduced the the longitudinal data reasonably well. The relaxation data were best reproduced by a model which had the ethylene rotating about the C_2 axis perpendicular to the plane of the molecule, while wobbling about the surface normal. However it is noted that use of the exponential form of the correlation function is a poor assumption in that the motional processes are non-stochastic.

T_2 measurements made in a field gradient were unable to detect the rate of translational diffusion at coverages below .4 monolayer, but the diffusion constant was found at coverages approaching a monolayer. It is argued that at low coverages T_1 relaxation is caused by an intra- molecular dipole-dipole mechanism while T_2 relaxation is caused by both intra- and inter-molecular dipole-dipole relaxation mechanisms.

To the Memory of
Ralph L. Whitney

Acknowledgements

In thanking some one always commits sins of omission, and we all owe much to many. In cases though there are people who need to be singled out.

I would like to thank Dr. Ian Gay not only for his help in this work, but because his clear thinking is inspirational, and his educational philosophy of a truly open nature. I thank Dr. Ted Wells for both his help and his enthusiasm, and for the use of much of his equipment. Not often does one single out an individual graduate student, but I owe much to Mr. Bob Ferguson for many good talks about this and other works, and for a great deal of help in computing.

I am most grateful for the financial assistance of the National Research Council, of Simon Fraser University's Chemistry Department, and the material support of the New Jersey Zinc Company.

Finally I would like to thank Bonnie Whitney for whom this whole undertaking may have been too costly.

TABLE OF CONTENTS

Title page.....	p i
Approval.....	p ii
Abstract.....	p iii
Dedication.....	p vi
Acknowledgements.....	p vii
Table of Contents.....	p viii
List of Tables.....	p xii
List of Figures.....	p xiii
The Notation Used in This thesis.....	p xiv
Chapter I Introduction.....	p 1
Surfaces and Catalysts.....	p 1
The Magnetic Resonance Spectroscopies.....	p 3
Statement of the Problem.....	p 5
The Structure of this Thesis.....	p 8
Chapter II Surface Dynamics and Models of	
Surfaces.....	p 9
Movement on the Surface.....	p 11
Heterogeneous Surfaces.....	p 13
Macroscopic Models and Measurements of	
Adsorption.....	p 13
Chapter III A Brief Summary of the Theory of	
Nuclear Magnetic Resonance and	
Relaxation.....	p 19
The Basic Phenomenon of Magnetic Resonance..	p 19
NMR in the Frequency Domain.....	p 23

NMR in the Time Domain.....	p 25
Saturation.....	p 26
Relaxation and the Bloch Equations.....	p 27
The Relation Between the Signal in the Time Domain and the Frequency Domain.....	p 31
Some Useful Pulse Experiments.....	p 33
T_1 Measurements.....	p 36
T_2 Measurements.....	p 38
An Experiment to Measure Diffusion.....	p 45
Chemical Shifts.....	p 45
Chapter IV Relaxation Analysis.....	p 48
Dipole-Dipole Relaxation.....	p 48
Other Mechanisms of Relaxation.....	p 55
Chapter V. The Theory of NMR and Relaxation Applied to Molecules Adsorbed on Surfaces.....	p 59
Differentiating Between Different Types of Dipole-Dipole Relaxation.....	p 60
A Model for Intra Molecular Relaxation of Surface Species.....	p 63
Chapter VI Survey of Work Done on ZnO.....	p 77
Zinc Oxide.....	p 78
Hydrogen Adsorption on ZnO.....	p 79
Ethylene on ZnO and Its Reaction with Hydrogen	80
Propene and the Butenes on ZnO.....	p 83
Chapter VII Adsorption Studies and Experimental	

Methods..... p 86

Adsorption Isotherms..... p 87

Sample Preparation, Errors and Precautions.. p 91

NMR Experimental Considerations..... p 92

Chemical Shift Measurements..... p 97

Fluorine Spectra..... p 101

Carbon Spectra..... p 102

Chapter VIII Nuclear Magnetic Resonance

 Measurements of Olefins Adsorbed

 on Zinc Oxide..... p 105

 Chemical Shift Studies..... p 105

 A series of Experiments with Fluorine

 Substituted Ethylenes..... p 114

 A Discussion of the Chemical Shifts..... p 121

 Information on the Structure of the

 Adsorbed Species..... p 125

 Some Experiments on ZnO Pellets..... p 128

Chapter IX Relaxation Studies of Ethylene

 On ZnO..... p 135

 Application of the Model of Intra-Molecular

 Dipole-Dipole Relaxation Through Anisotropic

 Rotation..... p 150

 A More Critical Appraisal of this Model..... p 163

 Comparison of Measured and Calculated Values

 of T_2 p 169

 Summary of the Conclusions to be Drawn from

the Relaxation Studies..... p 170

Chapter X Overall Conclusions and Further Work.. p 171

 Conclusions About measurements of Olefins

 on ZnO..... p 172

 Further Work..... p 175

Bibliography..... p 180

Appendix..... p 185

List of Tables

Table II-1	The Lifetime of an Adsorbed Molecule as a Function of the Heat of Adsorption...p 11
Table V-1	The Wigner Rotational Tensor of Rank 2....p 67
Table VIII-1	The Chemical Shifts of Some Hydrocarbons adsorbed on ZnO.....p 106
Table VIII-2	Fluorine and Proton Chemical Shifts of Free and Adsorbed Fluorine Derivatives of Ethylene.....p 112

List of Figures

Figure

II-1	Model of a Heterotactic Surface.....	p 14
II-2	A plot of Equation II-5.....	p 17
III-1	The Precession of a Dipole in a Field.....	p 21
III-2	The Effect of a Rotating Field.....	p 21
III-3	M Subjected to a 90 Degree Pulse.....	p 35
III-4	The Output Following a 90 Degree Pulse.....	p 35
III-5	The Output Following an Off Resonance 90 Degree Pulse.....	p 37
III-6	The Output of a 180-90 Pulse Experiment.....	p 39
III-7	The Carr-Purcell Experiment.....	p 41
III-8	The Meiboom Gill Experiment.....	p 42
III-9	The Output from a Meiboom Gill Experiment.....	p 44
IV-1	Plots of T_1 and T_2 vs. the Corelation Time.	p 55
V-1	The Euler Angles.....	p66
V-2	The Transformation.....	p 70
VII-1	The Isotherms of Ethylene on ZnO.....	p 88
VII-2	The Isosteres for Ethylene on ZnO.....	p 90
VIII-1	Ethane and Propane on ZnO.....	p 109
VIII-2	Ethylene and Propene on ZnO.....	p 110
VIII-3	Ethylene on ZnO (the Coverage Dependence).....	p 111
VIII-4	Chemical Shifts for Ethylene on ZnO.....	p 113
VIII-5	the Carbon Spectrum of Ethylene on ZnO.....	p 115
VIII-6	The Fluorine Spectrum of Some Derivatives of Ethylene.....	p 120

VIII-7	The Proton Spectrum of Ethylene on a ZnO Pellet	131
VIII-8	Acetaldehyde on ZnO.....	p 133
IX-1	T_1 vs $1/\text{Temp}$ for Ethylene on ZnO.....	p 136
IX-2	T_2 vs $1/\text{Temp}$ for Ethylene on ZnO.....	p 137
IX-3	T_1 and T_2 vs Coverage.....	p 138
IX-4	The Mass Spectra of Perdeuterated Ethylene Before and After Exposure to ZnO.....	p 143
IX-5	Equation IX-5 (High Coverage of Ethylene).....	p 147
IX-6	Equation IX-5 (Low Coverage of Ethylene).....	p 149
IX-7	Ethylene of a Surface Plane.....	p 152
IX-8	T_1 as a Function of the Wobble Angle.....	p 158
IX-9	T_1 Calc. vs $1/\text{Temp}$	p 158
IX-10	T_1 Calc vs $1/\text{Temp}$	p 161
IX-11	The Verhulst Function.....	p 161
IX-12	Calculated and Measured Values of T_1 for Ethylene on ZnO.....	p 164
IX-13	T_1 Calc vs $1/\text{Temp}$	p 167

Chapter I

Introduction

Surfaces and Catalysts

Solids are known first of all through their surfaces. Much of the interesting chemistry of solids happens at their surfaces, and there exists a large area of interest in what happens between such surfaces and substances in other phases particularly the gas and liquid phase.

The surface phenomena that occur between a gas or liquid and a solid surface make up the area of heterogenous catalysis; this and the phenomenon of adsorption itself have been of great interest to the chemist.

Both catalysts and adsorption on surfaces have proven exceedingly difficult to accurately describe and while models of these phenomena have been proposed, they remain far more simplistic than the phenomena themselves. One reason for this complexity is that most catalytic surfaces are very heterogeneous, having a wide distribution of site symmetries and often an equally wide distribution of adsorption energies at these sites.

During the first half of this century work in the area of surface chemistry was confined to the investigation of macroscopic properties; heats of adsorption, kinetics of adsorption and of surface

reactions, adsorption isotherms and surface areas obtained from them.

Two major barriers held back developments in the field. The first was lack of ultra high vacuums, since even at the best vacuum obtainable (roughly 10^{-6} torr) a surface could be contaminated by "background" species in seconds or less. The second was lack of instruments to examine the surface microscopically.

The last twenty years has seen the removal of both of these barriers. Ultra high vacuums allow one to make measurements on clean surfaces (Goldfinger 1970) and a host of new spectroscopies and improvements in older ones now encourages one to answer questions such as;

- 1) what species are present on the surface?
- 2) what site symmetries are present?
- 3) what is the nature of the chemical interaction; what is happening to the electrons.
- 4) what motions -- vibrational, rotational, diffusional, and exchange, are occurring.

No one tool can provide all the information about the molecular aspects of the surface. To date the most information has probably been gained using infra-red measurements (Eischens 1958, Hair 1967, Little 1966). Findings utilizing the newer techniques such as Mossbauer or Auger spectroscopy (Duke 1970, Boncher 1969, Goldanski 1970), low energy electron diffraction (LEED) (Edmonds

1969), electron spectroscopy (ESCA) (Siegbahn 1967) are now commonly being reported in the literature.

The Magnetic Resonance Spectroscopies

The magnetic resonance spectroscopies Electron Paramagnetic Resonance (EPR) and Nuclear Magnetic Resonance (NMR) are capable of giving information about structure, physical and chemical interactions, symmetry and motion.

The first of these depends upon the Zeeman splitting of the energy levels of the magnetic moment of an unpaired electron by a magnetic field. The exact experiment is described elsewhere (Slichter 1963) and its application to surface chemistry measurements have been described by Kokes (1967).

NMR depends on the Zeeman splitting of the energy levels of the magnetic moment of the nucleus by a magnetic field, and has become one of the major tools in chemistry. Its major advantage is the fact that subtle changes in physical or chemical environment, in structure, or in motion make for large changes in the position and shape of the resonance being measured, and yet the measurement has no apparent effect on these properties. It appears to be an ideal tool for the study of species adsorbed on surfaces.

NMR, however, has disadvantages too. It measures

properties over the whole sample, thus giving an average, but far more important is its relative insensitivity to small amounts of sample, a fact stemming from the small difference in population distribution between the Zeeman levels.

This second disadvantage has led to the fact that most of the NMR measurements done on surfaces have been performed on solids of high surface area with very large coverages (Packer 1967).

While such surfaces are often physically interesting, a large number of the chemically interesting surfaces do not have such large surface areas, and in many instances the interactions of greatest chemical interest take part at low coverages.

The majority of papers in this field have been on studies of physical rather than chemical adsorption. A large amount of work has been done on water adsorbed on several solids, and molecules such as benzene and sulfur hexafluoride on silica and alumina. Such work has been well reviewed (Resing 1968, Packer 1967, Pfeiffer 1972).

In more recent years some studies of chemical interactions have reached the literature, for example: Fraissard (1970, 1971).

In any area of surface chemistry it is important to correlate the findings with those of other spectroscopies

and of the classical techniques. Packer (1967) concludes an article on NMR measurements of adsorbed species with the statement:

"The investigation of a high surface area adsorbent solely by nuclear spin relaxation is unlikely to yield unambiguous information, but in conjunction with other methods it can give detailed information about the adsorbate-adsorbent interactions."

Statement of the Problem

When this study was undertaken there were no reports of NMR studies of chemisorption, so at its inception the question was really: Is it possible to study a catalytically interesting surface and adsorbate utilizing the spectrometers available? The spectrometers available were a new Varian XL-100 operating at 100 MHz and a highly modified semi-home built 15 MHz pulse NMR spectrometer. Both are described in more detail later on. Neither was designed to do catalytic research.


After some initial investigation into possible systems the answer to the first question seemed to be positive. Systems such as the light olefins on platinum, and the fluorine derivatives of the same on platinum, were found to produce measurable resonances. However the platinum had to be supported on high area silica and problems of separating the measurement of the interaction

of the olefin with silica, from that of olefin with platinum were foreseen.

It was also found that a resonance could be measured for olefins adsorbed on zinc oxide. This oxide surface is of chemical interest in that it catalyses the hydrogenation of olefins, the isomerization of olefins (Kokes 1972), the oxidation of olefins (Kubokawa 1973), the dehydrogenation of several alcohols (Kolboe 1969) $H_2 - D_2$ exchange (Dowden 1956) among others.

Catalysis by zinc oxide has been the subject of a large number of papers, among them some exceptionally complete work of the lab of Kokes and co-workers utilizing I. R. and mechanistic studies. These studies meant that information obtained from NMR could be interpreted in a better light and correlated with other measurements.

A myriad of questions were present. Zinc oxide acts as both an acid or a base. Would it be possible to determine if the surface were donating electrons to the olefin or vice-versa? Kokes had concluded that propene on zinc oxide was adsorbed partially as a pi-allyl complex. Would it be possible to "see" this structure on the surface? The butenes isomerize over zinc oxide. Could one see intermediate species or even "follow" the isomerization via NMR? The kinetics of olefin hydrogenation depends on migration across the surface. Can the motions of an olefin on zinc oxide -- the



so-called surface dynamics -- be measured and to what conclusion?

In seeking answers to these and related questions it was deemed advisable to use the same zinc oxide, or at least zinc oxide from the same supplier as that used by Kokes, thus enabling one to be more confident about information obtained from those studied. This created yet another major problem as this zinc oxide has both a relatively small surface area per gram, and a low bulk density, thus a low surface area per volume. For this reason concentrations of the adsorbed species measured were very low and the study was somewhat plagued by signal to noise problems.

During final stages of this project some theoretical questions arose. Much of the interpretation of this work and other work in the field has depended on a model of relaxation due to anisotropic motion at a surface developed by D. E. Woessner (1963). This model has been used to interpret relaxation data of water on several surfaces (Woessner 1963, 1969a, 1970a, b), benzene on silica (Woessner 1966), methanol on graphite (Riehl 1972) and methane on graphite (Anderson 1972).

This model was "reconstructed", and extended so that spectral densities could be calculated for situations where the spectral density is a function of the frequency and in a reference frame where motion about some symmetry

axis can be considered simultaneously with motion of this axis in relation to a surface normal. The "reconstruction" is presented in Chapter V, while the application of this model to ethylene adsorbed on zinc oxide is found in Chapter IX. In applying the model several assumptions of both this model and the Woessner model were shown to be fallible.

The Structure of This Thesis

It is conceivable that this thesis will be of interest to surface chemists who are not well acquainted with NMR, or perhaps even to those interested in NMR who are not well-acquainted with surface phenomena.

The thesis then includes a brief description of surface phenomena and studies thereof, a chapter on nuclear magnetic resonance, one on nuclear magnetic relaxation, a chapter outlining the effect of a surface on the interpretation of these measurements, and a chapter on catalytic properties of zinc oxide. The rest of the thesis is a description of the experiments carried out, and their interpretation both in the light of other works and in the light of a model developed herein, capable of interpreting relaxation of adsorbed species on a surface.

Chapter II

Surface Dynamics and Models of Surfaces

Our concern is with what is happening to the molecule while it is on the surface. We are interested both in the physical and chemical interactions between adsorbate and adsorbent, or adsorbate molecules, and the motion of the molecule on the surface. The motion of the molecule is of significance in any consideration of the kinetics of a reaction since it plays an important role in transportation of reaction intermediates or products, or in clearing sites where reactions may occur, and of course in the activation entropy for a reaction.

The whole process of gas adsorption should be viewed as a dynamic one. A molecule strikes the surface and is either specularly reflected or resides on the surface for some time and leaves again when it has gained enough energy to desorb. If the average residence time of a molecule which collides with surface is τ and n molecules strike each square cm of surface per second then each square cm should have $n\tau$ molecules adsorbed on it at equilibrium (i.e. when the number desorbing equals the number adsorbing). Because τ is critically dependent on temperature the relationship II-1 is often used (deBoer 1968)

$$\text{II-1 } \tau = \tau_0 \exp(dH/Rt)$$

where $1/\tau_0$ is related to the frequency of vibration of the adsorbed molecule perpendicular to the surface and dH is the heat of adsorption. τ_0 may be approximated using absolute reaction rate theory and may be considered equal to (deBoer 1968):

$$(1/\text{freq}) \exp(-S/R)$$

where S is the entropy of activation for desorption and freq is the vibration frequency normal to the plane.

Heats of adsorption of gases on solid surfaces run from 1 or 2 kcal/mole to well over 100 kcal/mole. As a general guideline molecules are considered to be physically adsorbed if their heats of adsorption are of the order of 1-10 kcal/mole, while chemical adsorption (chemisorption) is considered to involve heats of adsorption from 10-100 kcal/mole. Physisorption involves interactions of the van der Waals type, thus a better indicator of whether the interaction is physical or chemical is the ratio of the heat of adsorption of the gas to the heat of evaporation.

It is illustrative to calculate τ for several different heats of adsorption. Table II-I gives several examples (using $\tau_0 = 5 \times 10^{-14}$ secs and $T = 300$ degrees K).

dH(ads) (kcal/mole)	tau (seconds)
1	2.7×10^{-13}
10	9×10^{-7}
13	1.4×10^{-4}
15	4×10^{-3}
20	17
25	8×10^4

Table I -- The lifetime as a function of the heat of adsorption

Our model now, is of a system where a molecule collides with the surface and stays for some length of time varying from microseconds to years. Extending the model so that we can describe what goes on while the molecule is on the surface involves a description of the surface itself.

Movement on the Surface

Dacey (1965), deBoer (1968), and Ross and Oliver (1964) among others give descriptions of movement on different surfaces. The most idealized model is that of a plane where the energy of interaction between adsorbate and adsorbent is the same for every point on the plane. Such a system has a two dimensional spreading pressure and is describable by a two dimensional equation of state. At very low concentrations a two dimensional ideal gas law

holds while a two dimensional van der Waals type equation is required at higher concentrations to allow for lateral interactions between molecules.

Several systems where the interactions are weak (physical forces only) are describable by such models, notably Xe on mercury (Cassel 1936) and some of the alkanes on charcoal (deBoer 1952). For such cases the activation energy for diffusion is usually less than or close to RT .

More often diffusion on surfaces is characterized by an activation energy greater than RT . It is possible to still have a homogeneous surface; the adsorbed species going through an activated diffusion from site to site. Diffusion on such a surface can be described as a random walk process. deBoer (1968) describes the lifetime between hops by the equation II-2

$$\text{II-2} \quad \tau_{\text{diff}} = \tau_0 \exp(E_a/RT)$$

where E_a is the activation energy necessary for a particle to go from one site to another. τ_0 will again be related to the vibrations normal to the surface and may be taken to equal τ_0 of equation II-1. In this case the number of hops during the lifetime on the surface would be:

$$\text{II-3} \quad n = \exp\{(H-E_a)/RT\}$$

The heat of adsorption will always be greater than the activation energy of diffusion (Ross 1964). For a case where dH equal 10 kcal/mole and $E_a = 5$ kcal equation (3) shows that at 300 degrees K a molecule will hop about 6000 times during the 3×10^{-6} seconds it resides on the surface.

Heterogeneous Surfaces

A more realistic model of a surface features a distribution of heats of adsorption and diffusion (Somorjai 1972). Figure II-1 shows the energy barrier for diffusion across such a heterogeneous surface. Such a model includes 1) a distribution of well depths ($H(\text{ads})$), 2) a distribution of barrier heights associated with diffusion ($E_a \text{ diff}$), 3) deep wells (high energy site) associated with a high activation energy of diffusion, 4) a jump distance a which is the same as the distance between surface atoms. In practice it is difficult to determine the actual distribution of heats of adsorption although dH may be measured as a function of coverage by calorimetry, or derived from isotherms taken at various temperatures.

Macroscopic Models and Measurements of Adsorption

The most commonly made and one of the most useful of the classical measurements is the plotting of the amount

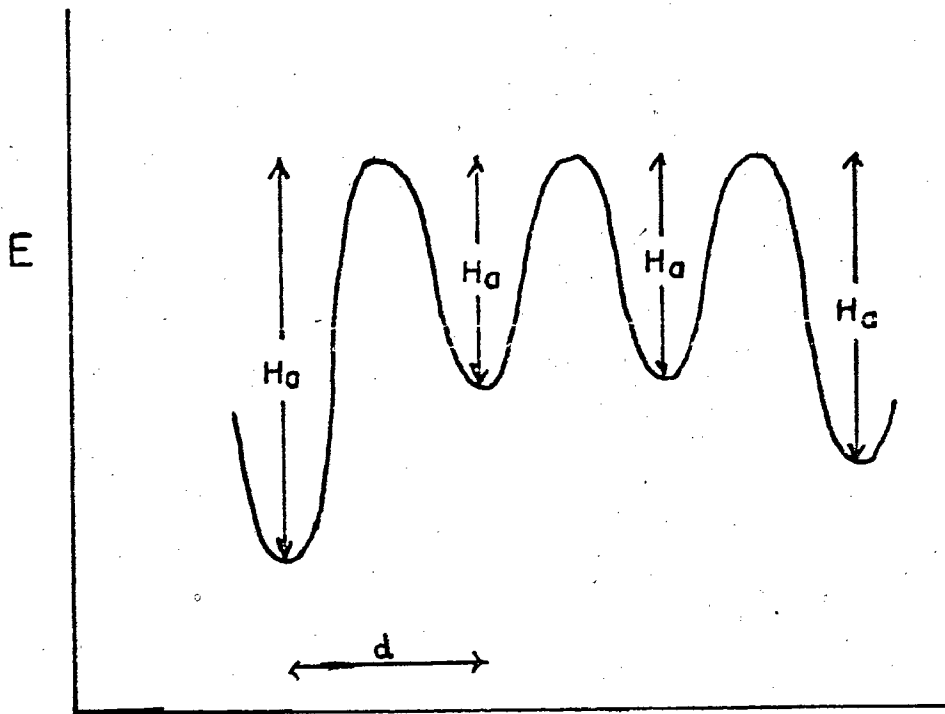


Figure II - 1

Model of a heterotactic surface.

of gas adsorbed against the pressure of the gas at constant temperature. Such plots are known as adsorption isotherms.

There are several characteristic shapes of such plots, the types being dependent on both adsorbate and adsorbent. A classification of the types of isotherms is given in Brunauer (1940).

The first theoretical isotherm was derived by Langmuir in 1916 (Langmuir 1916, 1918). It has since been derived from several different points of view (deBoer 1968).

The Langmuir isotherm model contains the assumptions that the heat of adsorption is the same for every site, is independent of other molecules on the surface, and that a molecule which strikes another adsorbed molecule will be reflected so that the upper limit to the adsorption is a monolayer. Often the Langmuir isotherm is approximated by gases chemisorbed on a surface at low coverage.

The expression for the Langmuir isotherm is most often seen in the form:

$$\text{II-5} \quad \theta = aP/(1+aP)$$

where theta equals the fraction of the surface covered, P is the equilibrium gas pressure above the surface and a is a constant relating to the rate of condensation on the surface to the rate of evaporation from the surface. A

plot of this isotherm is shown in figure II-2.

Another useful expression for an isotherm was derived by Brunaur, Emmett and Teller (BET) (Brunaur 1938) by extending the Langmuir model to allow for multilayer adsorption. The important added assumption is that the heat of evaporation for the second and subsequent layers is equal to the heat of evaporation from the bulk adsorbate.

The BET isotherm is most often seen in the form

$$\text{II-6 } P/V(P_0 - P) = 1/(V_m K) + (K-1)/(V_m K) \times P/P_0$$

where V is the volume adsorbed, V_m is the volume adsorbed in one complete monolayer, P is the pressure and P_0 is the saturation pressure of the adsorbate at a temperature of the experiment, k is a constant equal to $\exp((Q_a - Q_L)/RT)$ where Q_a is the heat of adsorption of the first layer and Q_L is the heat of vaporization of the bulk adsorbate. From II-6 it can be seen that a plot of $P/V(P_0 - P)$ vs P/P_0 should give a straight line. From such a plot one can determine V_m and thus if one knows the volume of one atom of the adsorbate, and makes some assumptions about packing on the surface, then the surface area of adsorbent can be determined.

Caution is necessary in using either of these isotherms since they are derived assuming a very homoenergetic surface and this assumption does not hold

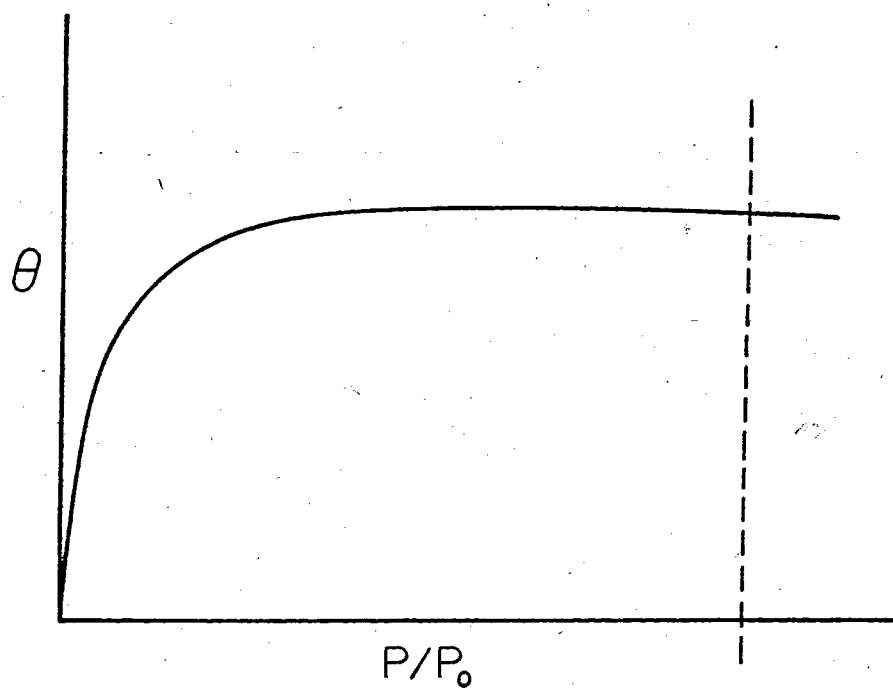


Figure II - 2

A plot of the form of equation II - 5 where P_0 is the saturation pressure of the adsorbate, and theta the fractional coverage.

true for many surfaces or adsorbates (Somorjai 1972).

Chapter III

A Brief Summary of the Theory of Nuclear Magnetic Resonance and Relaxation

The Basic Phenomena of Magnetic Resonance

This chapter and the next serve as an outline of NMR theory. They are admittedly incomplete and sometimes simplistic but hopefully will give the reader a feeling for the information to be gained from this tool.

A complete description of NMR theory can be found in several places notably Slichter (1963) or Abragam (1961). A description of the relaxation theory is found here as well, most of it following the classic paper of Bloembergen, Purcell and Pound (1948).

Nuclear Magnetic Resonance can be observed with any nuclei having a magnetic moment $\vec{\mu}$ not equal to zero. Classically the effect of a magnetic field \vec{H} on a magnetic moment $\vec{\mu}$ is to impart a torque \vec{L} on $\vec{\mu}$ equal to $\vec{\mu} \times \vec{H}$.

Such a torque is proportional to the time rate of change of the angular momentum $\omega = \hbar^{-1} \vec{L}$

$$\text{III-1 } \frac{d\vec{I}}{dt} = \vec{\mu} \times \vec{H}$$

The magnetic moment is proportional to the spin angular momentum, the proportionality constant being the so-called gyromagnetic ratio, γ .

$$\text{III-2} \quad \vec{M}_u = \gamma \cdot \vec{I} \quad \text{thus}$$

$$\text{III-3} \quad d\vec{M}_u/dt = \gamma \cdot (\vec{M}_u \times \vec{H})$$

The magnitude of \vec{I} and its component along the z axis are constants of motion, the rate of change of \vec{M}_u with time must be such that $\vec{I}(z)$ is constant and \vec{I} changes in direction only. The result of (3) then is a precession of \vec{M}_u about the direction of the field \vec{H} (commonly taken as the z direction) as in Figure 1. The solution to equation (3) is commonly found by translating to a rotating coordinate system. It can be shown (Slichter 1963) that the derivative of \vec{M}_u in the lab fixed frame $(d\vec{M}_u/dt)_{\text{lab}}$ is equal to the derivative in the rotating frame $(d\vec{M}_u/dt)_{\text{rot}}$ plus the cross product of the angular velocity of the rotating frame and the vector \vec{M}_u .

$$\text{III-4} \quad (d\vec{M}_u/dt)_{\text{lab}} = (d\vec{M}_u/dt)_{\text{rot}} + (\vec{\omega} \times \vec{M}_u)$$

$$\text{III-5} \quad (d\vec{M}_u/dt)_{\text{rot}} = \vec{M}_u \times (\gamma \vec{H} + \vec{\omega})$$

Equation III-5 is the same as III-3 if we replace \vec{H} by $H_0 + \omega/\gamma$. If we use a rotating frame such that:

$$\text{III-6} \quad \omega_0 = \gamma H_0 \quad ; \text{ then:}$$

$$\text{III-7} \quad (d\vec{M}_u/dt)_{\text{rot}} = 0.$$

that is the magnetic moment is fixed in the rotating frame. Translating back to the lab fixed frame we see

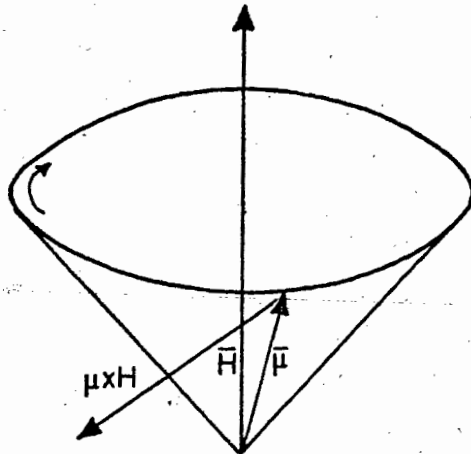


Figure III - 1
The precession of a dipole about a field.

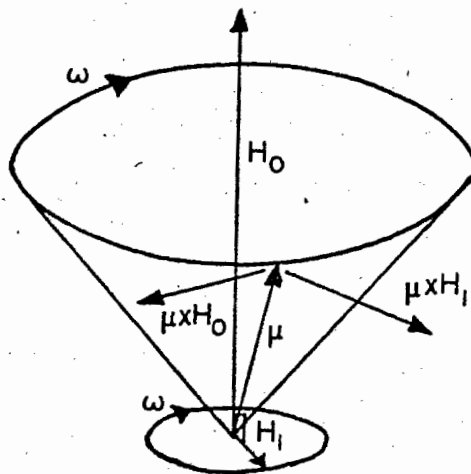


Figure III - 2
The effect on the dipole of a rotating field at right angles to the steady field.

that μ is a vector precessing at an angular velocity $\omega(o)$ given by equation III-6

$\omega(o)$ is known as the "Larmor frequency". It should be noted that this frequency is the same as that arrived at by looking at the system from a quantum mechanical point of view, see for example (Slichter 1963).

One of the beautiful things about the theory of magnetic resonance is that one is able to use either a classical or quantum mechanical formulation enabling one to see the model of what is occurring in rather simpler ways.

At this point we have been able to describe the magnetic dipole when placed in a magnetic field. It can be shown that the energy of a dipole in a magnetic field is simply $-\vec{\mu} \cdot \vec{H}_0$, that is, it is a function of the angle between the dipole and the field. Since this angle is not changing during the precession (see Figure I again), there is no change in energy.

If however, we add a second magnetic field \vec{H}_1 perpendicular to the first and rotating about the axis of \vec{H}_0 at some frequency, it can be seen that $\vec{\mu}$ will attempt to precess about this field as well. However, it cannot precess about both \vec{H}_1 and \vec{H}_0 unless H_1 is rotating at the same frequency as $\vec{\mu}$. The effect of H_1 is then to flip $\vec{\mu}$ so that the component of $\vec{\mu}$ on the axis of \vec{H}_0 is turned back and forth through 180 degrees.

This change in angle between $\vec{\mu}$ and \vec{H}_0 leads to a change in energy of the system.

As shown in Figure III-2 $\vec{\mu}$ can only precess about H_1 if H_1 rotates about H_0 at frequency ω , that is H_1 is in resonance with the precession of $\vec{\mu}$ about H_0 . One can measure the energy changes in the system either in the frequency domain (NMR Absorption or NMR Induction) or in the time domain (Pulse NMR). Since both techniques are employed in this research a short description of each will be given.

NMR in the Frequency Domain

We can produce H_1 rotating in the xy plane or its equivalent by applying an oscillating voltage to a coil of wire which has its axis perpendicular to H_0 . Actually this produces a linearly oscillating field H_x equal to $2 H_1 \cos(\omega \cdot t)$. Such a linearly oscillating field is equivalent to two rotating fields rotating in opposite directions with the same angular velocity. If the oscillating field is described by

$$\text{III-8 } H_x = 2 H_1 \cos(\omega \cdot t)$$

then the rotating fields will be described by:

$$H_x(1) = H_1 \cos(\omega \cdot t)$$

$$H_x(2) = H_1 \cos(\omega \cdot t)$$

$$H_y(1) = H_1 \sin(\omega \cdot t)$$

$$H_y(2) = -H_1 \sin(\omega \cdot \tau)$$

$$H_z(1) = 0$$

$$H_z(2) = 0$$

one of which will rotate in the same direction as the precessing dipole and will interact with it, the other having no effect.

The signal could be detected by making the H_1 coil with the sample inside it part of an LC circuit. The inductance L of the coil is a function of the susceptibility which changes drastically at resonance. The resonance condition could be met by stepwise changing the angular velocity ω of the oscillation of the H_1 field, or more commonly by leaving ω fixed and sweeping H_0 through the point of the resonance condition.

More commonly the signal is detected as a current induced by the precessing spins in a set of receiver coils at right angles to the transmitter coil and to $H(z)$ (the direction of H_0). The resonance condition is met as before.

The output of either detection device is a curve of amplitude of voltage or current vs. the frequency of the rotation of H_1 or versus the field H_0 .

NMR in the Time Domain

If we arrange for $H_x = H_1 \cos(\omega \cdot t)$ to have a frequency ω_0 such that $\omega_0 = \gamma \cdot H_0$ but turn H_x on for only a short period of time t_w we can expect that the magnetic dipole will follow H_1 for t_w . $\vec{\mu}$ then would precess through an angle $\theta = \gamma H_1 t_w$

and for example we could choose $\theta = -\pi$ which would invert the magnetic moment or choose $\theta = \pi/2$ which would turn the moment from the z axis into the xy plane. Detection of the movement of μ could be made in same way as for the frequency domain experiments. This is the basis for so-called pulse experiments in NMR. The relation between this transient response and the steady state response (frequency domain) will be shown after a description of the relaxation process.

The foregoing is of course very simplistic since it deals with a single isolated magnetic dipole. In reality we are forced to deal with a macroscopic sample containing a large ensemble of spins. A simple quantum approach to an isolated spin leads one to $2I + 1$ degenerate energy levels. The degeneracy is lifted when the nucleus is placed in a magnetic field. The energy of each level in the magnetic field is the eigen-value of the Hamiltonian (Abragam 1961):

$$\text{III-9 } \text{Ham} = - \gamma \hbar H_0 I_z$$

so $E = - \gamma \hbar H_0 m_I$ where m_I takes the integer or half integer values from $I, I-1, \dots, -I$; and the difference between any two energy levels is $\gamma \hbar H_0$. For $I = 1/2$, $m_I = \pm 1/2$ and we have a two energy level system completely analogous to the system previously described. The magnetic moment can be oriented along the field (in the lower energy level) or opposed to the field (in the upper energy level). An input of energy can flip \vec{M} from one orientation to the other or the nucleus from one energy level to the other.

Saturation

Consider now an ensemble of magnetic nuclei of spin $1/2$, with energy levels which differ by $\gamma \hbar H_0$. The ratio of population in the low level to the upper level is given by the Boltzmann equation:

$$\text{III-10 } n(1/2)/n(-1/2) = \exp(- \gamma \hbar H_0 / kt)$$

where $n(1/2)$ is the population of the energy level described by $m_I = 1/2$, $n(-1/2)$ the population of level $m_I = -1/2$. Gamma for a proton = 4257.6 hz/gauss. For a field of 23.4 K gauss the excess population in the lower level is only 16 in 1 million at $T = 300$ degrees K. Since we have equal probability of upward and downward radio frequency induced transitions and since the probability of spontaneous

emission is very small for a magnetic dipole (Abragam 1961) we can see the distinct possibility of equalizing the population of upper and lower states so that there will be no absorption of energy. This phenomenon is known as saturation.

Relaxation and the Bloch equations, T_1 and T_2 .

Experimentally one finds that saturating a sample is not so easy as the foregoing would suggest. We shall see that there are time variations in the local magnetic fields in a sample which cause the magnetization to come back to equilibrium.

I shall delay a description of these variations of field that cause the relaxation until I have outlined the description of the relaxation due to Bloch.

Before putting a sample in a magnetic field the x and z components of the net magnetization M are obviously equivalent (isotropic sample). In a large magnetic field however, we can see that there is a magnetization \vec{M}_z in the direction of the field (customarily taken as the z direction) while the x , and y components fall to zero.

If in a static field $\vec{H}_z = H_0$ we disturb $M_z = M_0$ then we observe that it will approach its old equilibrium M_0 in a way which is often adequately described by:

$$\text{III-11 } dM_z/dt = -(M_z - M_0) / T_1$$

That is equilibrium is approached exponentially with a time constant T_1 . Here M_0, M_x, M_y, M_z , are components of M in the lab fixed frame.

T_1 is known as the longitudinal relaxation time. Its inverse R_1 gives the rate that the component of magnetization along the field will approach its equilibrium value. T_1 is also known as the spin-lattice relaxation time since energy lost by the spins in going to the lower energy level is absorbed by the surrounding system, commonly known as the lattice.

We noted that $M_x = M_y = 0$ at equilibrium. If we disturb the system in such a way that we get a component of M in the xy plane then it will approach zero at a rate often adequately described by:

$$\text{III-12} \quad dM_x/dt = -M_x/T_2 \quad \text{and} \quad dM_y/dt = -M_y/T_2$$

T_2 is called the transverse relaxation time, since it describes the decay of the component of M which is transverse to the direction of the field. It is also known as the spin-spin relaxation time, since as we shall see it results from an interaction between the magnetic dipoles (spins).

Bloch assumed that in the presence of an applied D. C. field $H(0)$, and a much smaller r.f. field H_1 , that the motion due to relaxation could be added to the motion of the free spins (equation III-3) giving;

$$\text{III-13} \quad -dM/dt = M_x \cdot \gamma \cdot H - k(M_z - M_0) / T_1 \\ - (iM_x + jM_y) / T_2$$

where i, j, k are the normal unit vectors.

The solution to this equation is:

$$\text{III-14} \quad M_x = \tilde{M}_x \cos(\omega t) - \tilde{M}_y \sin(\omega t) \\ M_y = \tilde{M}_x \sin(\omega t) + \tilde{M}_y \cos(\omega t) \\ M_z = \tilde{M}_0 \{ [1 + \{\omega - \omega_0\}^2 T_2^2] / [1 + \{\omega - \omega_0\}^2] \} T_2^2 \\ + \gamma^2 H_1^2 T_1 T_2 \}$$

where \tilde{M}_x and \tilde{M}_y are the transverse components of M in a rotating frame, and have the values:

$$\text{III-15} \quad \tilde{M}_x = (\gamma A H_1 T_2^2 M_0) / \{ [1 + T_2^2 A^2] \\ + \gamma^2 H_1^2 T_1 T_2 \} \\ \tilde{M}_y = (\gamma \cdot H_1 T_2 M_0) / \{ [1 + T_2^2 A^2] \\ + \gamma^2 H_1^2 T_1 T_2 \}$$

$$\text{where } A = (\omega - \omega_0)$$

Thus the transverse components of the magnetization in the lab fixed frame are functions of time, and will produce a voltage of frequency ω in a coil.

If H_1 is small enough that the last term in the denominator is small in comparison to 1, saturation will not occur. In this case

$$\text{III-(16)} \quad \tilde{M}_y = \gamma H_1 M_0 T_2 / \{ [1 + A^2 T_2^2] \} \\ = \pi \gamma H_1 M_0 f\{A, T_2\}$$

$$\text{where } f\{A, T_2\} = 1/\pi \frac{T_2}{\{1+A^2 T_2^2\}}$$

which is the normalized Lorentzian shape function with a half width at half intensity of $1/T_2$.

It has become customary to look at this in terms of the magnetic susceptibility. Since we have a field $H_x = 2 H_1 \cos(\omega \cdot t)$ then we must have a magnetization M_x proportional to H_x , thus $M_x = \chi H_x$ where χ is the magnetic susceptibility. However, M_x , χ and H_x are all a function of ω and it is convenient to consider χ as having a real and imaginary part just as we can consider M_x and H_x to have a real and imaginary part. Equation (8) can be written as:

$$\text{III-17a } H_x(t) = 2 H_1 \text{Re}\{\exp i\omega t\} = \hat{H}_x(t)$$

$$\text{III-17b } M_x(t) = 2 H_1 \text{Re}\{\hat{\chi} \exp i\omega t\} = \hat{M}_x(t)$$

$$\text{where } \hat{\chi} = \chi' - i\chi''$$

and where the hats reminds us that we have written the quantities as complex numbers. III-(17b) may be rewritten then as:

$$\text{III-18 } M_x(t) = 2 H_1 \{\chi'(\omega) \cos \omega t - \chi''(\omega) \sin \omega t\}$$

A comparison with equation III-(14)

shows that:

$$\text{III-19 } \chi'(\omega) = \tilde{M}_x / 2 H_1$$

$$\chi''(\omega) = \tilde{M}_y / 2 H_1$$

and by substituting $X_0 \cdot H_0$ for M_0 , and ω_0 for gamma H_0 we can write:

$$\text{III-(20) (a) } \chi'(\omega) = \left(\frac{\pi}{2}\right) \cdot X_0 \cdot \omega_0 \cdot T_2 \cdot A f\{A, T_2\}$$

$$(b) \chi''(\omega) = \left(\frac{\pi}{2}\right) \cdot X_0 \cdot \omega_0 \cdot f\{A, T_2\}$$

so long as H_1 is small enough to avoid saturation. $f\{A, T_2\}$ is the normalized Lorentzian defined by (16). $\chi''(\omega)$ and $\chi'(\omega)$ are generally known as the absorption and the dispersion respectively. They are related to each other, the relationship being the Kramers-Kronig relations. Proof of these relations can be found in Abragam (1963 p. 93). Knowledge of $\chi'(\omega)$ at all frequencies gives $\chi''(\omega)$ at all frequencies.

The importance of $\chi''(\omega)$ is that it can also be determined theoretically from atomic (quantum mechanical) considerations giving us microscopic information from a macroscopic measurement.

The Relationship Between the Signal in the Time Domain and the Frequency Domain

We wish to know the magnetization $dM_x(t)$ produced at a time t due to a magnetic field $H_x(t')$ of duration dt' turned on at time t' where t' is earlier than t .

$dM_x(t)$ is proportional to $H_x(t')dt'$

We write

$$\text{III-(22)} \quad dM_x(t) = m(t-t')H_x(t')dt'$$

where the proportionality constant $m(t-t')$ depends on how long after the pulse of field that we wish to know $dM_x(t)$

The total magnetization at time t is the integral of equation (22).

$$\text{III-(23)} \quad M_x(t) = \int_{-\infty}^t m(t-t')H_x(t')dt'$$

As before we write $M_x(t)$ and $H_x(t')$ as complex numbers (always with the understanding that we are only considering the real part).

$$\text{III-23b} \quad \hat{M}_x(t) = M_x \exp(i\omega t) \quad , \quad \hat{H}_x(t) = H_x \exp(i\omega t)$$

Equation 23 now becomes:

$$\begin{aligned} \text{III-(24)} \quad \hat{M}_x(t) &= \exp(i\omega t) \int_{-\infty}^t m(t-t')H_x \exp(-i\omega t') dt' \\ &= H_x \exp(i\omega t) \int_0^{\infty} m(\tau) \exp(i\omega\tau) d(\tau) \end{aligned}$$

But previously (equation 17b) we wrote:

$$\hat{M}_x(t) = \hat{\chi}(\omega) \hat{H}_x(t)$$

where the hats remind us that the quantities are complex.

Comparison with (24) shows that:

$$\begin{aligned} \text{III-(25)} \quad \hat{\chi}(\omega) &= \int_0^{\infty} m(\tau) \exp i\omega\tau \quad d(\tau) \\ \text{or } \chi'(\omega) &= \int_0^{\infty} m(\tau) \cos \omega\tau \quad d(\tau) \\ \chi''(\omega) &= \int_0^{\infty} m(\tau) \sin \omega\tau \quad d(\tau) \end{aligned}$$

That is, in the pulse experiment we determine some quantity $M(\tau)$ whose Fourier transform is the quantity $\chi(\omega)$ we determine in the steady state experiment.

Similarly $M(\tau)$ is the Fourier transform of the complex susceptibility.

$$\text{III-26} \quad m(\tau) = 1/2\pi \int_{-\infty}^{\infty} \chi(\omega) \exp i\omega\tau \, d(\omega)$$

The information gained by an analysis of an experiment in the frequency domain tells us the information contained in the time domain experiment.

Some Useful Pulse NMR Experiments

Consider again a sample in a magnetic field H_0 in the z direction with a magnetization M , from the point of view of the rotating frame (see page 20). An r.f. field H_1 in the x direction at frequency $\omega = \text{gamma} \cdot H_0$, will cause M to precess about H_1 . If H_1 is turned on only for time t then M will only follow H_1 for that long. Consider t to be long enough to only turn M onto the y axis. (This is normally called a 90 degrees pulse). Suppose immediately after the pulse $M_z = 0$, $M_x = 0$ and $M_y = M_0$. Now M_y must decay to zero. If the apparatus is set up to detect signals along the x or y axis then the signal will decay with a time constant T_2 . This can be seen from a consideration of equations III-(12). Such a signal is generally known as a free induction decay or F.I.D.

The above picture denies the fact that M is composed of many individual spins. If the field was perfectly homogeneous then this would not matter and the above would be essentially correct. However, each of the individual spins is in a slightly different field. Since a pulse at ω_0 of duration t will contain all frequencies from $\omega_0 - 2\pi/t$ to $\omega_0 + 2\pi/t$, all the spins will still be turned onto the y' axis. However some will be going slower, some faster than ω_0 .

In the rotating frame we can picture some spins turning into the $x'y'$ quadrant others into the $-x'y'$ quadrant as in figure III-3 below. The signal now decays as the spins dephase in the $x'y'$ plane as well as decaying through the normal T_2 processes. The decay time constant is now T_2^* given by:

$$\text{III-(27)} \quad 1/T_2^* = 1/T_2 + 1/T(\text{in})$$

where $T(\text{in})$ is the time constant describing the process of dephasing in the $x'y'$ plane, caused by the inhomogeneity of the field.

The output from such an experiment would be a current decaying with time constant T_2^* as in Figure III-4.

If instead of using a pulse exactly at ω_0 , we use a pulse at $\omega_0 + d\omega$ then M will still be turned onto the xy plane as long as $d\omega$ is not too large. If we are detecting the signal with a phase sensitive detector which

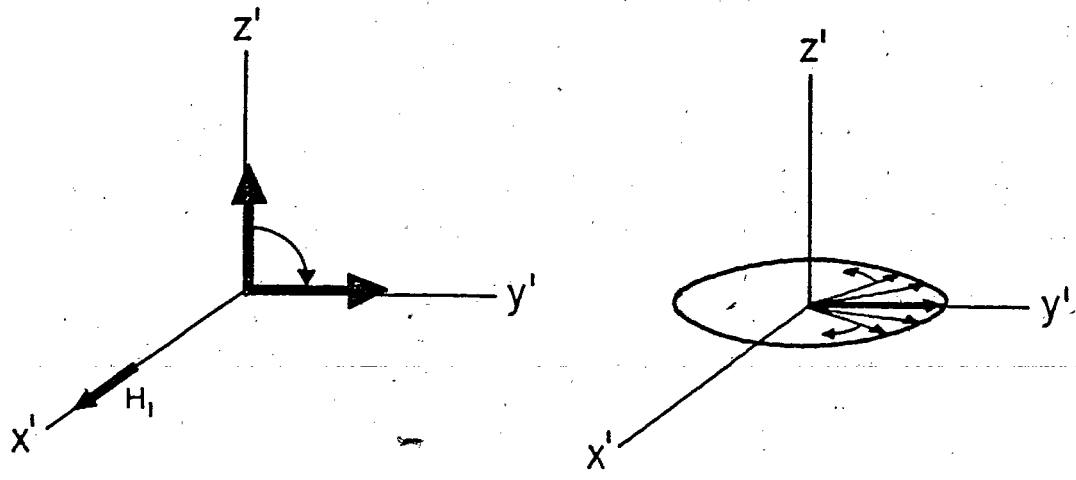


Figure III - 3
 M subjected to a 90 degree pulse is turned onto the y' axis
 The components of M begin to dephase in the $x'y'$ plane

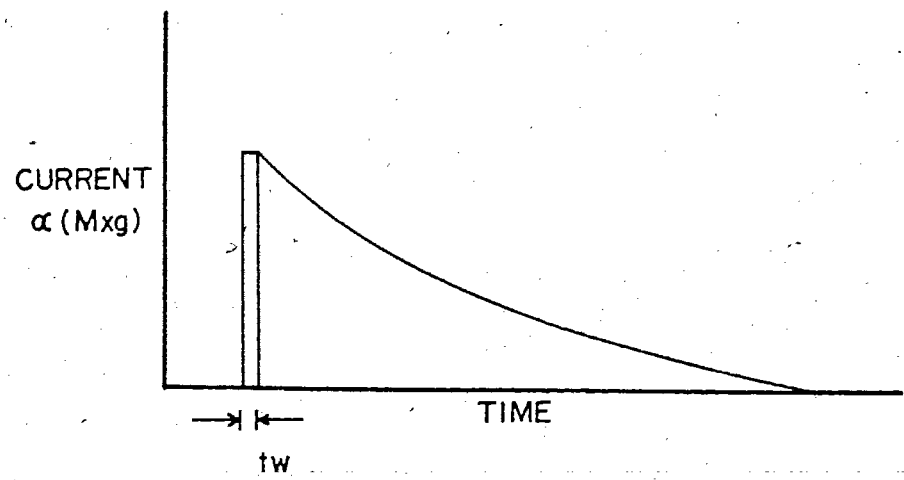


Figure III - 4
 The output following a 90 degree pulse about x' .
 t_w is the length of the pulse.

uses as a reference the phase of the input signal, then the output will be modulated as the xy component of M (now travelling faster or slower than the rotating frame) destructively and constructively interferes with the reference phase. The output will then look like Figure III-5.

The length of the pulse t can be varied so that M is turned through any number of degrees (although it should be short enough that T_1 and T_2 effects are negligible during t). For example a 180° degree pulse would then turn M_0 from the z axis to the $-z$ axis.

T_1 Measurements

As already mentioned, normally a spectrometer is set up to monitor the component of the magnetization in the xy plane, and thus from the Bloch equations, one can see means of measuring T_2 or at least T_2^* .

T_1 might be measured by measuring the height of the F. I. D. as a function the repetition rate of the 90° degree pulse, since the amplitude of M_z , tau seconds after a 90° degree pulse will be a function of T_1 .

A more common and precise way is to monitor the xy component of the magnetization by using a 180° degree pulse followed by a 90° degree pulse; both along the x axis. The 180° degree pulse turns the z component of the magnetization from M to $-M$. No signal is seen, as the

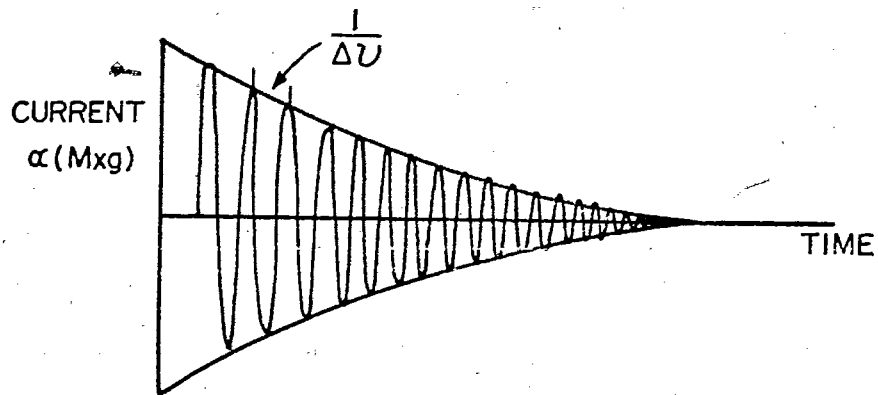


Figure III -5
The output following a 90 degree pulse which is off resonance by some amount $\Delta\nu$.

receiver "sees" only the xy component of M.

Tau seconds after the 180 degree pulse the sample is subjected to the 90 degree pulse. During the interval between pulses M was decaying with time constant T_1 . Now the initial amplitude of the F. I. D. following the 90 degree pulse will be a function of tau.

By measuring the amplitude of the F. I. D. as a function of tau one can easily determine T_1 , from equation III-11. or the integral of III-11.

$$\text{III-28 } M_z = M_0 (1 - 2\exp(-t/T_1))$$

Typical output is diagrammed in Figure III-6.

T_2 Measurements

Accurate measurement of T_2 is a problem since in both c. w. experiments and normal 90 degree pulse experiments one is actually measuring T_2^* , and furthermore one must be certain in c.w. experiments not to saturate the sample; (see equations III-15).

Carr and Purcell (1954) developed a multiple pulse experiment for measuring T_2 which was later modified by Meiboom and Gill (1958). The Carr-Purcell pulse train is a 90 degree pulse about the x axis followed by a 180 degree pulse at time tau, followed by another at time 3 tau, which is in turn followed by more 180 degree pulses every 2 tau, i.e. the train is 90 degrees - tau - 180

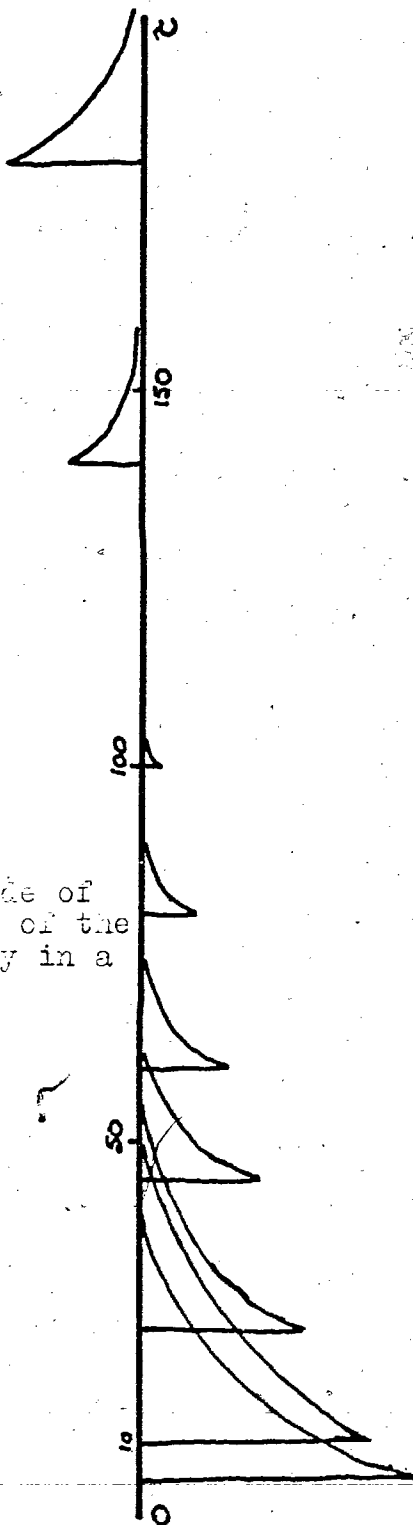


Figure III - 6

The initial amplitude of a FID as a function of the repetition frequency in a 180-90 T_1 pulse experiment.

degrees - 2 tau - 180 degrees - ...).

A consideration of Figure III-7 shows the experiment. All pulses are along the x' axis, and the diagrams are as seen in the rotating frame.

Upon being hit with a 90 degree pulse M is turned about x' to the y' axis (a); because of the inhomogeneous field M_y now starts to dephase in the $x'y'$ plane (b); the 180 degree pulse now turns those components of M in the $x'y'$ quadrant (those with $\omega > \omega_0$) into the $x(-y)$ quadrant, and those in the $(-x)y$ quadrant (those with $\omega < \omega_0$) into the $(-x)(-y)$ quadrant (c); those components that had $\omega > \omega_0$ are now going to rephase with those with $\omega < \omega_0$ along the $(-y)$ axis (d) and will produce a current maximum in the receiver at time 2 tau; a further 180 degree pulse at time 3 tau carries the components in the $x(-y)$ quadrant to the xy quadrant, and those in the $(-x)(-y)$ quadrant to the $(-x)y$ quadrant (e); where they rephase along the y axis producing another current maximum now at time 4 tau (f). Subsequent 180 degree pulses at times 5 tau, 7tau ... etc produce signals usually referred to as echos at times 6 tau, 8 tau etc.

The amplitude of the echos is dependent upon the spacing time tau, and to the real T_2 , (see for example Farrar 1971). It can also depend on the rate of diffusion as will be seen shortly. A close consideration of the above leads one to the conclusion that errors in the pulse

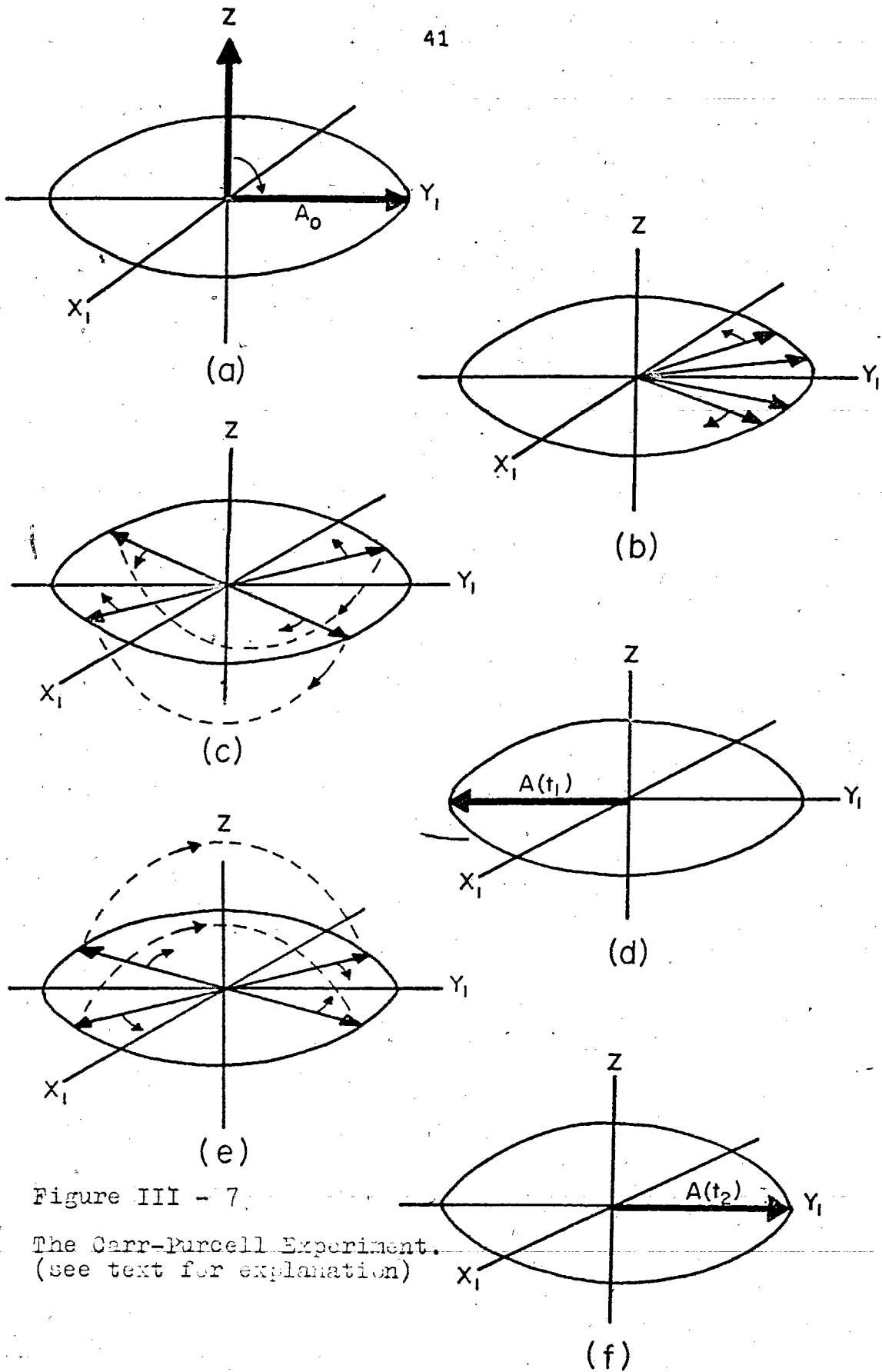


Figure III - 7.

The Carr-Purcell Experiment.
 (see text for explanation)

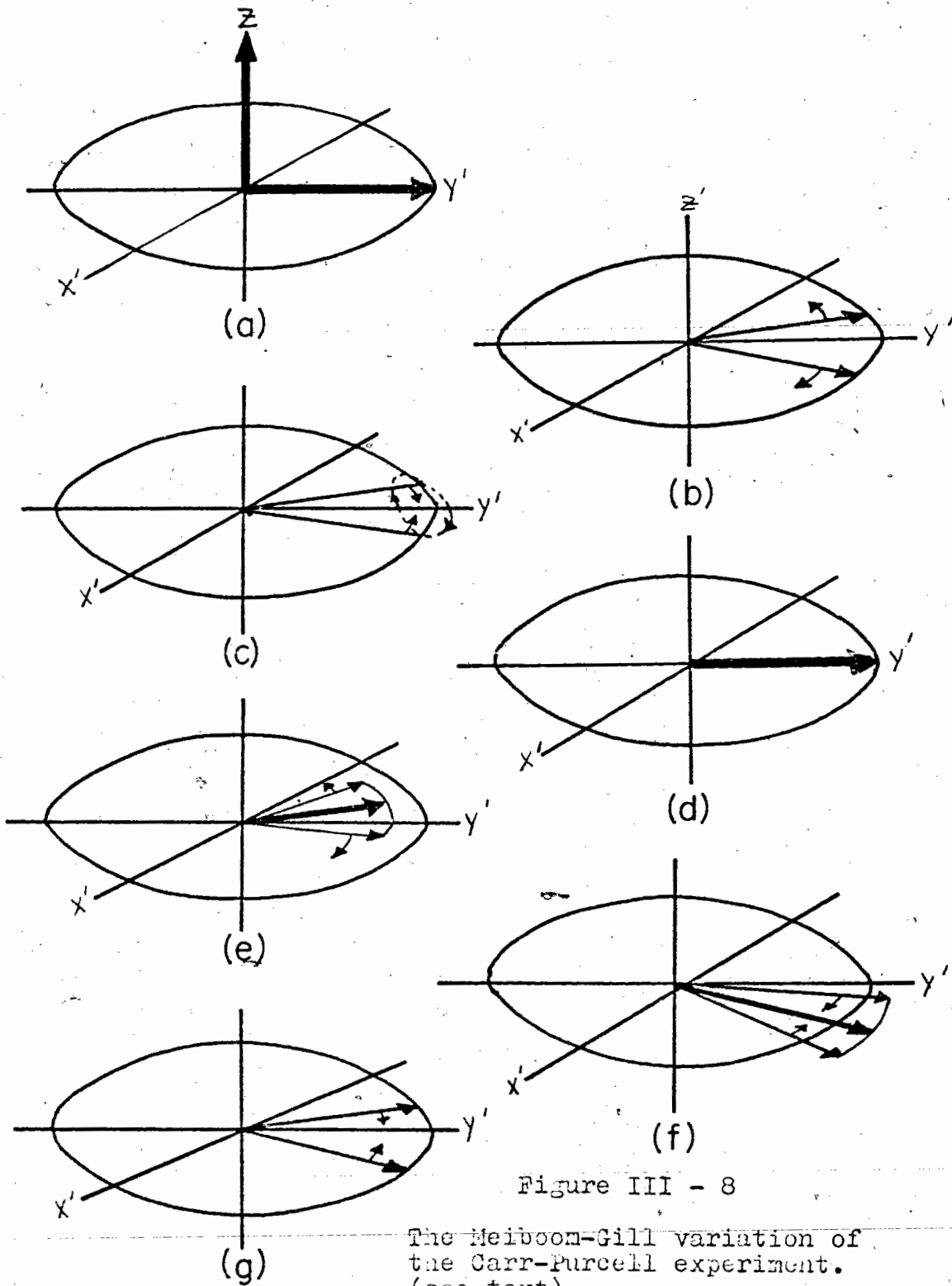


Figure III - 8

The Meiboom-Gill variation of the Carr-Purcell experiment. (see text)

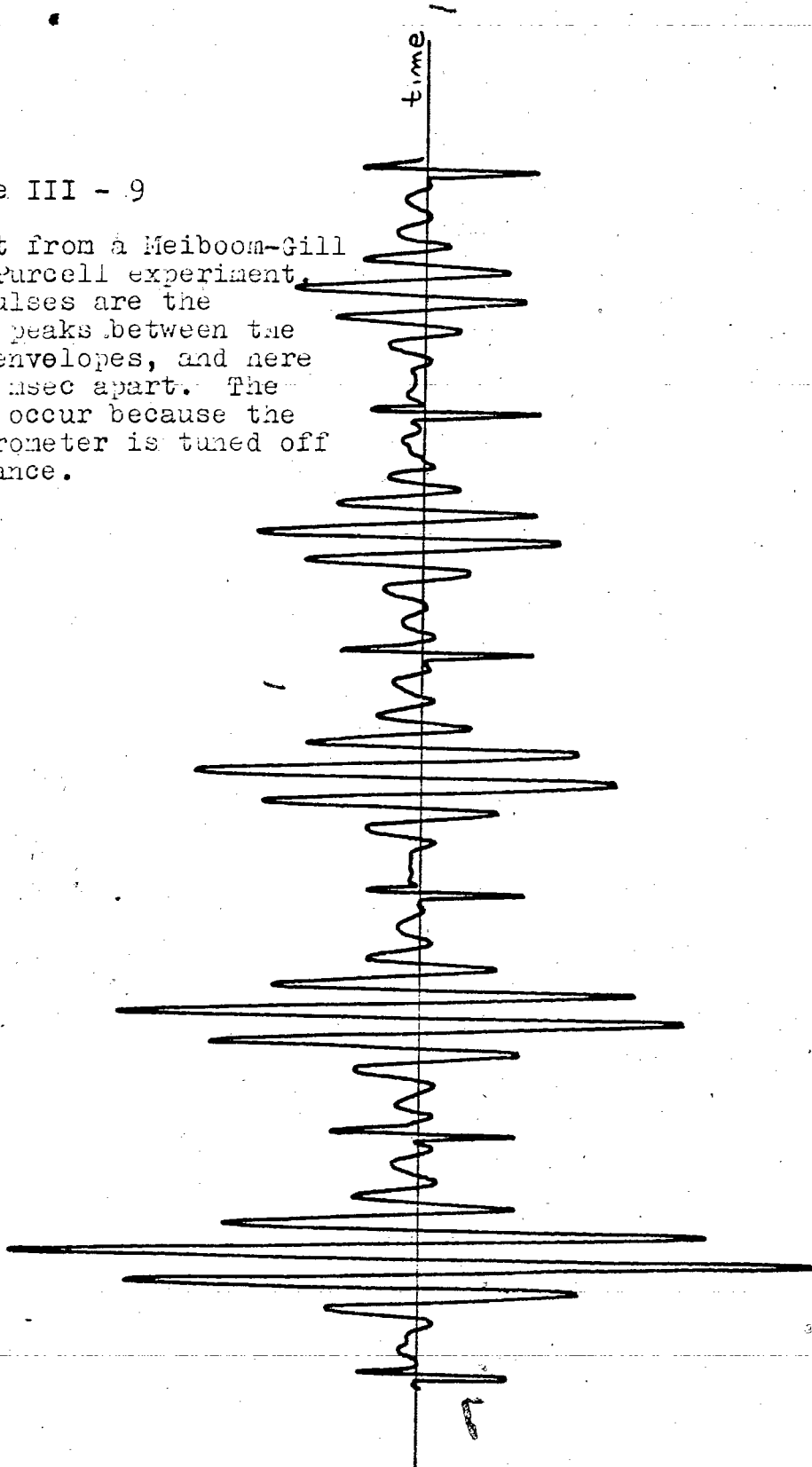
width are cumulative in this experiment.

The variation of the Carr-Purcell experiment proposed by Meiboom and Gill (1958) uses a 90° - τ - 180° - 2τ - 180° - ... pulse train as before but the phases of the 90° and 180° degree pulses are 90° degrees apart. This is the same as applying the 180° degree pulse along the y axis. Figure III-8 shows the result of this variation. Following a 90° degree pulse about the x' axis (rotating frame); M_z is tipped to the y' axis (a); then begins to dephase in the $x'y'$ plane (b); the 180° degree pulse, effectively along y , carries components of M in the $x'y'$ quadrant to the $(-x')y'$ quadrant and those in the $(-x')y'$ quadrant to the $x'y'$ quadrant (c); they rephase along the y' axis producing an echo (d). Subsequent 180° degree pulses exchange components from the $x'y'$ to the $(-x')y'$ and vice versa and are followed by an echo. If the 180° degree pulse is less than 180° degrees then the components of M are carried to a place out of the xy plane (as in the Carr-Purcell experiment) (e) they rephase with slightly smaller amplitude than they would have if the pulse had been of the proper length (f); but the next 180° degree pulse is of the right length to return then exactly to the xy plane (g). The errors in the Meiboom-Gill variation due to improper pulse lengths cancel out.

Figure III-9 shows the output of a Meiboom-Gill variation of a Carr-Purcell experiment, following the

Figure III - 9

Output from a Meiboom-Gill Carr-Purcell experiment. The pulses are the sharp peaks between the beat envelopes, and here are 5 msec apart. The beats occur because the spectrometer is tuned off resonance.



first 180 degrees pulse. In this case the spectrometer has been tuned off resonance, a practice which means that the 90 degree and 180 degree pulses are less well defined.

An Experiment to Measure Diffusion

The actual amplitude of the echo at time 2τ is equal to (Carr 1954):

$$\text{II-29} \quad A(\text{echo}) = K \exp[-t/T_2 - 1/3 \gamma^2 \cdot G^2 D \tau^2 t]$$

where G is the spatial gradient of the magnetic field and D is the diffusion constant. Effectively this means that if a nucleus moves to an area where the magnetic field is different then the measured relaxation time will be shorter. Measurements of the amplitude of the echo as a function of τ can lead one to a value for the diffusion constant.

Chemical Shifts

Each chemically different species when placed in a magnetic field will experience a slightly different field and thus resonate at a different frequency. This leads to the phenomenon of chemical shifts, which is the chief characteristic of NMR spectroscopy that has made it such a valuable tool in chemistry.

The different fields at the nuclei with different electronic environments result from the orbital motion

induced in the electrons when placed in a magnetic field. The moving electrons produce a secondary field which interacts with the nucleus as before. The induced current and thus the secondary field is proportional to the applied field H_0 , so that the field at which a particular nucleus will resonate is given by:

$$\text{III-30 } H_i = H_0 \{1 - \sigma_i\}$$

where σ_i is the screening constant or shielding coefficient. In a constant field each chemically different nucleus will resonate at a different frequency. Generally the new frequency will be lower than the frequency of the bare nucleus since the effect of the secondary field is to bring the energy levels closer together. In a fixed frequency, swept field experiment the same situation results in having to use a higher field to get the nucleus to resonate.

Since it is difficult to measure an absolute value of a magnetic field, chemical shifts are generally measured from a standard reference. The amount of the chemical shift is proportional to the magnetic field in which the experiment is carried out and the shifts are usually measured in parts per million (ppm). Thus

$$\begin{aligned} \text{III-31 } \delta &= \{H_i - H(\text{ref})\} / H_0 \quad \times 10^6 \\ &= -\{\omega_i - \omega(\text{ref})\} / \omega_0 \quad \times 10^6 \end{aligned}$$

where δ is the chemical shift in parts per million.

In most of the proton work Tetra methyl silane (TMS) is used for the standard. By way of illustration methyl protons in n-alkanes have chemical shifts of the order of 1 ppm down field from TMS (usually quoted as -1 ppm), while the methylene protons have chemical shifts of from -1 1/4 to -2 ppm. Olefinic protons in alkenes on the other hand have shifts of the order of -5 ppm.

If the reference sample used is separate from the sample being measured then a correction must be applied for the difference in bulk susceptibilities of the two samples involved.

This correction is a function of the shape of the sample and is such that no correction is necessary for a sphere. For a cylinder the actual chemical shift δ (real) is found by:

$$\text{III-32} \quad \delta \text{ (real)} = \delta \text{ (obs)} + 2\pi/3 \{X_v(\text{ref}) - X_v(\text{sample})\}$$

where δ (obs) = the observed chemical shift and X_v are the volume susceptibilities of the reference and sample substances respectively.

Since the correction involved is not derived in any of the standard texts although it is stated in some (Pople 1959) and since it is not obvious, it is derived in appendix A.

Chapter IV

Relaxation Analysis

Dipole-Dipole Relaxation

An analysis of NMR relaxation (measurement of T_1 and T_2) gives information about the molecular dynamics of the system involved. A consideration of what causes the relaxation to take place or more exactly, the nature of the coupling between the spins and their environment, is necessary.

If one considers a system composed of many dipoles it is not surprising that these dipoles will be coupled to each other since each will produce a magnetic field at another dipole approximately equal to $\vec{\mu}/r^3$ where $\vec{\mu}$ is the dipole moment and r is the distance between the dipoles. (For a proton at chemical bond distances from another proton $\mu/r^3 = \text{ca. } 1 \text{ gauss}$ which can either oppose or reinforce H_0 so this coupling is considerable.) Such coupling is known as dipole-dipole coupling.

However the strength of this interaction alone does not determine T_1 and T_2 since a modulation of coupling at an appropriate frequency is necessary. This modulation is generally caused by the molecular dynamics.

It is instructive to consider the picture first from a classical point of view.

Each dipole causes a small field \vec{h} at each other dipole. As before (Chapter III) a field \vec{h} produces a torque $\vec{h} \times \vec{M}$ on \vec{M} . Consider \vec{h} and \vec{M} in the rotating frame so that:

$$\vec{h} = i\vec{h}_x' + j\vec{h}_y' + k\vec{h}_z' \quad \text{and} \quad \vec{M} = i\vec{M}_x' + j\vec{M}_y' + k\vec{M}_z'$$

$$\text{IV-1 } (\vec{h} \times \vec{M}) \text{ (rotating frame)} = i(\vec{h}_y' \vec{M}_z' - \vec{h}_z' \vec{M}_y') \\ + j(\vec{h}_z' \vec{M}_x' - \vec{h}_x' \vec{M}_z') + k(\vec{h}_x' \vec{M}_y' - \vec{h}_y' \vec{M}_x')$$

As with the field \vec{H} , \vec{h} can not effectively couple with \vec{M} unless it has frequency $\omega(0)$, however we can consider any process having frequencies centered at ω to be made up of Fourier components from 0 to ω . It will be the size of the Fourier component at $\omega(0)$ that will determine whether the movement of \vec{h} can effectively couple with \vec{M} .

Equation IV-1 shows that of the components of \vec{h} in the rotating frame, \vec{h}_x' is coupled to \vec{M}_y' and to \vec{M}_z' , \vec{h}_y' is coupled to \vec{M}_x' and \vec{M}_z' while \vec{h}_z' is coupled to \vec{M}_x' and \vec{M}_y' . From our previous definitions of T_1 and T_2 we can see that fluctuation of \vec{h}_x' and \vec{h}_y' lead to T_1 and T_2 relaxation, whereas fluctuation of \vec{h}_z' leads to T_2 relaxation only.

A further consideration shows that T_2 can only be shorter or as long as T_1 . If \vec{h}_x' and \vec{h}_y' are static (in the rotating frame) then in the lab fixed frame they are moving at high frequency (of the order of $\omega(0)$).

These high frequency components affect both T_1 and T_2 . However if $\vec{h}\omega'$ is static or has a low frequency $\vec{h}\omega$ will also be static leading to a low frequency or zero frequency contribution to T_2 only. In summary, T_2 processes are induced by both high and low frequencies, T_1 processes by high frequencies only.

The semiclassical and the purely quantum mechanical approach to dipole-dipole relaxation are outlined in Chapter 8 of Abragam and also in the paper of Bloombergen Purcell and Pound (Bloombergen 1948).

Generally the Hamiltonian of the system is written as the sum of the Hamiltonian describing the interaction between $\vec{\mu}$ and the static field (the Zeeman energy) and and the interaction energy between the dipoles.

$$\text{IV-2 } \text{Ham}(\text{total}) = \text{Ham}(\text{Zeeman}) + \text{Ham}(\text{dipole})$$

where $\text{Ham}(\text{Zeeman}) = \gamma \hbar H_0 \sum_j I_z^{(j)}$ which has eigenvalues $\hbar E(M) = -\gamma \hbar H_0 M$ where M takes $2I+1$ values from I to $-I$.

The perturbing Hamiltonian dipole can be derived considering the classical interaction between two dipoles $\vec{\mu}_1$ and $\vec{\mu}_2$.

$$\text{IV-3 } (\vec{\mu}_1 \cdot \vec{\mu}_2 / r^3) - 3(\mu_1 \cdot \vec{r})(\mu_2 \cdot \vec{r}) / r^5$$

where r is the distance between μ_1 and μ_2 and \vec{r} is the vector between them.

By writing \vec{M}_{u_1} and \vec{M}_{u_2} as the operators $\gamma_1 \hbar \mathbf{I}$,
and $\gamma_2 \hbar \mathbf{I}$ the perturbing Hamiltonian for a two
spin system can be written as (Abragam 1961):

$$\text{IV-4 } \hbar \text{ Ham}_{\text{dipole}} = \sum_{\mathbf{q}} F(\mathbf{q}) \cdot A(\mathbf{q})$$

where $A(\mathbf{q})$ and $F(\mathbf{q})$ are tensors of rank 2.

The $A(\mathbf{q})$ are operators acting on the spin variables
(i.e. they are space quantized and thus independent of
time).

$$\text{IV-5 } A_0 = \alpha \{-2/3 I_z S_z + 1/6 (I_+ S_- + I_- S_+)\}$$

$$A_1 = \alpha \{I_z S_+ + I_+ S_z\}$$

$$A_2 = 1/2 \cdot \alpha \cdot I_+ S_+$$

where I and S are the angular momentum quantum
numbers of the two respective spins,

$$\text{where } \alpha = -3/2 \gamma_1 \gamma_2 \hbar$$

and where I_+ , S_+ , I_- , S_- are the ladder operators.

The $F(\mathbf{q})$ are random functions of time which describe
the relative position of the two spins. They are related
to the spherical harmonics of order 2, $Y_{2M}(\theta, \phi)$, by:

$$\text{IV-6 } F_0 = 1/\vec{r}_{ij}^3 \cdot (16\pi/5)^{1/2} Y_{20}(\theta_{ij}, \phi_{ij})$$

$$F_1 = 1/\vec{r}_{ij}^3 \cdot (8\pi/15)^{1/2} Y_{21}(\theta_{ij}, \phi_{ij})$$

$$F_2 = 1/\vec{r}_{ij}^3 \cdot (32\pi/15)^{1/2} Y_{22}(\theta_{ij}, \phi_{ij})$$

These functions change with time since \vec{r} may vary with

time, and θ_{ij}, ϕ_{ij} (representing the Euler angles between \vec{r}_{ij} and the magnetic field H_0) varies with time if \vec{r}_{ij} moves.

Each of the $F_i(t)$ spatially describes the state of the system at a time t . Consider the system at a time τ later; $F_i(t+\tau)$ now describes the new state.

The function $F_i(t+\tau) \cdot F_i(t)$ tells how the initial state of the system is correlated to the new state. However we have a complete ensemble of individual states so that we average over the whole ensemble.

$\langle F_i^*(t+\tau) \cdot F_i(t) \rangle$ (where $\langle \rangle$ denotes the average) tells how the average of $F_i(t)$ is correlated to the average of $F_i(t+\tau)$

$$\text{IV-9} \quad \langle F_i(t+\tau) \cdot F_i(t) \rangle = G_i(\tau)$$

is called the correlation function of $F_i(t)$.

The correlation function determines the so-called "spectral density" of the interaction which produces the relaxation. The spectral density is the Fourier transform of $G_i(\tau)$

$$\text{IV-10} \quad J_i(\omega) = \int_{-\infty}^{\infty} G_i(\tau) \exp(-i\omega\tau) d\tau$$

In order to determine the correlation function one needs a model for the molecular motion. In practice, particularly for any but very simple systems, it is assumed that the correlation function may be written as:

$$\begin{aligned} \text{IV-11 } G(\tau) &= \langle F(t+\tau)^* F(t) \rangle \\ &= \langle F(t)^* F(t) \rangle \exp(-\tau/\tau_c) \end{aligned}$$

where τ_c is called the correlation time and characterizes the time scale of the molecular motion. In particular if $\tau < \tau_c$ the system will not have changed measurably, whereas if $\tau > \tau_c$ it will have changed significantly.

For this approximation equation (10) becomes

$$\text{IV-12 } J_i(\omega) = \langle F_i^*(t) F_i(t) \rangle \approx 2\tau_c / (1 + \omega^2 \tau_c^2)$$

where one can make the assumption that τ_c is the same for each of the functions $F_0(t)$, $F_1(t)$ and $F_2(t)$, so long as one expects isotropic motion.

The importance of the $J_i(\omega)$ is that expressions for T_1 and T_2 for two spin systems where only the dipole-dipole relaxation mechanism need be considered have been derived in terms of these quantities (Bloombergen 1948, Abragam 1961).

For the case of intramolecular dipole-dipole relaxation between like spins the expressions are

$$\text{IV-13 } 1/T_1 = 3/2 \gamma^4 \hbar^2 I\{I+1\} \{J_1(\omega) + J_2(2\omega)\}$$

$$\begin{aligned} \text{IV-14 } 1/T_2 &= \gamma^4 \hbar^2 I\{I+1\} \{3/8 J_0(0) + 15/4 J_1(\omega) \\ &+ 3/8 J_2(2\omega)\} \end{aligned}$$

If we make the assumption that the correlation functions can be written as in equation 11 then evaluating the spectral densities which are in the form of equation (12) we get for $I = 1/2$

$$\text{IV-15 } 1/T_1 = K \left\{ \tau_c / (1 + \omega_0^2 \tau_c^2) + 4 \tau_2 / (1 + 4 \omega_0^2 \tau_2^2) \right\}$$

$$\text{IV-16 } 1/T_2 = K/2 \left\{ 3 \tau_c + 5 \tau_c / (1 + \omega_0^2 \tau_c^2) + 2 \tau_2 / (1 + 4 \omega_0^2 \tau_2^2) \right\}$$

$$\text{where } K = 3 \gamma^4 \hbar^2 / 10 r^6$$

Some caution is necessary here. The equations (13) and (14) are gross simplifications valid for a system where only two spins are interacting and where motion is completely isotropic. The equations (15) and (16) introduce an assumption about the algebraic form of the correlation functions and are a pretty coarse approximation.

However equations (15) and (16) do point out some interesting differences between T_1 and T_2 and their relationship to the correlation time. Note that as the correlation time gets shorter (as it would when the temperature increased) that T_1 goes through a minimum and rises to a point where τ_c approaches 0. T_2 on the other hand is approximately constant when τ_c is long (motion is slow) and increases almost linearly as τ_c .

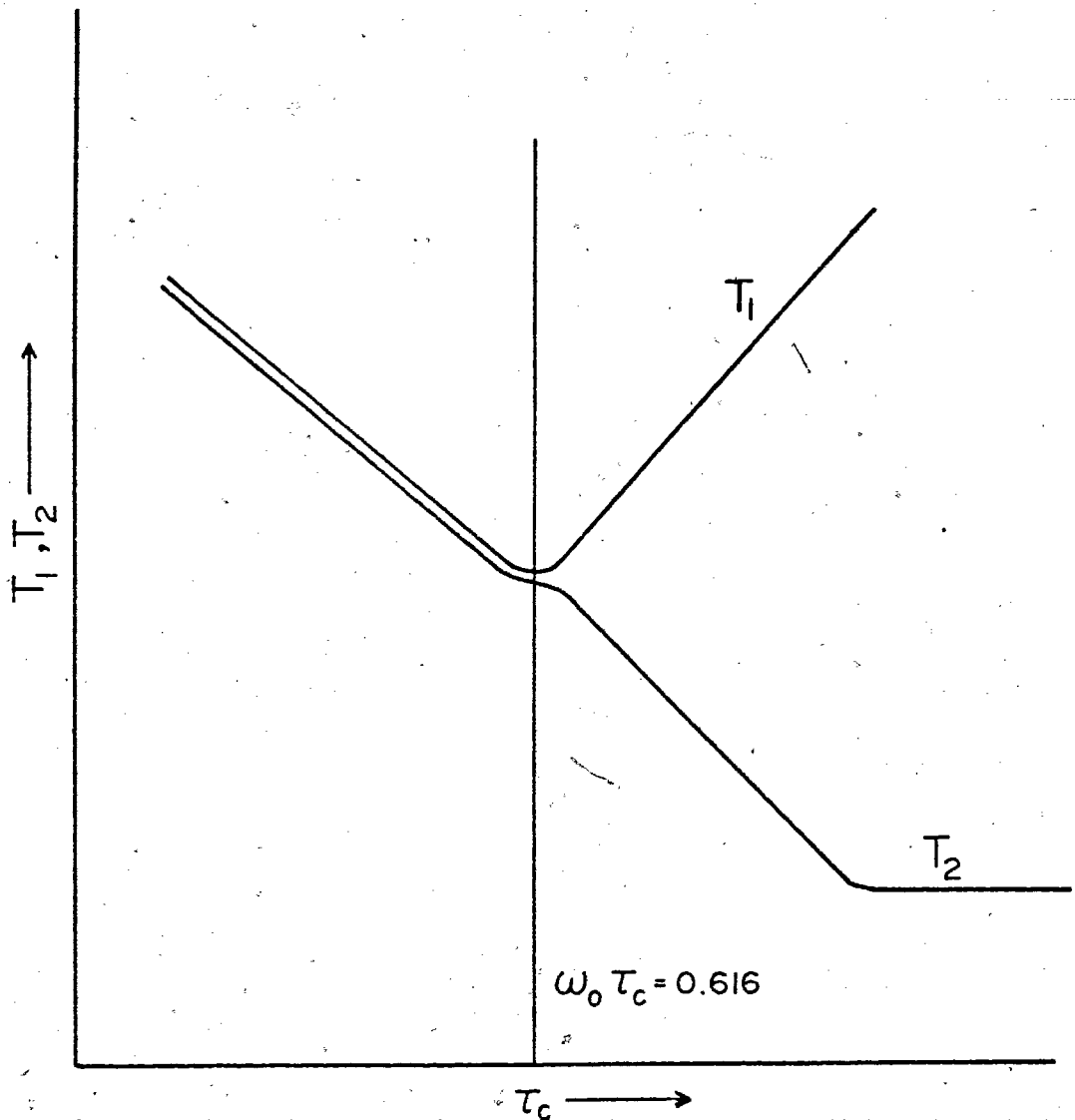


Figure IV - 1
Plots of the functions IV - 15 and IV - 16

gets shorter.

Plots of equations (15) and (16) are shown in figure IV-I. It can be noted that for this model the minimum in T_1 occurs when $\omega_0 \cdot \tau_c = .616$ and that the ratio of T_1 / T_2 at this point is 1.6, then if the data were to fit this model (τ_c can be varied by varying the temperature) then the correlation time would be known for these set of circumstances.

It should be stressed again that this model is simplistic in that (1) it is based on only 2 interacting spins, (2) the motion involved must be isotropic, (3) the motion is characterized by a single correlation time.

Such conditions are seldom found in surfaces where one expects and finds more than one correlation time or even a distribution of correlation times, where different correlation times may determine T_1 and T_2 where the motion is not necessarily isotropic on the average, and where we may want to look at systems more complicated than those where there are only 2 spins interacting.

Other Mechanisms of Relaxation

There are other possible couplings between a spin and its environment, and if these are modulated by some motion any of them can result in a relaxation mechanism.

A mechanism formally very similar to dipole-dipole relaxation is the coupling between a nuclear spin and an

electronic spin with a non-vanishing wave function at the nucleus. Such an interaction is ordinarily of larger magnitude than the Zeeman coupling between the nuclear moment and the applied field. Of greater interest in NMR is the case where there is a large electronic moment (unpaired spin) in the nearby environment such as the case of having paramagnetic impurities in a solution. In this case the coupling acts as a perturbation on the Zeeman levels as before, can cause transitions between levels, and thus relaxation.

A second important relaxation mechanism occurs when I is greater or equal to 1 and the nucleus has a quadrupole. The coupling between the quadrupole moment and electric field gradients results in a relaxation mechanism which when present usually dominates that of dipole-dipole relaxation.

Other mechanisms of interest include relaxation brought about when the electron shielding coefficient is a non-diagonal tensor, scalar couplings where one spin is coupled to another via the chemical bonds between them, and a spin rotation interaction with a coupling between the magnetic moment and the total angular momentum of the molecule.

It goes almost without saying that if one expects to get useful information from a system then either a method must be devised to separate the different relaxation

mechanisms, or the system must be chosen so that only one mechanism arises or totally dominates.

CHAPTER 5

The Theory of NMR and Relaxation Applied to Molecules
Adsorbed on Surfaces

Several reviews and many papers exist on applications of NMR to the study of species adsorbed on surfaces, and no attempt will be made here to summarize them. Review articles have been written by H. Winkler (1961), H. A. Resing (1968), K. J. Packer (1967), more recently by H. Pfeifer (1972), and again by Resing (1972).

One expects several changes in the relaxation mechanisms of molecules after they become adsorbed on a surface. The most obvious change is a result of a change of the motion in as much as there is some potential between the surface and the adsorbed species, and because motion may now be restricted to a plane or a "cave" as in a zeolite. One expects too that molecules that formerly rotated isotropically may now have a preferential axis of rotation. If the molecule in the bulk phase relaxed through some intermolecular dipole-dipole mechanism then one would expect this to be severely altered on a surface, the relaxation in this case becoming coverage dependent. One would expect relaxation caused by dipole dipole interactions with magnetic dipoles associated with the surface, as for example with hydroxyls on an oxide surface. Obviously a surface could enhance relaxation if it

contained paramagnetic species.

Since molecules can still rotate on the surface one expects intramolecular dipole-dipole mechanisms to be important, although the formalisms of such will be different than in solutions since one no longer has an isotropic medium, and certain motions may no longer take place.

Most of the work done to date has involved the assumption that relaxation is through intramolecular dipole-dipole coupling (Pfeiffer 1971). We shall consider some ways of examining this assumption. Both intramolecular and intermolecular relaxation mechanisms involve a surface coverage dependence, the first because the "density" of coverage determines the kinds of motions allowable, the second for obvious reasons.

Differentiating Between Different Types of Dipole-Dipole Relaxation

It is completely feasible for the relaxation to be through different types of dipole dipole interactions. These may be:

- (1) intramolecular dipole-dipole
- (2) intermolecular dipole-dipole
- (3) interaction with surface dipoles (a particular case of 2)
- (4) interaction with surface electron paramagnetic

species.

One can differentiate between these possible mechanisms as follows. If the system being investigated is one containing protons then comparison between the relaxation rates of the normal molecule to a sample prepared with a partially deuterated species will separate the first two mechanisms from the last two. Partial deuteration will not change the fraction of protons interacting with either surface hydroxyls or paramagnetic centers. No change in the relaxation rate suggests mechanism (3) or (4) predominates. These two may be separated by looking at relaxation on a surface that has been deuterated. One can of course choose a system where mechanism four is of no importance. However, it may be treated theoretically (Packer 1967).

If a molecule is relaxing by means of an intramolecular dipole-dipole mechanism then one expects no change in the relaxation time between a sample composed of a mixture of fully deuterated and undeuterated adsorbate species. A change in relaxation times implies an intermolecular interaction. It is obvious that one needs to be careful that exchange does not occur between the hydrogens and deuteriums of the species adsorbed, since in this case an intramolecular process will also change the relaxation times.

On any heterogeneous surface there is the possibility

of multiphase behaviour. That is molecules may be adsorbed on one type of site which causes different relaxation behaviour from another type of site. In this case one would expect to measure different relaxation times if the sites exhibited different chemical shifts, or a relaxation curve which was the sum of 2 (or more) exponentials if the sites exhibited the same chemical shift. Analysis of systems that exhibit multiphase behaviour can give information about the populations of both sites and the activation energies involved in transfer from one phase to another. The situation has been treated theoretically by Zimmerman and Brittin (Zimmerman 1957b), Woessner and Zimmerman (Woessner 1963b), and Woessner (1961).

Analysis of such systems depends on data which allow for the deconvolution of two Lorentzians (or more) superimposed on each other, or equivalently two superimposed exponential curves. Since one can always expect a better fit by doubling the parameters in a least squares problem one needs a good statistical argument to convince oneself that the deconvolution is real.

The only systems treated in this manner have large surface areas and usually large coverages; such systems as water on silica gel (Woessner 1963) or benzene on silica gel (Woessner 1966). The reader is referred to the review by Pfeifer (1971) for a further analysis.

A Model for Intra-Molecular Relaxation of Surface Species

Even if translational diffusion is a major mechanism of relaxation in the bulk phase, it may be expected to be of lesser importance on a surface especially at low coverage since the interaction still depends on an r^{-6} term.

The large majority of work published assumes that intramolecular relaxation is the only mechanism involved (Packer 1967).

The following is a model for intramolecular relaxation which allows one to account for the changes in molecular motion expected when the molecule becomes adsorbed on a surface.

Analysis of the relaxation is dependent on knowledge of the spectral density which in turn depends on the correlation function of the spherical harmonics of rank 2. However the F_i are known explicitly only in a molecule fixed frame. For consideration of relaxation on a surface one needs to know these functions in a frame fixed to the surface.

Such a transformation has been carried out by Woessner and Zimmerman (Woessner 1962) from trigonometric considerations, and has been extended (Woessner 1966) to allow for motion about a symmetry axis while the symmetry

axis moves in relation to a surface normal. This extension is extremely cumbersome and has only been carried out for systems where $\omega \tau \ll 1$ (systems where the $J_i(\omega)$ are independent of ω).

This assumption does not hold for a system near the point where T_1 passes through a minimum (see Figure 1, Chapter IV).

The correlation functions $\langle F^*(t+\tau) \cdot F(t) \rangle$ as written in Chapter IV have arguments θ and ϕ which are the longitudinal and azimuthal angles which the vector r_{ij} makes with the magnetic field H_0 , that is they are given in the lab fixed frame. As stated above one only knows these functions explicitly in the molecule fixed frame (Huntress 1968).

An expression is derived herein by using the Wigner rotation matrices $D_{M'M}^J$ (Rose 1957). The result is a completely general expression capable of describing many different motions on the surface and which has the advantage over Woessner's transformation (Woessner 1966) in that all $J_i(\omega)$ are derived simultaneously.

The transformation is carried out on the function in the molecule fixed frame, carrying these first into a rotational axis fixed frame, then to a surface fixed frame, and finally to the lab fixed frame.

In the molecule fixed frame we can place the molecule in any manner that is convenient. θ and ϕ describe

the longitudinal and azimuthal angles of r_{ij} with this frame. $Y_{2M}(\theta\phi)$ when translated to the lab fixed frame will describe the interaction between the two dipoles. Because we would like to consider motion about several different axes of rotation we translate first to an "axis of rotation" fixed axis system.

The spherical harmonics in this coordinate system are found from the expression:

$$V-1 \quad Y_{2M_2}(\theta_2\phi_2) = \sum_{M_1} D_{M_1 M_2}^2(\alpha, \beta, \delta_1) Y_{2M_1}(\theta\phi)$$

where the $D_{M' M}^2(\alpha, \beta, \delta_1)$ is the second rank Wigner rotation matrix in arguments $\alpha(1)$, $\beta(1)$, $\gamma(1)$, and where the angles are the Euler angles between the molecule fixed frame and the rotational axis fixed frame.

The Euler angles used are shown in Figure V-1. $D_{M' M}^2$ is given in Table V-1, and was derived from the relationship (Rose 1957):

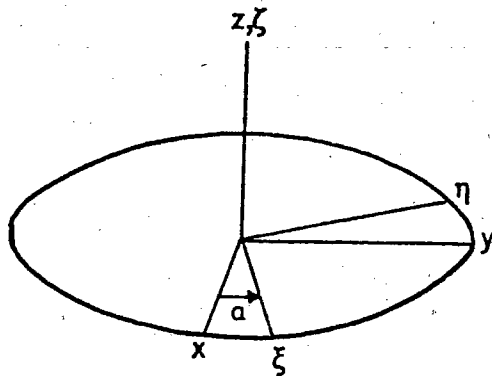
$$D_{M M'}^J = \sum_t (-1)^t \frac{\sqrt{(J+M)!(J-M)!(J+M')!(J-M')!}}{(J+M-t)!(J-M-t)!(t)!(t-M+M')!} (\cos\theta/2)^A (\sin\theta/2)^B$$

$$A = 2J + M - M' - 2t \quad B = 2t - M + M'$$

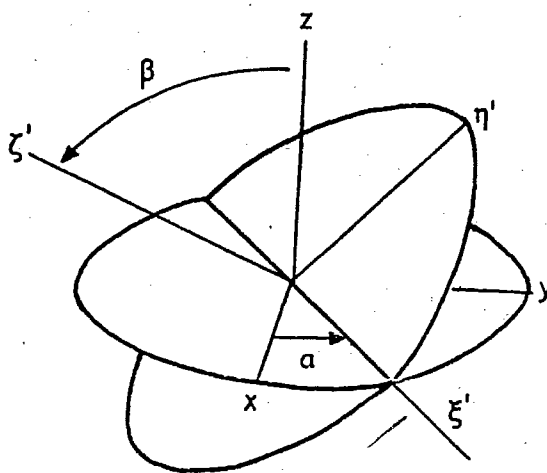
This new set of spherical harmonics is now translated to a surface fixed frame where one axis is the normal to the surface. The random functions in this frame become:

$$V-2 \quad Y_{2M_3}(\theta_3\phi_3) = \sum_{M_2} D_{M_2 M_3}^2(\alpha, \beta, \delta_2) \sum_{M_1} D_{M_1 M_2}^2(\alpha, \beta, \delta_1) Y_{2M_1}(\theta\phi)$$

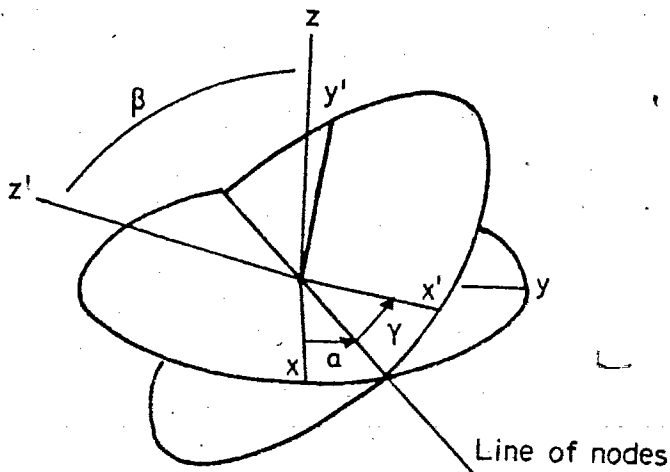
where $\alpha(2)$ $\beta(2)$ $\gamma(2)$ are the Euler angles



(a)



(b)



(c)

Figure V - 1
The Euler angles alpha, beta, gamma.

5

5

$M' \backslash M$	$M=2$	$M=1$	$M=0$	$M=-1$	$M=-2$
$M'=2$	$\frac{1}{4}(1+\cos\beta)^2 e^{-2ia} e^{2iy}$	$-\frac{1}{2}\sin\beta(1+\cos\beta) e^{2ia} e^{-iy}$	$\frac{\sqrt{6}}{4}\sin^2\beta e^{-2ia}$	$-\frac{1}{2}\sin\beta(1-\cos\beta) e^{-2ia} e^{iy}$	$\frac{1}{4}(1-\cos\beta)^2 e^{-2ia} e^{2iy}$
$M'=1$	$\frac{1}{2}\sin\beta(1+\cos\beta) e^{-ia} e^{-2iy}$	$\frac{1}{2}(\cos^2\beta - \sin^2\beta - \cos\beta) e^{-ia} e^{-iy}$	$-\frac{\sqrt{6}}{2}\sin\beta\cos\beta e^{-ia}$	$\frac{1}{2}(\sin^2\beta - \cos^2\beta + \cos\beta) e^{-ia} e^{iy}$	$-\frac{1}{2}\sin\beta(1-\cos\beta) e^{-ia} e^{2iy}$
$M'=0$	$\frac{\sqrt{6}}{4}\sin^2\beta e^{-2iy}$	$+\frac{\sqrt{6}}{2}\sin\beta\cos\beta e^{-iy}$	$\frac{1}{2}(3\cos^2\beta - 1) e^0$	$-\frac{\sqrt{6}}{2}\cos\beta\sin\beta e^{iy}$	$\frac{\sqrt{6}}{4}\sin^2\beta e^{2iy}$
$M'=-1$	$\frac{1}{2}\sin\beta(1-\cos\beta) e^{ia} e^{-2iy}$	$\frac{1}{2}(\sin^2\beta - \cos^2\beta + \cos\beta) e^{ia} e^{-iy}$	$\frac{\sqrt{6}}{2}\sin\beta\cos\beta e^{ia}$	$\frac{1}{2}(\cos^2\beta - \sin^2\beta - \cos\beta) e^{ia} e^{iy}$	$-\frac{1}{2}\sin\beta(1+\cos\beta) e^{ia} e^{2iy}$
$M'=-2$	$\frac{1}{4}(1-\cos\beta)^2 e^{2ia} e^{-2iy}$	$+\frac{1}{2}\sin\beta(1-\cos\beta) e^{2ia} e^{-iy}$	$\frac{\sqrt{6}}{4}\sin\beta e^{2ia} e^{iy}$	$\frac{1}{2}\sin\beta(1+\cos\beta) e^{2ia} e^{iy}$	$\frac{1}{4}(1+\cos\beta)^2 e^{2ia} e^{2iy}$

Table V-1 The Wigner rotational tensor of rank 2

between the rotational axis fixed frame and the surface fixed frame.

Finally we need to translate to the lab fixed frame where one axis is fixed by the magnetic field H_0 . The random functions become:

$$V-3 \quad Y_{2M_4}(\theta_4, \phi_4) = \sum_{M_3} D_{M_3, M_4}^2(\alpha_3, \beta_3, \gamma_3) \sum_{M_2} D_{M_2, M_3}^2(\alpha_2, \beta_2, \gamma_2) \sum_{M_1} D_{M_1, M_2}^2(\alpha_1, \beta_1, \gamma_1) Y_{2M_1}(\theta, \phi)$$

To form the correlation functions describing the motion one forms expressions which are complex conjugates of (1), (2), and (3), but with Euler angles taken at times $t+\tau$. This means that the motion will be carried in the Wigner matrices. However we do not want any motion in $\alpha(3)$, $\beta(3)$ and $\gamma(3)$ (the angles between the surface fixed frame and the lab fixed frame) and furthermore want all $\alpha(3)$, $\beta(3)$ and $\gamma(3)$ to be allowed as there are all orientations of surfaces in the lab frame.

Taking advantage of the relation: (Rose 1957)

$$V-4 \quad \frac{1}{8\pi} \int_{\text{all space}} D_{MM'}^J D_{M''M'''}^{J*} d\Omega = \frac{1}{(2J+1)} \delta_{MM''} \delta_{M'M'''}$$

one ends up with 5 correlation functions of the form:

$$V-5 \quad \frac{1}{5} \langle Y_{2M}(\theta_3, \phi_3) Y_{2M'}^*(\theta_3', \phi_3') \rangle \delta_{MM'}$$

but this collapses to the normal 3 functions since:

$$V-6 \quad \langle Y_{2M}(\theta, \phi) Y_{2M'}^*(\theta', \phi') \rangle = \langle Y_{2-M}(\theta, \phi) Y_{2-M}^*(\theta', \phi') \rangle$$

In writing expression 5 with the Kroneker delta one is assuming that no cross correlation terms exist, that is the average value of the component of one random function on another is equal to zero.

The explicit functions described by 5 are:

$$\begin{aligned}
 \text{V-7} \quad & \langle Y_{2M}(\theta_3 \phi_3) Y_{2M}^*(\theta_3' \phi_3') \rangle \\
 & = \{ \langle D_{2M}^2(\alpha_2 \beta_2 \gamma_2) D_{2M}^{2*}(\alpha_2' \beta_2' \gamma_2') \rangle + \langle D_{-2M}^2(\alpha_2 \beta_2 \gamma_2) D_{-2M}^{2*}(\alpha_2' \beta_2' \gamma_2') \rangle \} \\
 & \cdot \langle Y_{22}(\theta_2 \phi_2) Y_{22}^*(\theta_2' \phi_2') \rangle \\
 & + \{ \langle D_{1M}^2(\alpha_2 \beta_2 \gamma_2) D_{1M}^{2*}(\alpha_2' \beta_2' \gamma_2') \rangle + \langle D_{-1M}^2(\alpha_2 \beta_2 \gamma_2) D_{-1M}^{2*}(\alpha_2' \beta_2' \gamma_2') \rangle \} \\
 & \cdot \langle Y_{21}(\theta_2 \phi_2) Y_{21}^*(\theta_2' \phi_2') \rangle \\
 & + \langle D_{0M}^2(\alpha_2 \beta_2 \gamma_2) D_{0M}^{2*}(\alpha_2' \beta_2' \gamma_2') \rangle \cdot \langle Y_{20}(\theta_2 \phi_2) Y_{20}^*(\theta_2' \phi_2') \rangle
 \end{aligned}$$

where $M = 0, 1, \text{ and } 2$. Each of the terms in $\theta_2(2)$ and $\phi_2(2)$ are formed from an expression exactly analogous to (7) but with the arguments of the D 's in $\alpha_2(1)$, $\beta_2(1)$ and $\gamma_2(1)$, and the arguments of the Y 's in θ_2 and ϕ_2 (which are of course time independent).

The motions are carried in the two sets of Wigner matrices. Motions in $\alpha_2(1)$, $\beta_2(1)$ and $\gamma_2(1)$ can describe rotations about any axis by suitable arrangement of the molecule in the molecule fixed frame. Motions in $\alpha_2(2)$, $\beta_2(2)$, $\gamma_2(2)$ describe the motion of this rotation axis in relation to the surface normal.

The complete transformation is represented graphically in figure V-2

A major problem in relaxation analysis is to

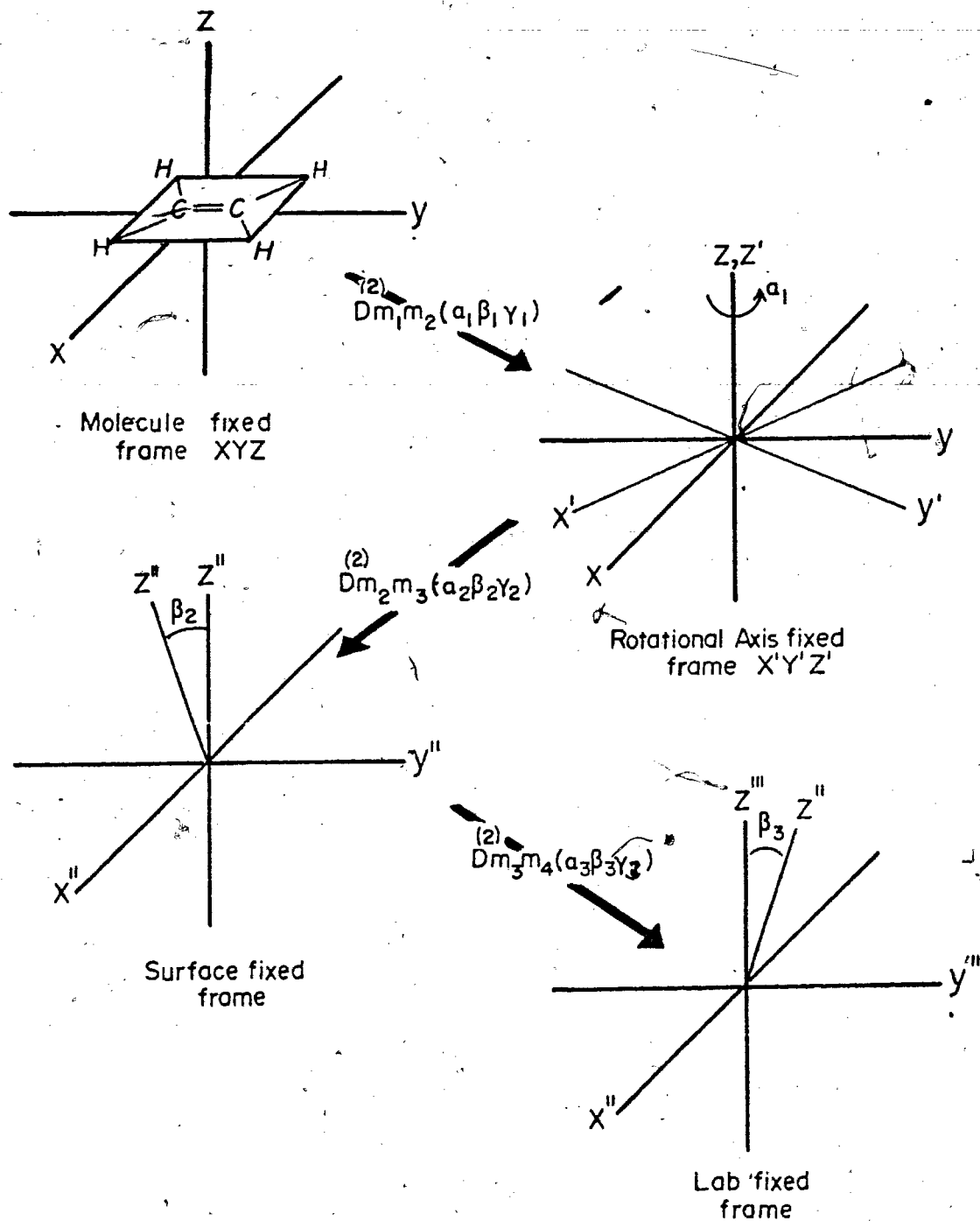


Figure V - 2

The complete transformation.

determine the exact form of the correlation functions. Woessner has derived an expression for these functions for ellipsoids undergoing Brownian motion (Woessner 1962b) based on work of Perrin (Perrin 1934). Huntress has derived a similar expression (Huntress 1968) based on the work of Favro (Favro 1960) and has included expressions for other kinds of relaxation mechanism involving anisotropic reorientation. Both of these models involve the assumption of a continuous isotropic medium. The more difficult case where the medium is anisotropic, i.e. where the frictional constant is replaced by a frictional tensor of rank two has been dealt with (Steele 1963a, b, c) but the problem seems incapable of solution for the general case of an asymmetric top.

At the same time there are a number of naive assumptions that one can make about the form of those functions. Often the assumption is made that the correlation function is of the form $\exp(t/\tau_c)$ (Abragam 1961, Bloombergen, Purcell and Pound 1948). This means that for sufficiently long tau the correlation function approaches zero, that is on the average there is no relationship between the vector r_{ij} at time t and at time t+tau as tau approaches infinity.

In using a correlation function in this form one is assuming a stochastic diffusion process and is depending on the interruption of the motion by collisional or other

processes, since if the motion simply continued then the correlation function would not decay with time.

A more complete derivation of this form of the correlation function may be found in Hertz (1967), where he points out an exact solution for the rotation of a spherical molecule having this form, but reminds one that τ is the time constant which "characterizes the time dependence of the correlation function" not the time dependence of the system.

The work of Woessner and Zimmerman (Woessner 1963) and Woessner (1962a) involves a stochastic diffusion process describing motion among a large number of equilibrium positions. The results of this model are that average values of the form:

$$\langle \exp(i\alpha) \exp(-i\alpha') \rangle$$

are equal to $\exp(-\tau/\tau_\alpha)$;

those of the form:

$$\langle \exp(i2\alpha) \exp(-i2\alpha') \rangle$$

are equal to $\exp(-4\tau/\tau_\alpha)$; and the average values in arguments of the longitudinal angles are equal to the average value of the square of the function times $\exp(-\tau/\tau_\alpha)$.

It must be emphasized at this point that motions in α (1) (rotations about a symmetry axis) must not be

correlated with the motion of the axis. It should also be pointed out that each of the transformations carried out which has time dependence in it leads to $2M+1 = 5$ correlation times. In practice one is unlikely to be able to separate these, and it is a realistic assumption to make the time constant for motions of beta in each D_{MN}^J equal, and the time constant for motion in alpha for each equal, although tau (alpha 2) would not likely equal tau (alpha 1) of course. If one uses the assumptions outlined above in equation 7, the result can then be evaluated explicitly. The reader is reminded that the correlation function given in equation 8 are in the surface fixed frame and are multiplied by 1/5 to bring them to the lab fixed frame.

$$\begin{aligned}
 \text{V-8a} \quad \langle Y_{20}(t) Y_{20}^*(t+\tau) \rangle &= 3/4 \langle \sin^4 \beta_2 \rangle \langle Y_{22}(\theta_2 \phi_2) Y_{22}^*(\theta_2' \phi_2') \rangle \\
 &\exp(-4\tau/\tau_{\alpha_2}) \exp(-\tau/\tau_{\beta_2}) \\
 &+ 3 \langle \sin^2 \beta_2 \cos^2 \beta_2 \rangle \langle Y_{21}(\theta_2 \phi_2) Y_{21}^*(\theta_2' \phi_2') \rangle \\
 &\exp(-\tau/\tau_{\alpha_2}) \exp(-\tau/\tau_{\beta_2}) \\
 &+ 1/4 \langle (3 \cos \beta_2 - 1)^2 \rangle \langle Y_{20}(\theta_2 \phi_2) Y_{20}^*(\theta_2' \phi_2') \rangle \exp(-\tau/\tau_{\beta_2})
 \end{aligned}$$

$$\begin{aligned}
 \text{V-8b} \quad \langle Y_{21}(t) Y_{21}^*(t+\tau) \rangle &= \{ 1/4 \langle \sin^2 \beta_2 (1 + \cos \beta_2)^2 \rangle \\
 &+ 1/4 \langle \sin^2 \beta_2 (-\cos \beta_2)^2 \rangle \} \langle Y_{22}(\theta_2 \phi_2) Y_{22}^*(\theta_2' \phi_2') \rangle \\
 &\exp(-4\tau/\tau_{\alpha_2}) \exp(-\tau/\tau_{\beta_2}) \\
 &+ \{ 1/4 \langle (\cos^2 \beta_2 - \sin^2 \beta_2 - \cos \beta_2)^2 \rangle + 1/4 \langle (\sin^2 \beta_2 - \cos \beta_2^2 + \cos \beta_2)^2 \rangle \} \\
 &\langle Y_{21}(\theta_2 \phi_2) Y_{21}^*(\theta_2' \phi_2') \rangle \exp(-\tau/\tau_{\alpha_2}) \exp(-\tau/\tau_{\beta_2}) \\
 &+ 3/2 \langle \sin^2 \beta_2 \cos^2 \beta_2 \rangle \langle Y_{20}(\theta_2 \phi_2) Y_{20}^*(\theta_2' \phi_2') \rangle \exp(-\tau/\tau_{\beta_2})
 \end{aligned}$$

$$\begin{aligned}
 V-8c \quad \langle Y_{22}(t) Y_{22}^*(t+\tau) \rangle &= \{ 1/16 \langle (1 + \cos \theta_2)^4 \rangle \\
 &+ 1/16 \langle (1 - \cos \theta_2)^4 \rangle \} \langle Y_{22}(\theta_2 \phi_2) Y_{22}^*(\theta_2' \phi_2') \rangle \exp(-4\tau/\tau_{\theta_2}) \\
 &\exp(-\tau/\tau_{\beta_2}) \\
 &+ \{ 1/4 \langle \sin^2 \theta_2 (1 + \cos \theta_2)^2 \rangle + 1/4 \langle \sin^2 \theta_2 (1 - \cos \theta_2)^2 \rangle \} \\
 &\langle Y_{21}(\theta_2 \phi_2) Y_{21}(\theta_2' \phi_2') \rangle \exp(-\tau/\tau_{\theta_2}) \exp(-\tau/\tau_{\alpha_1}) \\
 &+ 3/8 \langle \sin^4 \theta_2 \rangle \langle Y_{20}(\theta_2 \phi_2) Y_{20}^*(\theta_2' \phi_2') \rangle \exp(-\tau/\tau_{\beta_2})
 \end{aligned}$$

where:

$$\begin{aligned}
 V-9a \quad \langle Y_{20}(\theta_2 \phi_2) Y_{20}(\theta_2' \phi_2') \rangle &= 3/4 \langle \sin^4 \theta_2 \rangle \sin^4 \theta \exp(-\tau/\tau_{\theta_2}) \\
 &\exp(-\tau/\tau_{\alpha_1}) \\
 &+ 3 \langle \sin^2 \theta_2 \cos^2 \theta_2 \rangle \sin^2 \theta \cos^2 \theta \exp(-\tau/\tau_{\theta_2}) \\
 &\exp(-\tau/\tau_{\alpha_1}) \\
 &+ 1/4 \langle (3 \cos^2 \theta_2 - 1) \rangle (3 \cos^2 \theta - 1) \exp(-\tau/\tau_{\theta_2})
 \end{aligned}$$

$$\begin{aligned}
 V-9b \quad \langle Y_{21}(\theta_2 \phi_2) Y_{21}^*(\theta_2' \phi_2') \rangle &= \{ 1/4 \sin^2 \theta_2 (1 + \cos \theta_2)^2 \} \\
 &+ 1/4 \langle \sin^2 \theta_2 (1 - \cos \theta_2)^2 \rangle \} \sin^4 \theta \exp(-4\tau/\tau_{\theta_2}) \\
 &\exp(-\tau/\tau_{\alpha_1}) \\
 &+ \{ 1/4 \langle \cos^2 \theta_2 - \sin^2 \theta_2 - \cos \theta_2 \rangle + 1/4 \langle \sin^2 \theta_2 - \cos^2 \theta_2 + \cos \theta_2 \rangle \} \\
 &\sin^2 \theta \cos^2 \theta \exp(-\tau/\tau_{\theta_2}) \exp(-\tau/\tau_{\alpha_1}) \\
 &+ 3/2 \langle \sin^2 \theta_2 \cos^2 \theta_2 \rangle (3 \cos^2 \theta - 1) \exp(-\tau/\tau_{\theta_2})
 \end{aligned}$$

$$\begin{aligned}
 V-9c \quad \langle Y_{22}(\theta_2 \phi_2) Y_{22}^*(\theta_2' \phi_2') \rangle &= \{ 1/16 \langle (1 + \cos \theta_2)^4 \rangle \\
 &+ 1/16 \langle (1 - \cos \theta_2)^4 \rangle \} \sin^4 \theta \exp(-4\tau/\tau_{\theta_2}) \\
 &\exp(-\tau/\tau_{\alpha_1}) \\
 &+ \{ 1/4 \langle \sin^2 \theta_2 (1 + \cos \theta_2)^2 \rangle + \langle \sin^2 \theta_2 (1 - \cos \theta_2)^2 \rangle \} \\
 &\sin^2 \theta \cos^2 \theta \exp(-\tau/\tau_{\theta_2}) \exp(-\tau/\tau_{\alpha_1}) \\
 &+ 3/8 \langle \sin^4 \theta_2 \rangle (3 \cos^2 \theta - 1) \exp(-\tau/\tau_{\theta_2})
 \end{aligned}$$

If one sets up a rotation using a molecule fixed frame such that $\beta(1) = 0$, (and thus $\tau(\beta 1) = \text{infinity}$) then on substitution of equations 9 into 8 some interesting things become evident. Each of the correlation functions has a term depending only on $\tau(\beta 2)$ and other terms that depend on both $\tau(\beta 2)$, $\tau(\alpha 2)$ and $\tau(\alpha 1)$.

$\tau(\beta 2)$ is the time constant that describes the motion of a rotation axis about a surface normal, thus it could be used to describe a wobble as in Woessner's 1966 model. It is quite conceivable that such a time constant is longer than $\tau(\alpha 1)$ the time constant for a rotation about this symmetry or rotational axis.

Since $1/T_1$ and $1/T_2$ will depend on the functions expressed in 8 and 9 through the relationships given in Chapter IV one now expects that a graph in $\ln T_1$ versus $1/\text{Temperature}$ to be somewhat different than figure IV-1.

If we only consider rotation about a single symmetry axis then we are left with 3 correlation times. Each of these can be "frozen out" (had their effect minimized) by measuring T_1 and T_2 as a function of temperature. The graph of $\ln T_1$ versus $1/\text{temperature}$ would then have 3 minima, so long as the correlation times for each motion were significantly different. If rotations were energetically feasible about more than 1 symmetry axis and were at a different rate than the other rotations, then

one would expect a minimum for each of these.

Generally it is impossible to assign these minima to particular motions. One can only measure T_1 as a function of temperature, and if more than one minima exists, assign them to different motions in as logical a way as possible and then see if the measured relaxation times compare with those derived from the expressions of Chapter IV. The problem becomes an indeterminable one unless some other experiments are carried out which can back up these assignments.

chapter 6

Survey of Work Done on ZnO

Zinc oxide was first reported to function as a catalyst for olefin hydrogenation in 1940 (Woodman 1940). It is an interesting catalyst to study since, the kinetics of olefin hydrogenation over this catalyst are simpler than over metals (Dent 1969a), the oxide is confined to one oxidation state thus precluding reactions with rather than on the surface, it is transparent in the infra-red thus allowing for identification of surface species, it is diamagnetic thus allowing for simpler NMR studies, and finally it is now being manufactured commercially so that work being done in one lab is easier to correlate with work being done in another (if both use the same supplier).

The olefin, hydrogen, ZnO system has been studied by Pliskin et al. (Eichens 1962) using I.R., Kesauulu et al. (Naryana 1970) using conductivity measurements, Cvetanovic et al. (Baranski 1971) using Temperature Programmed Desorption (TPD), Teichner et al. (1963, 1967, 1968), using conventional kinetic methods, I.R. and conductivity and most thoroughly by Kokes and co-workers (1969, 1970, 1971, 1972) using I.R. conventional kinetic methods and a number of isotope experiments.

Teichner's studies were carried out at higher temperatures than Kokes and show a more complex system

than is in evidence at lower temperatures. The results summarized below are mostly those of Kokes and co-workers except where noted.

Zinc Oxide

Zinc oxide has a structure of alternating cation and anion layers in a hexagonal close packed manner (Wurtzite structure) (Krylov 1970). A model of a stoichiometric zinc oxide crystal is given by Dent (1969a, p. 3786). The $000\bar{1}$ plane is seen as a layer of oxide ions in the same format as the 0001 plane, but spaced so that the zinc is only .53 angstroms below the surface, and the spaces between the oxide spheres of radius .58 angstroms.

In practice ZnO is a metal excess n type semiconductor. Doping with either electron acceptors or donors has no effect on its activity for hydrogenation (Gerscner 1963), suggesting that its catalytic properties for this reaction are not a function of the electronic structure of the solid. Taylor et al. (1954) and Teichner et al. (1963) both observed oxygen poisoning and concluded that the activity was a function of non-stoichiometry (i.e. the deficiency of oxygen); a conclusion inconsistent with the doping experiments.

A large amount has been written in regards to correlating the activity of catalysts to the number of d electrons (Clark 1970, Krylov 1970). Such correlations

have not shed much light on olefin hydrogenation over oxides, where good catalysts have been found with structures from d^0 (alumina) to d^{10} (ZnO).

Hydrogen Adsorption on ZnO

At ambient temperatures Kokes et al. (1969a) found two types of hydrogen chemisorption on ZnO. The first is adsorbed rapidly, can be removed by pumping and covers about 5% of the surface (Kokes used Kadox 25 supplied by the New Jersey Zinc Company which has a surface area of 8 - 10 $m^2/gm.$) independent of the amount of the second kind of hydrogen. The second type of hydrogen goes on more slowly (but the first of it may be rapid) and can not be removed by pumping except at elevated temperatures.

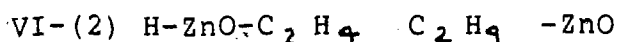
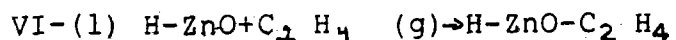
Only type I hydrogen gives rise to bands in the IR. Kokes concludes from his studies that type I chemisorption is a heterolytic cleavage forming an O-H and a Zn-H on the surface. He terms the active Zn-O site an acid base pair and uses this concept in interpreting much of his work. He found that the type II chemisorption does not enter into the hydrogenation at room temperature. Kokes also found that type I chemisorption was not poisoned by oxygen and that the oxide was still active even if prepared in such a way as to make it stoichiometric. However type I chemisorption and hydrogenation of olefins is poisoned by water leading to the conclusion that the previous

observations of oxygen poisoning were observations of a reaction of oxygen with surface hydrogen blocking type 1 sites.

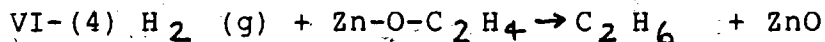
Ethylene on ZnO and its Reaction with Hydrogen

The heat of adsorption of ethylene on ZnO is about 14 kcal/mole vs. 3.2 kcal/mole for its heat of vaporization, suggesting that ethylene is indeed weakly chemisorbed onto the surface. (The heat of adsorption for ethane on ZnO is approximately 5 kcal/mole and its heat of vapourization is 3.5 kcal/mole suggesting that ethane is physisorbed on ZnO.)

One can picture the following set of reactions between ethylene and a zinc oxide surface previously treated with hydrogen.

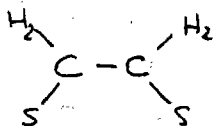


There are a multitude of questions involved in such a picture. One would like to know the nature of the bonding associated with reaction (1) and (2) and the nature of the hydrogen in reactions (2) and (3). There are other possibilities such as simultaneous transfer of two hydrogens onto a C_2H_4 as in a Rideal mechanism (Rideal 1938).

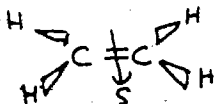


One would also like to know if the reactions are in fact reversible at the temperatures of interest, and to know if there are other reactions other than those depicted above. Kokes' studies reveal that the ethylene is adsorbed on some site different than the type 1 Hydrogen since ethylene adsorption is not poisoned by water. (The ethylene I. R. spectra did not change significantly on a catalyst treated with water, while the I. R. spectra of type 1 hydrogen was unobservable under such conditions.)

From I. R. studies it is evident that the ethylene double bond is not broken in the adsorbed species excluding species such as:



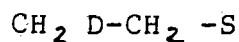
Kokes concludes that the ethylene is bonded as a pi complex vis:



Although there are no firm grounds to conclude what kind of site S is, Kokes suggests that it is an O^- . He bases his conclusion firstly on his model of ZnO which has the Zn^{++} sequestered between 3 O^- sites thus causing steric hindrance for a pi bond to interact with a Zn^{++} ,

and the fact that the spectrum of deuterium and ethylene adsorbed on ZnO in each other's presence shows no change for the Zn-D band intensity, while the O-D band drops to about 60% of its normal value for that concentration.

Upon admitting a small amount of D_2 to ethylene adsorbed on the oxide surface a single band appears in the C-D paraffinic stretching region (suggesting a monodeutero species) and the double bond stretch (at 1600 cm^{-1}) reduces in intensity or disappears. Kokes concludes that an ethyl species is formed as in reaction (2), vis.

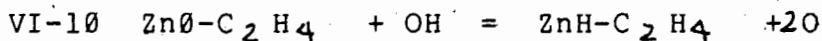
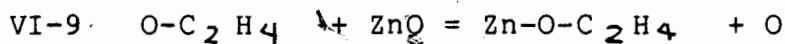
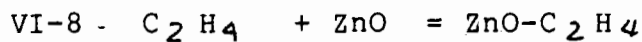
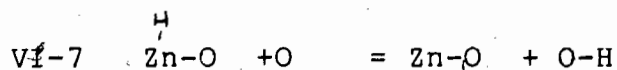
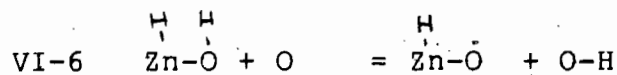
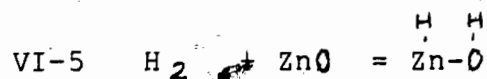


He also concludes that S here is a Zinc ion, steric hindrance being of less importance for the more directional sigma bond.

The product formed on deuteration of ethylene over ZnO is only $C_2H_4D_2$ leading one to the conclusion that reaction VI-2 is not reversible. (A reaction similar to VI-2 over metals is reversible since deuteration of ethylene over metals leads to a distribution of products of the form $C_2H_{(6-x)}D_x$ (Bond 1962).) The formation of an ethyl complex rejects the idea of a Rideal mechanism (reaction VI-4). Support for this rejection also comes from the fact that no hydrogenation occurs when the surface is poisoned by water despite the fact that the amount of ethylene adsorbed and the ethylene

I. R. spectrum is unchanged, on a ZnO surface so poisoned.

Several other processes may also be occurring on the surface.



where the O are surface oxygen species. Equation 5 represents the adsorption of type 1 hydrogen as discussed before. Equation 9 and VI-1 represent adsorption of the ethylene. Equations 6, 7, 9 and 10 represent surface diffusion of the ethylene and hydrogen.

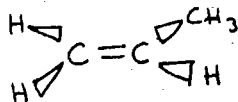
Propene and the Butenes on ZnO

There are at least two different species of propene on ZnO, a fact easily verified since evacuation of the gas from the surface at room temperature leaves about .37 std cm³/gm of propene on the surface (Kadox 25) and this is not removed until the surface is heated to about 125 degrees C.

The complete analysis of this system including analysis of the species $\text{CH}_3-\text{CH}-\text{CD}_2$, $\text{CD}_3-\text{CH}=\text{CH}_2$, $\text{CH}_3-\text{CD}=\text{CD}_2$, $\text{CD}_3-\text{CH}=\text{CD}_2$, $\text{CD}_3-\text{CD}=\text{CD}_2$ has also been done by Dent and Kokes (1970).

The relevant conclusions are that;

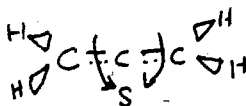
(1) The weakly bonded species is bonded to the surface as a pi complex comparable to the ethylene system, vis;



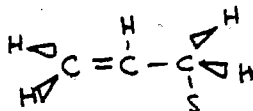
(2) The strongly bonded propene adsorbs dissociatively forming an adsorbed complex and an OH (or OD) species.

(3) The hydrogen-carbon bond broken was a methyl hydrogen.

(4) The strongly adsorbed complex is a pi-allyl species vis:



rather than the system:



(5) Kokes speculates that the adsorption site S for the pi-allyl species is a Zinc ion.

(6) He points out that the pi allyl species would be almost immobile on the surface.

ZnO also acts as a catalyst for butene isomerization. Again two species are formed on adsorption which Kokes et

al. (1971) conclude are a pi species and a pi allyl species. They conclude that isomerization occurs with the pi allyl species probably acting as an intermediate with cis-trans and double bond migration taking place simultaneously, i.e. the cis - trans isomerization does not involve but-1-ene as an intermediate.

Chapter 7

Adsorption Studies and Experimental Methods

The catalyst of main interest in this study was Zinc oxide provided by the New Jersey Zinc Company and labelled Kadox 25. In order to better characterize the surface some standard adsorption studies were done.

To begin with the surface area was measured to find the effect of different methods of preparation. Areas were determined using the BET method (equation II-6). Nitrogen gas was used as the adsorbate with the standard assumption that the cross sectional area of a nitrogen molecule is 16.2 square angstroms (Young 1962).

The area of the ZnO after outgassing at 150 degrees C for 48 hours was found to be 10 ± 1 square meters /gram.

The standard treatment used in these experiments was that of Kokes et al. (Dent 1969a) and was used so that these studies could be as closely correlated with theirs as possible.

The treatment consisted of evacuating the sample at 450 degrees C for 2 hours at a pressure of $< 10^{-5}$ torr, followed by heating in 160 torr of oxygen at 450 degrees C for a further 2 hours with a liquid nitrogen trap in the system; this followed by cooling and further evacuation at $P < 10^{-5}$ torr for one hour.

After such a treatment samples were found to have

areas ranging from 8.6 to 9.0 m²/gm. Repeated treatment did not subsequently lower the area substantially further. Samples were generally only treated once and then discarded.

The oxygen treatment was used to assure a stoichiometric ratio of zinc to oxygen. Treating the sample as above but omitting the oxygen treatment results in a much grayer powder, presumably an oxide with a stoichiometric excess of Zn.

The area following this second kind of treatment was not significantly different even if the evacuation was continued at 450 degrees for 2 days.

Treatment with hydrogen at elevated temperatures should further increase the stoichiometric excess of zinc. After outgassing a sample at 450 degrees C for 2 hours, and then heating in hydrogen for 2 hours at 450 degrees it was found that the area had decreased to < 3 m²/gm. Treating at only 300 degrees C in hydrogen did not reduce the area.

Adsorption Isotherms

The adsorption isotherms of C₂H₄ on ZnO were measured at 0 degrees C, 28 degrees C, 35 degrees C and 50 degrees C and are shown in figure VII-I.

Isosteres of the form log P versus 1/T were plotted from which one obtains the isosteric heats of adsorption

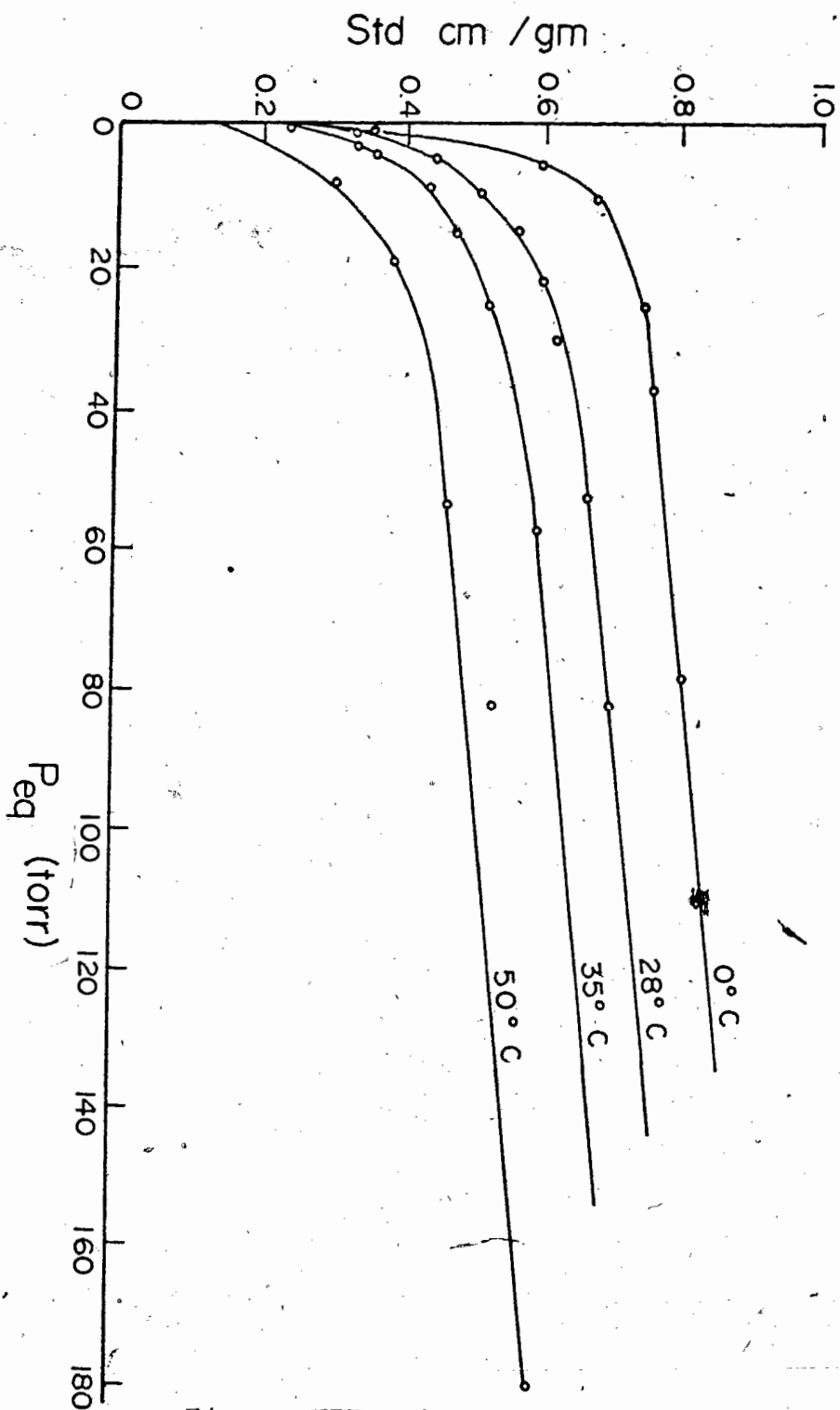


Figure VII - 1
The isotherms of ethylene adsorbed on ZnO

by using the Clausius-Clapeyron equation in the form

$$\text{VII-1 } d \ln p / d(1/T) = Q(\theta) / R$$

Isosteres are shown in Figure VII-2. The heats of adsorption calculated from these were 13.3 kcal/mole at a coverage of .25 std cm³/gram, 12.6 kcal/mole at a coverage of .4 std. cm³/gram and 14.5 kcal/mole at a coverage of .6 std cm³/gram, and 11.3 kcal/mole at a coverage of .7 std cm³/gm. These were not deemed to be significantly different. They do suggest however, that in this range of coverages that the surface is quite homotactic. The latter suggests that the adsorption is becoming more physical in nature, and indeed this coverage is past the area of the inflection of the isotherms.

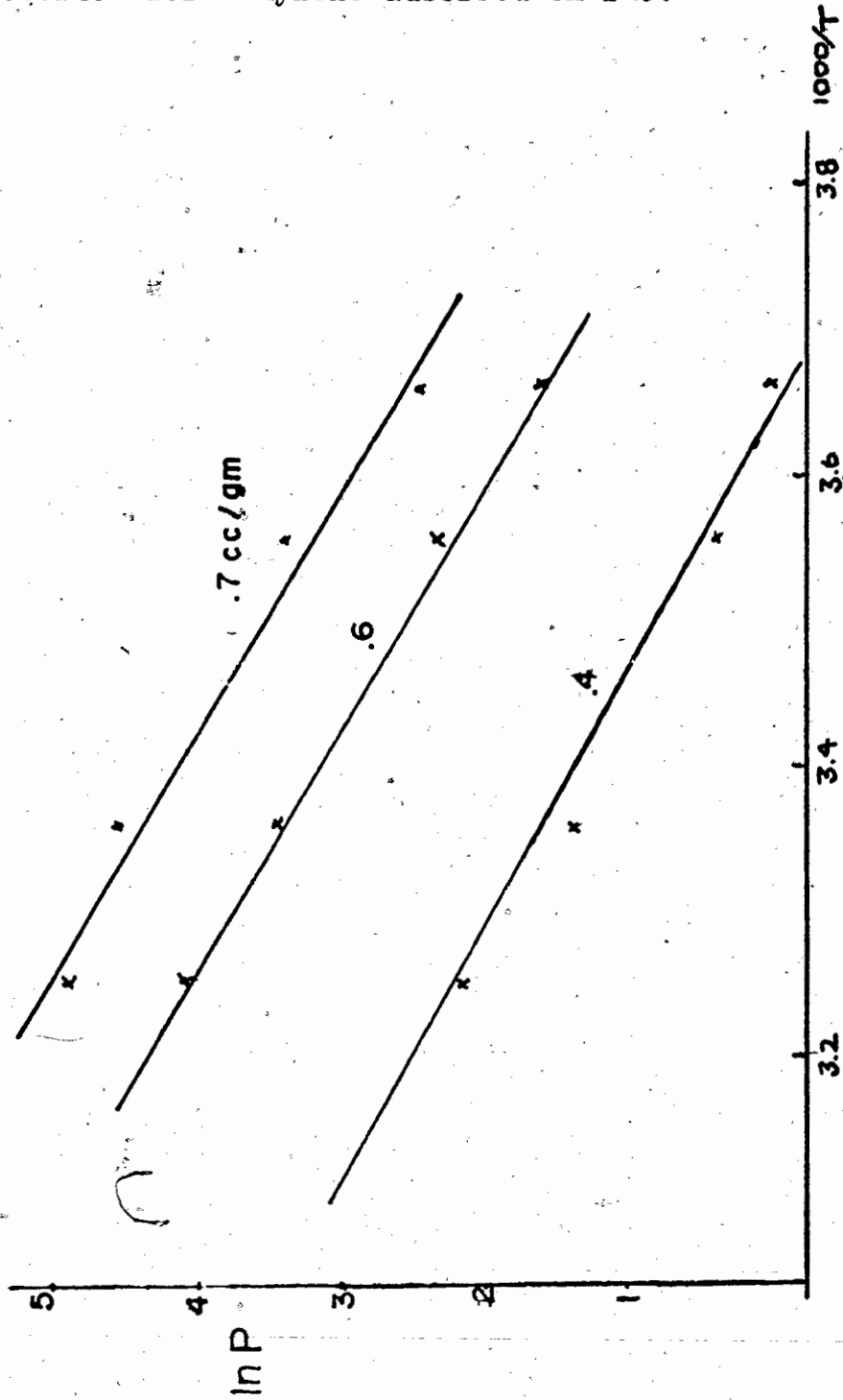
Isotherms for C H on the ZnO prepared without the oxygen treatment, or with the hydrogen treatment at 300 degrees C, were also measured, and did not differ significantly from those where the oxygen treatment had been used.

The area of an ethylene molecule was calculated, assuming a carbon-carbon bond length of 1.34 angstroms, a carbon-hydrogen bond length of 1.07 angstroms and a Van der Waals' radius of hydrogen of 1.2 angstroms, to be 21 square angstroms.

This meant that a statistical monolayer of ethylene on the zinc oxide used was equivalent to 1.58 std

Figure VII - 2

Isosteres for ethylene adsorbed on ZnO.



cm^3/gram . The inflection point on the C_2H_4 isotherm at room temperature is around $.6 \text{ std cm}^3/\text{gram}$, representing approximately $.4$ of a monolayer.

Sample Preparation; Errors and Precautions

Sample preparation was carried out with a rather conventional mercury diffusion vacuum line. The sample preparation area had a gas burette calibrated by weighing empty, and full of distilled water. The manometer was of the volume compensating type and allowed for a measureable change in volume of 30 cm^3 (60%). The manometer was mercury filled. A calibrated McLeod gauge was also used. Height differences in the manometer were measured with a cathetometer equipped with a vernier and accurate to $\pm .01$ mm. Pressure readings were then accurate to $\pm .02$ mm of Hg.

Volumes of those parts of the rack calibrated by helium expansion were accurate to $\pm .1\%$. Volumes of sample tubes were determined by helium expansion to $.2\%$. However, to save measuring the volume of each sample tube, several were manufactured at once with the same external dimensions, then the volume was measured by helium expansion. The difference was found to be within $.1 \text{ cm}^3$ which was taken as the error in measurement in subsequent calculations. This represented an error of $\pm 1\%$. The amount of gas adsorbed on a sample was calculated from the

pressure drop on allowing the gas into the sample tube containing the adsorbent. (All gases were assumed to be ideal.) Amounts of gas adsorbed were accurate from between 1% for low coverages ($.3 \text{ std cm}^3/\text{gram}$) to 10% for high coverages ($1.4 \text{ std cm}^3/\text{gram}$).

In preparing samples to find the relationship between T_1 , T_2 and temperature at constant coverage another source of uncertainty was involved. It was necessary to prepare a separate sample for each temperature. This involved not just knowing the amount adsorbed, but preparing each sample so they would have a set amount adsorbed at the desired temperature. It was found to be impractical to produce a set coverage to better than $\pm 5\%$, although at low coverages or low temperatures it was much easier and most were within $\pm 2\%$.

It should also be noted that the surface area was not measured for each individual sample since it is a reasonable assumption that as long as the treatment was the same there would be little variation in the area.

NMR Experimental Considerations

Both steady-state (frequency domain) and pulse (time domain) NMR measurements were done in this study.

Steady state measurements were done utilizing a Varian model XL-100 spectrometer operating at 100 MHz. It was employed in a fixed field, swept frequency mode. The

probe was a standard Varian V-4415 cross coil, equipped with a dewar for variable temperature experiments and allowing for 12 mm sample tubes. The temperature was controlled with a Varian temperature controller.

T_2 and chemical shift measurements were taken from XL-100 spectra. Measurements of T_2 were optimized by running the data into a model 1064 Fab-ri-Tek Instrument Computer, and then punching the digitized data out on paper tape. The paper tapes were then transcribed to magnetic tape using a PDP model 15 computer and a magnetic tape drive. The magnetic tapes were then used to read the data into an IBM 360/50 computer. By this method data could be fit by the method of least squares to functional expressions.

This whole process was not trivial, in fact I can only conclude that experiments involving so many steps should be avoided. Currently of course on line computers make such experiments infinitely easier.

T_2 's were found by least squares fitting the data to a Lorentzian, once the data were in the IBM 360/50.

Broadening of lines due to inhomogeneity of the field was minimized by carefully trimming up the field. This was done utilizing either a 5% solution of TMS in a 12 mm tube, or neat TMS in a coaxial capillary surrounded by ZnO. The second method was discontinued as it was felt that one was adjusting the homogeneity over only a small

diameter, whereas the desired measurement was being made over a larger diameter. However, there was no empirical evidence to suggest that one method was any better than the other, since there was no measurable difference between signals obtained with a sample spinning or not spinning in the field.

Care was taken to insure that the H_1 field would not saturate the sample. The power was turned down well below the point where it would visibly effect peak shape, and then the gain was increased to compensate. This of course led to a smaller signal/noise ratio. For some samples a comparison of the digitized data was made by calculating T_2 from the least square fit as a function of H_1 power, so as to determine the point that one was saturating the sample.

Time domain experiments were performed at 15 MHz using a system previously described (Collins 1973). The probe was home built and is a cross coil type with a dewared insert for variable temperature experiments.

Temperature studies at 15 MHz were a greater problem than at 100 MHz since the temperature controller was of much poorer quality. For frequency domain experiments, temperatures were usually kept within $\pm 1/2$ degrees C, although were considered to be within ± 1 degrees C. For the time domain experiments however the temperatures were difficult if not impossible to control within ± 2 degrees

C. Measurements were discarded if the temperature changed more than this amount, where it was important. As seen later the activation energies of the relaxation processes turn out to be of the order of 2 kcal/mole so that such temperature variation is not as significant as it might have been.

T_1 measurements were obtained by utilizing 180 degrees - tau - 90 degrees pulse trains. The averaged amplitude after a fixed number of spectra was measured as a function of tau and then these amplitudes were least squares fit to the expression

$$\text{VII-2 } \ln\{A(0) - A(t)\} = \ln 2A(0) - t/T_1$$

which follows from the expression (see equation III-28)

$$\text{VII-3 } A(t) = A(0) (1 - 2\exp(-t/T_1))$$

Toward the end of these studies a new Nicolet model 1080 instrument computer enabled one to make on line fourier transforms of free induction decays. This enabled one to measure the area of a fourier transformed free induction decay as a function of tau in a 180 - tau - 90 experiment. However, this was not deemed significantly more accurate than the previous method of taking the height of the free induction decay a fixed time after the 90 degrees pulse. It did have the advantage of a digitized signal to noise ratio, allowing better error

estimates

Points to fit to equation VII-2 were measured with an error of from 5 to 15% usually 10 to 15 points were used to fit the exponential.

Standard deviations of fit were generally of the order of .1% with the standard deviation of the slope of the line being of the same order. It was felt however, that the error in measurement was generally higher, probably of the order of 1 or 2%.

The size of error decreased as coverage increased, and increased as temperature decreased.

Signal/noise problems were common in this study. For samples with a coverage of .6 std cm^3/gram and with 4 equivalent protons a signal to noise of about 8 to 1 could be obtained at room temperature (.6 std cm^3/gram is equivalent to about 10^{-2} Molar). For samples with lower coverage the signal to noise was more than proportionately worse, because the line widths went up as the coverage went down. At .3 std cm^3/gram the signal/noise was about 3 to 1 for a single XL-100 scan. Similarly the signal to noise did not improve with lower temperature (as the Boltzman factor would predict) since the effect of a shortening T_2 predominated, for example the signal to noise ratio was in the order of 1:1 for a sample which had .35 std cm^3/gram of ethylene at 10 degrees C.

T_2 measurements were also performed at 15 MHz using

a Meiboom-Gill variation of the Carr-Purcell experiment as outlined in Chapter III.

In this experiment a Tektronix 2661 rate generator was used to simultaneously trigger a Tektronix 2663 pulse generator set to deliver a 90 degree pulse, and the Nicolet 1080 instrument computer. The first delay of tau seconds was set on the 1080, that is, a second Tektronix 2663 set to deliver a 180 degree pulse was triggered by the Nicolet model 1080 at the end of the delay time. Data were being fed to the 1080 after this pulse. Subsequent 180 degree pulses were triggered at the end of n channels using a pulse from the 1080 such that $n \cdot (\text{dwell time/channel}) = 2 \tau$.

The experiment was repeated (after approximately 5 T_1 's) and signal averaged for generally 1024 times or as necessary. T_2 was determined by measuring the amplitude of the echoes at 2 tau, 4 tau, 6 tau . . . and least squares fitting them to:

$$\text{VII-4 } \ln A/A(0) = -t/T_2$$

$$\text{or to } \ln A/A(0) = -t/T_2 - 1/3 \gamma^3 G^2 D \tau^2 t$$

(where G is the field gradient, and D the diffusion constant) depending on the field gradient. The errors for these experiments are described in chapter IX along with the results.

Chemical Shift Measurements

Chemical shift measurements for ^1H were made on the XL-100, and were measured usually against an external standard while the spectrometer was externally locked on a water sample. It was found that the external lock did not wander, and that one could achieve reproducible results in this fashion.

Two problems arose however. The first was the well known and somewhat difficult problem of correcting for differences in magnetic susceptibilities between a known standard and the sample being measured. The second was a less known problem associated with locking on an external sample and measuring samples of different susceptibilities. This second problem relates to the design of the probe.

The probe is designed with two receiver coils; one for the observe channel, one for the external lock channel. This second coil contains a sample of water permanently mounted in it, and is placed as close to the first coil as possible, since it is the basis of the feedback mechanism which keeps the field constant at that spot. It can easily be shown by observing the lock signal, that this signal is shifted when a sample is placed in the observe coil. In response to this shift,

the main field must shift in the opposite direction. If the samples placed in the probe are of different susceptibilities they will cause different amounts of this 'lock shift', and that difference needs to be known in order to gain reliable chemical shift information.

For the samples used in this study it was found that the lock shifted downfield by .4 ppm for the regularly used standard __a sample which was 6% TMS, 20% chloroform, and 74% deuterated acetone. The samples containing ZnO powder caused a 'lock shift' of .2 ppm downfield. The field shifted up by .4 ppm for the standard, but only .2 ppm for the ZnO samples.

It is difficult to know however how much of this difference is taken up by the feedback loop. It would be better not to have to add this correction.

The other correction that must be added is for the difference in magnetic susceptibility.

Theoretical corrections for the difference in magnetic susceptibility were made using the formula derived in the appendix.

$$\text{VII-6 } \delta(\text{cor}) = \delta(\text{meas}) + 2\pi/3 \{X(\text{ref}) - X(\text{sam})\}$$

The susceptibility for TMS was taken from Emsley Feeney and Sutcliff (Emsley et al. 1965) and is listed as $-.54 \times 10^{-6}$. The volume susceptibility for ZnO was calculated using the data of Trew (Trew et al. 1965) who list the

molar susceptibility of ZnO as -27.8×10^{-6} . Using the densities of the ZnO powder and pellet as measured, the calculated volume susceptibility for the powder and pellet are $-.19 \times 10^{-6}$ and $-.95 \times 10^{-6}$ respectively.

The calculated correction factor ignoring contributions from adsorbed species (less than .1%) are $-.7$ ppm for the powder and $+ .8$ ppm for the ZnO pellet.

It is not unlikely that the susceptibility of the ZnO powder is different than that calculated from the molar susceptibility because of surface effects. This would make this correction inaccurate.

It would be nice to have an empirical correction. Measurements were made on a variety of samples of TMS adsorbed on ZnO, and on TMS in a capillary inside a ZnO sample. Caution is necessary, as one does not know that TMS is not shifted from TMS in the free state upon adsorption. TMS in a capillary inside the ZnO should not be shifted at all. The fact that it was was the clue that led to the discovery of the 'lock shift' already discussed.

The shifts for TMS adsorbed on ZnO were found to be coverage dependent, being .2, .3, .45, .55, .55 ppm from TMS liquid, for samples with coverages of .36, .6, 1.0, 2.0, 3.0 std cm^3/gm respectively.

The shift of the TMS on ZnO at high coverage should approach the shift for bulk TMS except for the difference

in magnetic susceptibility caused by the ZnO. This shift of .55 ppm is then the empirical correction.

Using this correction has a further advantage in that one need not concern oneself with the 'lock shift' discussed earlier. The shift in the lock is the same for both TMS on ZnO and for other gases on ZnO.

For these reasons then the magnetic susceptibility correction applied in this work was the empirical correction, that is the correction applied was -.55 ppm, this being the measured shift of TMS physically adsorbed on ZnO, measured from the position of liquid TMS.

For comparison of gas phase chemical shifts to adsorbed state chemical shifts, careful consideration must be given to the reference used in the gas phase measurements. The correct comparison is made utilizing a gas phase measurement which uses gas phase TMS as a reference, while if the reference were liquid TMS a correction of 1.1 ppm needs to be applied.

The errors in the chemical shift measurements depend on the line width and S/N ratio. Errors varied from less than .05 ppm for high coverages to .2 ppm for low coverages.

F^{19} Spectra

The 15 MHz NMR spectrometer was also used to measure resonances of some other nuclei on surfaces.

F^{19} spectra of C_2H_3F , $(1,1)C_2H_2F_2$,

C_2F_3H , and C_2F_4 adsorbed on ZnO were recorded, using signal averaging of the free induction decay following a 90 degree pulse, and subsequently taking the Fourier transform to determine the frequency domain spectra. Chemical shifts from these spectra were measured by recording the F. I. D. of CF_3COOH immediately before and after the experiment, Fourier transforming it, and comparing the channel number that the peak of CF_3COOH spectrum was in with the C. N. of the peak of the adsorbed species spectrum.

C^{13} Spectra

It is a cryptic comment on technology and the state of the art, that when this study was initiated (1970) we were very pleased to be able to obtain H^1 spectra of adsorbed species on a rather low area surface, while toward the end we were talking of natural abundance C^{13} experiments. (C^{13} has a natural abundance of 1.1% and a gamma about 1/4 the gamma of a proton.)

C^{13} experiments using C_2H_4 on ZnO were initiated after Gay (1974) succeeded in recording spectra of acetone, cis- and trans-2 butene, and ethylene on silica. The silica had a surface area of over 600 m^2/gm and a higher bulk density than the ZnO. In fact in the case of C_2H_4 /silica he managed to get about 38 std cm^3 of adsorbed C_2H_4 on a column about 4 cm. high. In comparison with C_2H_4 /ZnO there was about 3 std cm^3 in

a comparable volume of sample.

One method of getting more C_2H_4 into the sample tube is to increase the bulk density of the adsorbent. In order to accomplish this we made a small pellet press of diameter .95 cm. and used this to press pellets which would just fit the inside of a 12 mm. sample tube. The bulk density was increased from .6 gms/cm³ to 3 gms/cm³ yet there was only a small reduction in surface area, from 9 M² to 8.6 m² on the sample measured.

By increasing the pressure of C_2H_4 over the sample to 1100 torr the amount adsorbed turned out to be 1 std cm³/gm but with the increased bulk density this represented almost 4 times as much sample as before for comparable coverage.

Since the vacuum rack in this experiment was not designed to measure pressures above 1.7 atmospheres a sample was prepared by freezing down a large measured quantity (68000 torr-cm³) of C_2H_4 into an NMR tube of volume 12.8 cm³ which had 6.8 gms. of the high density ZnO in it. The amount of C_2H_4 adsorbed could only be estimated by extrapolating the measured isotherms. In order to do this the measured isotherm points were least squared fit to the BET equation and that function was extrapolated. Since measured points were only known for pressure values up to 1.5 atmospheres this can only provide a rough estimate. The coverage for this sample

was estimated to be 1.4 std cm^3/gm from the B. E. T. and 1.5 std cm^3/gm from comparison of H^1 peak amplitudes with those of a sample of known coverage.

114,000 scans at 2 per second produce a C^{13} spectrum with a signal to noise ratio of approximately 3 to 1.

Chapter VIII

Nuclear Magnetic Resonance Measurements of Olefins
Adsorbed on Zinc Oxide

Chemical Shift Studies

It is of interest to determine whether electrons are being donated to a surface, or are coming from a surface during a chemisorption process. Both surface potential measurements and infrared studies of adsorbed species have been used in the past to help determine which case holds for a certain system.

NMR is an ideal tool for determining which happens, since as discussed in Chapter 3 the presence of electrons around the nucleus causes a change in the field at the nucleus. This change can be measured as a so-called chemical shift and is directly related to the electron density at a nucleus. Thus a donation of electrons to a surface will result in a deshielding of the nucleus, and for a fixed frequency experiment one would have to go to a lower field to find the resonance, or alternatively in a fixed field experiment to higher frequencies to find the resonance.

^1H spectra of ethylene, propene, the butenes and for comparison butane and ethane as well as ^{19}F spectra of $\text{C}_2\text{H}_3\text{F}$, $\text{C}_2\text{H}_2\text{F}_2$, $\text{C}_2\text{F}_3\text{H}$, and C_2F_4 , and ^{13}C

TABLE VIII - 1

The Chemical Shifts of Some Hydrocarbons adsorbed on Zinc Oxide (compared with the same substances in a free state). In ppm, corrected by $-.55$ ppm.

molecule	CH ₃	CH ₂	olefinic	ref
ethane	-.85			Reddy 1961
ethane(ads)	-.91			
butane	-.95	-1.3		Spiesecke 1961
butane(ads)	-.98	-1.3		
ethylene			-5.29*	Bovey 1967
			-5.35	BothnerBy 1961
			-5.4**	this work
ethylene(ads)			-6.6 to -5.5+	
propene	-1.65		-5.7, -4.9, -5.0	Reddy 1961
propene(ads)	-1.8		-6.3, -5.5	
TMS	0			
TMS(ads)	+.25 to .55 (uncorrected)			

* in TMS

**corrected for difference in magnetic susceptibility

by -1.1 ppm using TMS liquid as a reference.

+depending on coverage; largest shift for lowest coverage

spectra of C_2H_4 were measured to determine the chemical shifts involved. The chemical shift of ethylene was also measured as a function of coverage.

Chemical shifts of adsorbed species on ZnO powder were corrected by $-.55$ parts per million as discussed in Chapter 7. Table VIII-1 shows the chemical shifts of free and adsorbed molecules. The chemical shifts of free molecules were taken from other works and references to these are given in the table.

The physically adsorbed molecules (ethane, butane and TMS) experience a slight shift downfield of the free molecules.

The more strongly adsorbed olefins however show pronounced 1H chemical shifts downfield for the olefinic protons, and smaller shifts for the methyl protons of propene.

For adsorbed ethylene the chemical shift was measured as a function of coverage. At high coverages the slight downfield shift of physisorbed species was noted, while for low coverages larger downfield shifts were noted.

Spin-spin splittings were not resolved for any of the adsorbed species except in the ^{13}C spectrum of ethylene, but the CH_3 , CH_2 and olefinic protons were resolved.

On all 1H spectra the chemical shift is shown relative to TMS and is shown corrected and uncorrected for the difference in susceptibilities of ZnO and TMS.

The spectra of ethane and propane adsorbed on ZnO are shown in Figure VIII-1. Line widths are narrower than for comparable coverages of olefins and chemical shift differences between free and adsorbed phases suggest a further shielding of the nucleus, an observation made for all physisorbed species. The change in shielding is discussed later as a physical phenomenon. This and the narrower linewidth are consistent with the low heats of adsorption of these two gases on ZnO.

Figure VIII-2 shows the spectra of ethylene and propene at coverages of .6 and .69 $\text{std cm}^3/\text{gm}$ of ZnO respectively, at 38 degrees C. Figures VIII-3 and 4 illustrate the change in chemical shift and in line width for different coverages of ethylene.

The δH shifts for adsorbed ethylene are all moved downfield from ethylene in a free state, with the greatest downfield shifts for lowest coverage. What we are observing is a deshielding of electrons most probably brought about by donation of electrons by the ethylene to the surface. That such donation is coverage dependent is not at all surprising since one expects that at low coverage adsorbed species find the most energetically favourable sites, and that the number of electrons withdrawn per molecule adsorbed will be higher at these sites. When the coverage gets higher adsorption is somewhat less favourable and the deshielding is not as

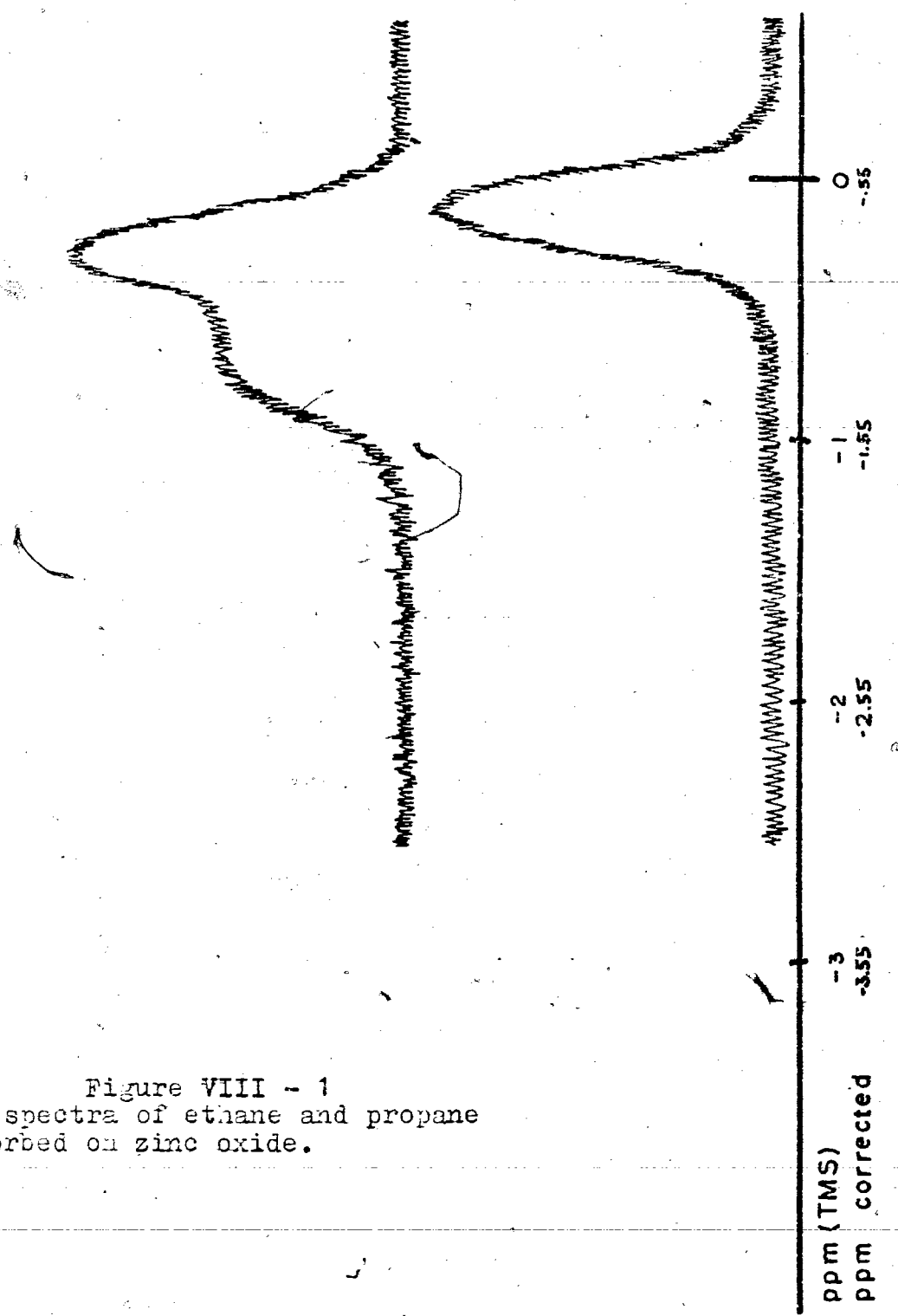


Figure VIII - 1
The spectra of ethane and propane
adsorbed on zinc oxide.

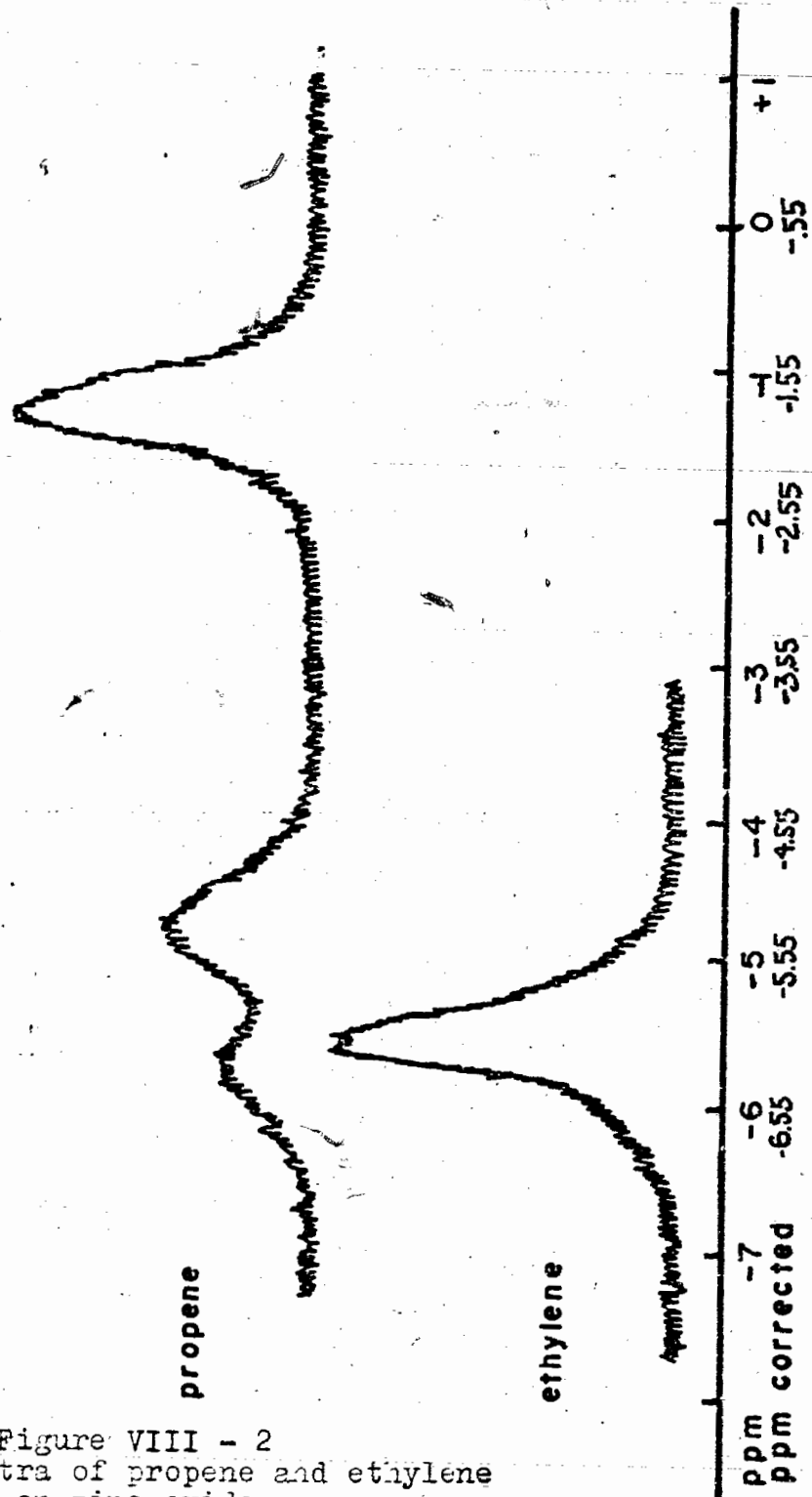


Figure VIII - 2
The spectra of propene and ethylene
adsorbed on zinc oxide.

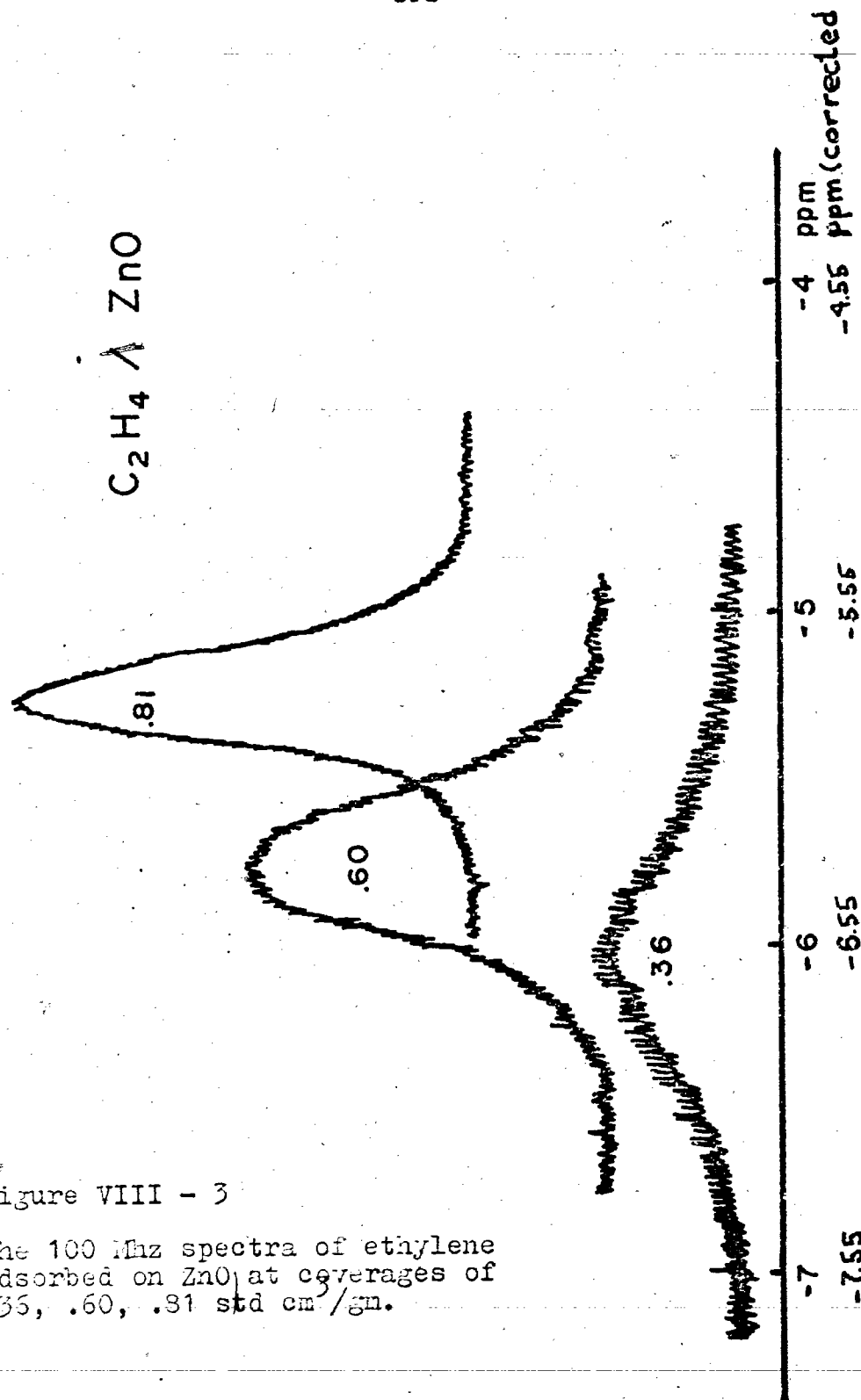
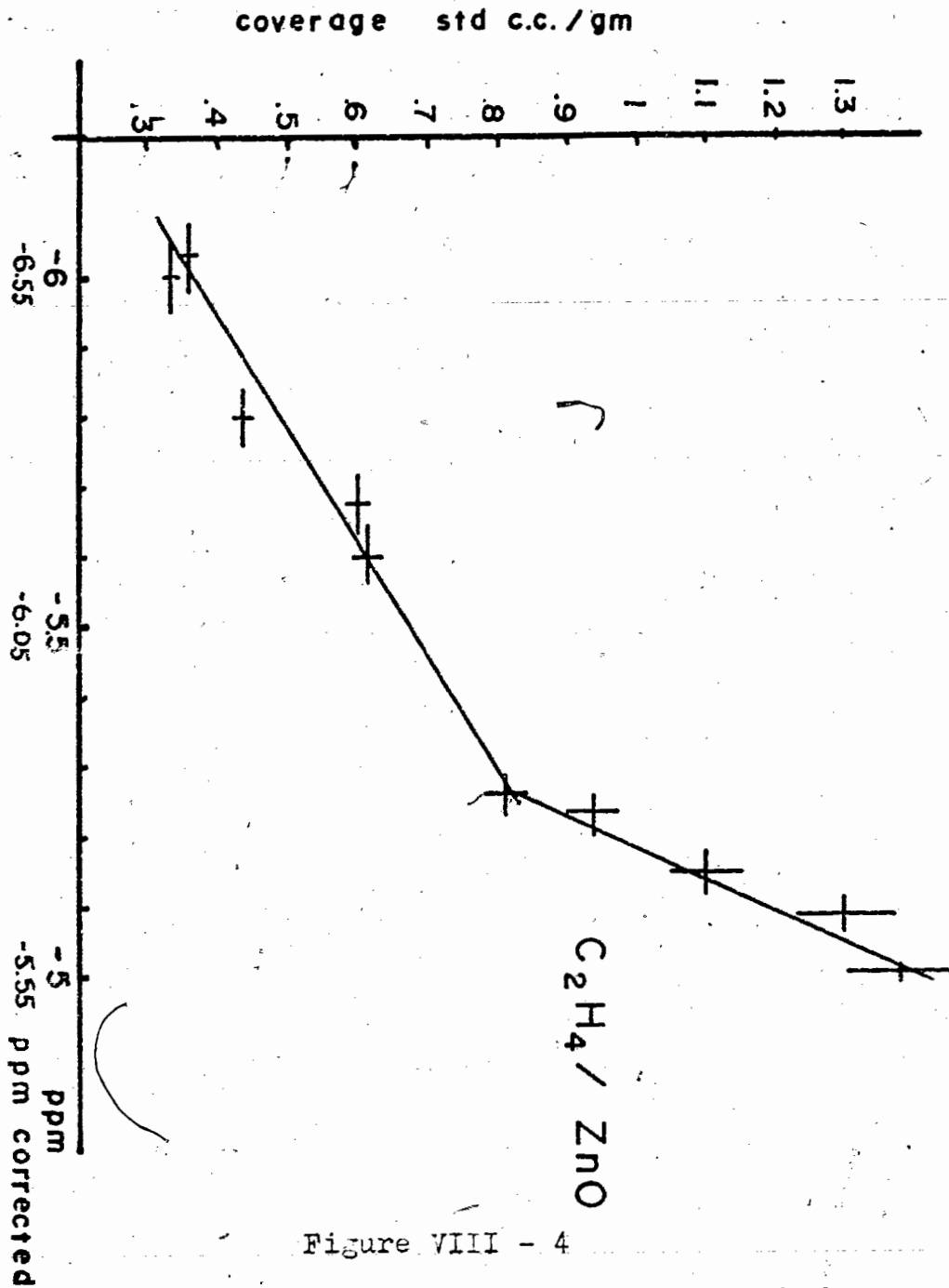


Figure VIII - 3

The 100 Mc spectra of ethylene adsorbed on ZnO at coverages of .35, .60, .81 std cm²/gn.

great. It seems worth noting that the inflection point in Figure VIII-4 is very near the inflection point in the adsorption isotherm of C_2H_4 on ZnO (Figure VIII-4). Both points indicate the area where further adsorption is expected to be more physical and less chemical in nature. This change in chemical shift as a function of coverage is admittedly at odds with the isosteric heat data; a point discussed later.

1H chemical shifts are not very large so that to provide a more convincing argument the ^{13}C chemical shift was measured for a specially prepared C_2H_4 on ZnO sample. Some precautionary remarks are necessary. The sample used was ZnO compressed such that the bulk density was ca. 3 gms/cm^3 . (The nitrogen BET surface area of another sample treated this way was unchanged within experimental error.) However there were no direct means available to measure the quantity of gas adsorbed at high pressure. As described earlier, the sample was subjected to approximately 11 atmospheres of C_2H_4 . The coverage was estimated by 2 separate methods. The first from a linear extrapolation of the C_2H_4 BET isotherm. The second by comparing NMR peak amplitudes (1H spectra) with a sample of known coverage. The first implied a coverage of $1.4 \text{ std cm}^3/\text{gm}$ the second $1.5 \text{ std cm}^3/\text{gm}$. 1H chemical shifts for this sample were displaced upfield from free C_2H_4 when corrected.



The chemical shift of ethylene adsorbed on ZnO as a function of coverage.

The ^{13}C spectrum is shown in figure VIII-5, along with that of benzene (both taken at 15 MHz). The chemical shift of the adsorbed C H is 4.6 ppm upfield of C_6H_6 (lig) (uncorrected for susceptibility) whereas C_2H_4 in a free state is 5.2 ppm upfield of C_6H_6 . One expects very little contribution to the spectrum from gaseous C_2H_4 since the concentration of gaseous species at the ZnO plug (which excluded much of the space) was lower than the concentration of adsorbed species, and the repetition rate (500 msec) was fast enough such that the gaseous species would be considerably saturated, a fact verified by turning the sample upside down so that the ZnO plug was not in the receiver coils, and trying to collect a spectrum using the same repetition rates as before.

The theoretical magnetic susceptibility correction for the ZnO pellet was .8 ppm, while the empirical correction (being the difference in chemical shift between TMS adsorbed on the pellet and TMS liquid), was only .4 ppm. This latter correction was used. The volume susceptibility of liquid benzene is $-.625 \times 10^{-6}$ (Pople 1959) so the correction to be applied when using benzene as a reference calculated from equation VII - 6 is +.1 ppm..

Despite the high fraction of physisorbed species, the chemical shift of the carbon is downfield by .5ppm. The

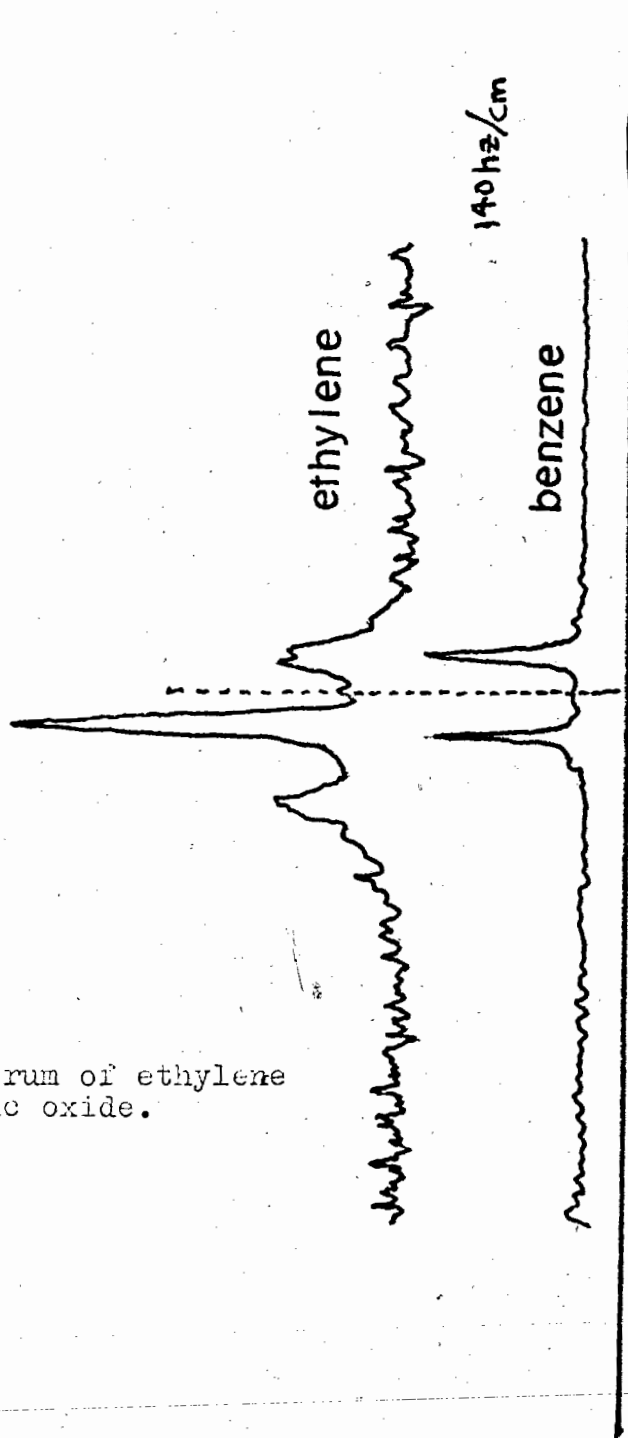


Figure VIII - 5

The carbon spectrum of ethylene adsorbed on zinc oxide.

carbons then are partially deshielded.

A Series of Experiments with ^{19}F Substituted Ethylenes

^{19}F NMR has a much wider chemical shift window (Emsley et al. 1965 Vol. II) and also tends to show larger chemical shifts on changes of environment than do protons (Ibid). Samples were prepared with $\text{C}_2\text{F}_3\text{H}$, (1,1) $\text{C}_2\text{F}_2\text{H}_2$, C_2FH_3 , and C_2F_4 adsorbed on ZnO in hopes of comparing the deshielding of the ^{19}F nuclei with the deshielding of the protons and ^{13}C in C_2H_4 .

A larger linewidth (c. 700 hz for $\text{C}_2\text{H}_3\text{F}$) led to signal to noise problems when using coverages in the order of .6 std cm/gm. To circumvent this the spectra were taken by fourier transforming the sum of several hundred free induction decays taken at 15 MHz. Chemical shifts were measured from an external reference the position of which was recorded before and after to account for field drift. The diamagnetic susceptibility correction is +.2 ppm, considerably less than the error in measurement in this case, the increased error being due to the large line width plus the reduced field used.

Table VIII-2 lists the observed chemical shifts measured in ppm upfield from CF_3COOH for the fluoro substituted ethylenes adsorbed and in solution. The shifts of the compounds in solution are taken from the

Table VIII-2
 Fluorine and proton chemical shifts of free and adsorbed
 fluorine derivatives of ethylene relative to fluoro-
 acetic acid

molecule	shift free	ref	shift(ads)*	change*
C_2F_4	+56	Parshall 1965	+63	7
C_2F_3H	26,50,108	Mooreland 1965	28,55,136	2,5,28
	21.6,47.5,126 ++		29.0,56.7,135.7 ++	
(1,1) $C_2F_2H_2$	4.8	Shvo 1965	12	7.4,9.2,9.7 7
			10.9++	
C_2FH_3	35.4	Banwell 1961	50	15
			43++	

* errors are \pm 3 ppm

++ These measurements taken much later by F.T. at 100Mhz

proton measurements +

C_2F_3H	-6.5	Smith 1967	-6.6	-.1
(1,1) $C_2F_2H_2$	-3.8	Ihrig 1972	-3.8(3.5++)	0
C_2FH_3	4.0,4.4,6.2	Emsley 1966	-4.3,-4.6,	-.3,-.2
			(-4.15)(-4.6)++	
			-6.4	-.2
			(-6.5)++	

+corrected by -.55 ppm

*errors are \pm .1

proton measurements of free molecules were made in
 carbon tetra-chloride with TMS internal

literature and the references are given in the table 2. Table 2 also lists the proton chemical shifts of the same molecules adsorbed relative to TMS (corrected by $-.55$ ppm for difference in diamagnetic susceptibility) and the corresponding ^1H chemical shifts of "free" molecules.

Figure VIII-6 shows the 15 MHz spectra of the compounds.

A close consideration of Table VIII-2 points to the fact that there is different shielding involved with the fluorine derivatives of ethylene adsorbed on ZnO than with ethylene adsorbed on ZnO. The change in chemical shift is large for some fluorines implying a chemical interaction, but in all cases it is to a higher field suggesting that there is greater electron density at ^{19}F nuclei. We must conclude for these large shifts that electrons are coming from the surface in contrast to what appears to be happening for ethylene.

Dent and Kokes (1972) view ZnO as an acid base cation pair and state:

". . . hence the catalyst depends not only on the proton affinity of the oxide but also on the carbanion affinity of the cation. The acidity of the cation may determine the basicity of the catalyst. Specific interactions, i.e. effects of ion structure on the basicity of the interaction are likely to be evident when the carbanions differ radically in structure."

R

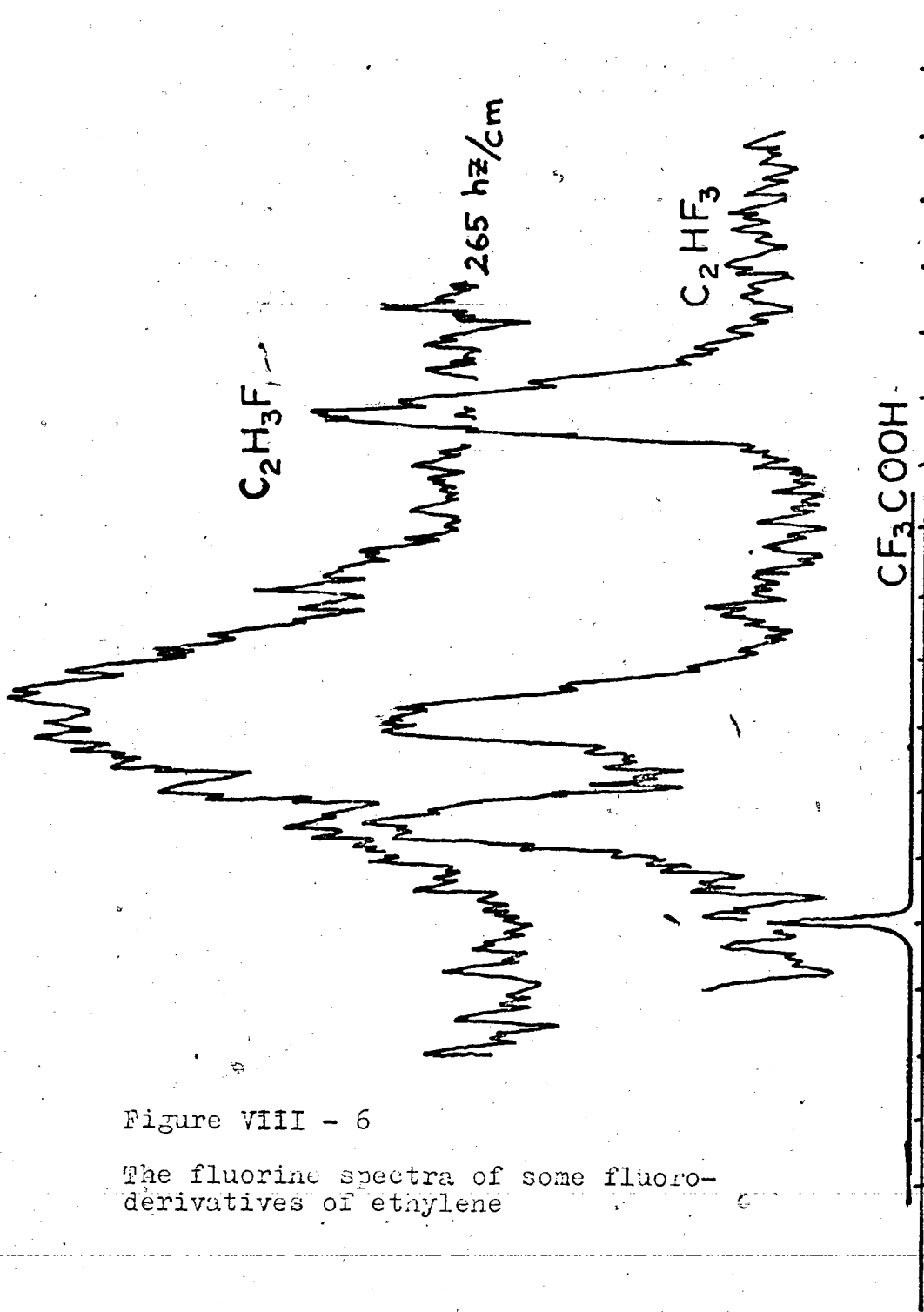


Figure VIII - 6

The fluorine spectra of some fluoro-derivatives of ethylene

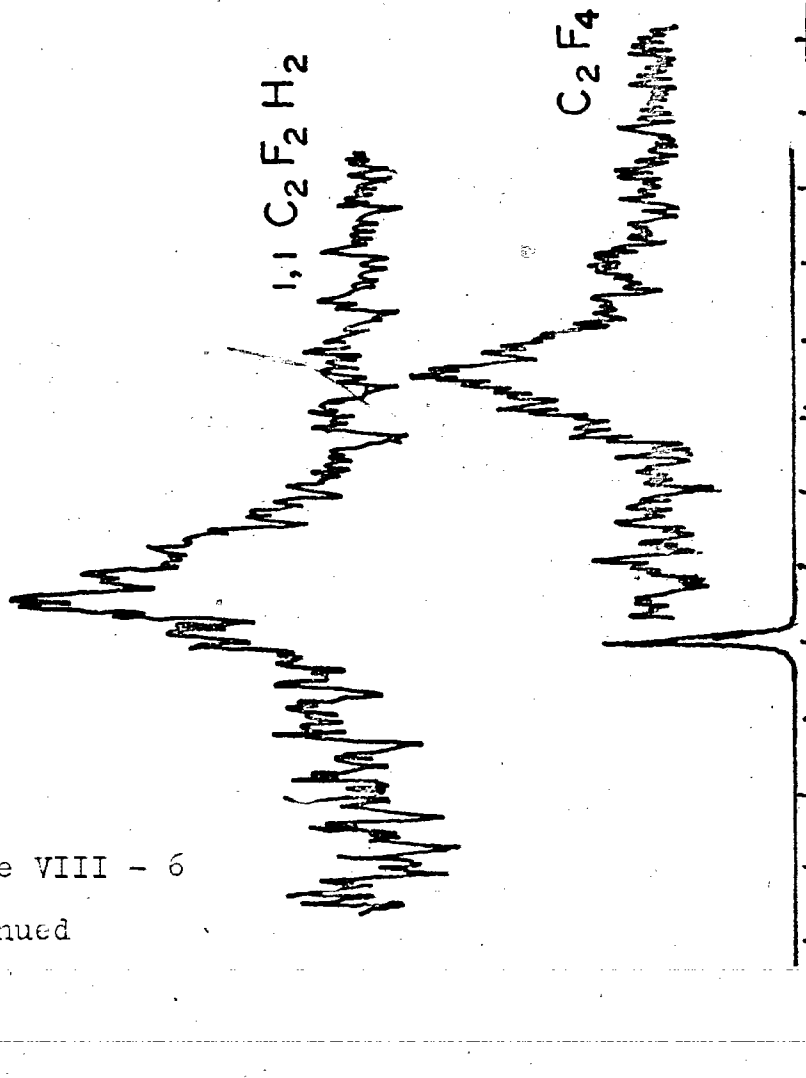


Figure VIII - 6
continued

Fluorinated ethylenes are bound to be more acidic than the unsubstituted ethylene and zinc oxide does indeed seem to respond to this difference rather drastically. In looking back on the data the size of the chemical shift is consistent with the large line widths, since strong interactions would lead to more immobile species thus shortening T_2 .

NOTE ADDED AT A LATER DATE

Measurements taken in this laboratory after this thesis was written suggest that the conclusions drawn about the fluorine derivatives of ethylene may not be valid. It was found that the chemical shifts of these species adsorbed on ZnO were not greatly different than the gas phase shifts. In all cases the comparisons made were made using liquid phase data. It is even possible that the measurements made here were predominantly made on gas phase molecules.

A Discussion About the Chemical Shifts

At this point it becomes prudent to discuss the ^1H and ^{13}C chemical shifts of the adsorbed complexes since it was rather glibly assumed that the negative shift for olefinic protons meant donation of electrons to the surface, and the shifts for the physisorbed species have not been explained.

As noted in Chapter 3 the field at a nucleus can be

described by

$$H = (1 - \sigma) H(o)$$

where sigma is a tensor describing the "shielding" of the nucleus by the surrounding electrons. A positive sigma leads to a weaker field at the nucleus and thus a necessity to go to a higher field in a fixed frequency experiment in order to obtain resonance.

Buckingham (1960) suggests considering sigma to be composed of a screening constant for the isolated molecule sigma (gas) plus a screening constant for the surrounding medium. This second part has in his opinion four different contributions, thus

$$\sigma(\text{medium}) = \sigma(b) + \sigma(a) + \sigma(\text{omega}) + \sigma(E)$$

where sigma (b) is the contribution which is proportional to the bulk magnetic susceptibility of the medium, sigma (a) accounts for the anisotropy in susceptibility of the surrounding molecules, sigma (omega) is due to Van der Waals forces, and (E) accounts for electric field effects caused by charge distributions in the neighbouring molecules.

In going from a gaseous to a condensed phase in a cylindrical sample tube, the necessary correction to apply will be $\frac{2}{3} \pi \chi_v$ of the condensed phase (assuming χ_v

of the gas phase is zero). I have only corrected for the difference in χ due to the ZnO but under the conditions at which these shifts were measured this will be the overwhelming amount of the correction.

$\Sigma(\omega)$ is brought about by the distortion of the electronic environment by the attractions of nearest neighbours, and an increase in paramagnetic screening due to assymmetric distortions caused by collisions. Both factors are negative and thus lead to downfield shifts.

$\Sigma(a)$ is that part of the shielding constant which is due to the anisotropic susceptibility of the medium. It is the cause of the upfield shift for molecules dissolved in aromatic solvents, and the downfield shifts for molecules dissolved in solvent such as CS_2 (Zimmerman 1957, Bothner-By 1957). Expressions have been derived for $\Sigma(a)$ (Buckingham 1960, Stephen 1958) for some solvents although no expression has been derived for surface interactions. Certainly there is a susceptibility anisotropy at a surface, which could cause small shifts. Presumably some of this would be compensated for by using TMS adsorbed on ZnO as a reference.

$\Sigma(E)$ arises from the polar effect caused by the perturbation of the electronic structure of the molecule by an electric field resulting from the surrounding medium. The effect then is only important for polar

molecules and will not be further considered except to say that the large downfield chemical shift accompanying hydrogen bonding is a sigma (E) effect, and if adsorption interferes with hydrogen bonding as in water adsorbed on silica then an upfield shift should occur as indeed it does (Pickett 1970).

The slight shifts for the physisorbed species, and the larger shifts for the chemisorbed species, or some part of it can be explained on the basis of Van der Waals effects.

Both methane and ethylene display downfield shifts when going from the gas to the liquid phase (Gordon 1961) or as the gas pressure is increased (Raynes 1962). The van der Waals shift was $-.4\rho$ ppm (where ρ is the density in gm/ml for ethylene. This implies that the shift will get larger as the density (coverage) goes up. This is in direct contrast to our ethylene case where the largest shifts are for the lowest concentrations. However it is remarkably like the TMS on ZnO where the shifts on adsorption are a function of coverage with the largest shift for the largest coverage.

For the ethylene case the shift is much greater, and in the other direction. The best conclusion is electron donation to the surface with a corresponding deshielding of the nuclei involved.

The change in chemical shift as a function of

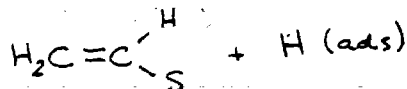
coverage is somewhat in contrast to the isosteric heat values (see chapter 7). Some of this is likely caused by greater donation of electrons per molecule at lower coverage. Some of the change is the same effect one observes for TMS on ZnO. As the coverage increases the shift moves upfield due to Van der Waals interactions. However one is still perplexed by the magnitude of this coverage dependence, in view of the rather constant heats.

There is an obvious point here, and that is a cataloging of chemical shifts of adsorbates versus coverage on a large number of surfaces with reference to their gas phases would be very useful for interpreting adsorbate adsorbent interactions, would undoubtedly correlate to other surface measurements, and would certainly add to our understanding of catalysis.

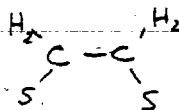
Information on the Structure of the Adsorbed Species

Figure VIII-2 and VIII-3 reveal some information on the structure of the adsorbed species.

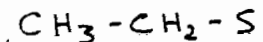
For ethylene the single resonance in the olefinic region would exclude such structures as:



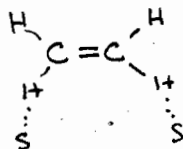
or



or



or



but allows for either a π -complex as proposed by Dent and Kokes (1970c) or a structure with all 4 hydrogens, hydrogen bonded to the surface, a structure which is unlikely because of the surface dimensions and symmetries involved, and because it would make the species quite immobile, in direct contrast to the relaxation data obtained on this system.

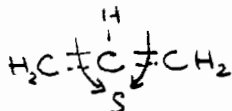
The possibility that the single resonance is in reality composed of two or more resonances with some distribution of chemical shifts was investigated in two ways.

Firstly the digitized data obtained from the C. W. experiment at 100 MHz was least squares fit to a sum of Lorentzians, and the improvement in fit compared to the fit for a single Lorentzian giving consideration to the number of parameters added. There was no statistical evidence to conclude that there were superimposed Lorentzians.

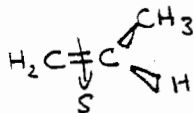
If there were a distribution of chemical shifts involved then the measured peak width and thus T_2 should

be field dependent. T_2 's were also measured at 15 MHz both by least squares fitting an off resonance F. I. D. and by the Meiboom-Gill variation of the Carr Purcell experiment. Within experimental error the differences were too small to suggest such field dependence.

The situation is more complex for propene. Dent and Kokes (1970a, b) find that propene adsorption on ZnO leads to both a strongly bound state for which they propose a pi-allyl structure:



and a more weakly bound state thought to be a π complex:



which can be desorbed by pumping at room temperature. It was found that approximately .38 std cm^3/gm of propene was left on the surface after pumping on it at room temperature. Such a quantity should be relatively easy to see if it were like the ethylene where coverages of less than .3 std cm^3/gm gave a good spectrum.

C. W. measurements on the XL-100 were without any result for such a sample. Even an average of 8 C. W. experiments showed no peak whatsoever. The simplest explanation of this would be that the tight binding produces a line width too broad to be observed with this

instrument.

A higher coverage of propene produced the spectrum shown in figure 2, which is considered to be only the loosely bound species. The spectrum is consistent with a pi complex since no methylene resonance was found, and the chemical shift displacement on adsorption is much greater for the olefinic protons than for the methyl protons. The observation of only two bands in the olefinic region is not surprising since two of the free molecule chemical shifts are nearly the same in comparison with the observed line widths for the absorbed species. Two thousand scans at 15 MHz (time domain spectra) produced a peak for the tightly bound propene species but unfortunately it is difficult to draw conclusions from it since it has a line width greater than the chemical shift window.

Some Experiments on ZnO Pellets

As previously outlined, in order to increase the number of molecules within the receiver coils, some samples were prepared with Zinc oxide compressed so that the bulk density was increased by a factor of 5. BET surface measurements on such a sample were only 5% less, the area of surface per cm² of sample was then up by a factor of 5.

Spectra taken of molecules adsorbed on these pellets were however not as straight forward as planned.

The samples were treated in the same way that the powders were treated, although more time was allowed for outgassing because of increased diffusion problems. Typically they were heated to 450 degrees in vacuum for 6 - 10 hours, treated in 150 torr of oxygen with liquid nitrogen trap in the system for 2 hours and then outgassed at room temperature for 10 to 24 hours.

Typical results of such a sample with .8 std cm^3/gm of ethylene adsorbed on it are shown in Figure VIII-7. The ratio of amplitudes of the lowfield to highfield peak was coverage dependent (at low coverages it was bigger at high coverages smaller); the line widths were considerably larger than corresponding coverages on the powder, and the chemical shift of the lowfield peak varied over 2 parts per million. Temperature studies were carried out, and the two peaks did not coalesce, or even tend to upon heating to 150 degrees C. Several samples were outgassed in vacuum, whereupon it was found that the gas could only be recovered quantitatively with heating to about 100 degrees C.

Mass spectra were taken of the evolved gases. They showed peaks at 44, 28, 27, 26, 25, 18 and 17. In outgassing a sample at 0 degrees C and then taking off a fraction at 100 degrees C, the first showed little evidence of a 44 peak and only a slight 18, 17 peak, while the second showed a much larger 44, and 18, 17 peak. Mass

spectra cracking patterns were compared with those of acetaldehyde and ethylene oxide run under the same conditions, and NMR spectra of these two compounds adsorbed on Zinc oxide pellets and powder were run for comparison. Both experiments showed conclusively that the second peak was not due to ethylene oxide or acetaldehyde.

The spectra of acetaldehyde adsorbed on ZnO is shown in figure VIII - 8 . The ethylene oxide adsorbed on ZnO was too broad to observe, despite a high coverage.

The mass spectra were however consistent with the formation of CO_2 and H_2O from ethylene and oxygen. The second peak (the downfield one) behaves in the same fashion as water on zinc oxide, that is its chemical shift is very coverage dependent. This has been explained by interference with hydrogen bond formation upon adsorption (Pickett 1970).

Kubokawa et al. (1973) have studied the oxidation of ethylene, propene and the butenes over ZnO to produce CO_2 and H_2O , but with gas phase and adsorbed oxygen present.

At this point it was concluded that oxidation was occurring on the surface due to a stoichiometric excess of oxygen remaining from the oxygen treatment which was unable to diffuse out of the pellet. Subsequent experiments showed that the peak to low field still remained even on pellets outgassed at 450 degrees for 16

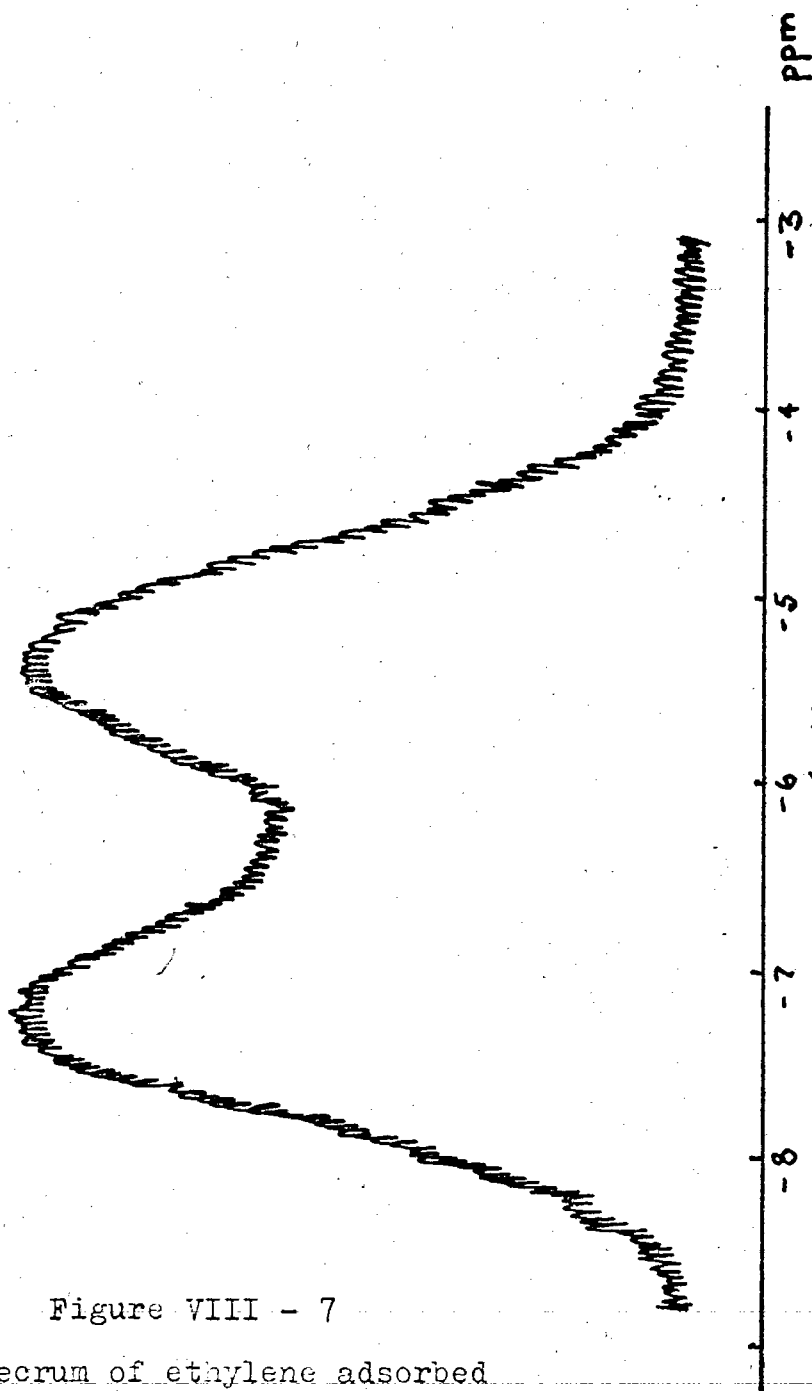


Figure VIII - 7

^1H spectrum of ethylene adsorbed
on a ZnO pellet.

hours that were given no oxygen treatment. However the only conclusion that seemed likely was that the compression of the zinc oxide traps enough excess oxygen which subsequently is not readily outgassed. This excess oxygen is responsible for the oxidation of the olefin to CO_2 and H_2O . It seems unlikely that the olefin reduces the zinc oxide, since this would have readily shown up in the infra-red studies of Kokes et al. (Dent 1972).

The two predominant reasons for wanting to do the studies on ZnO pellets were to try and get a spectrum of the tightly bound propene; which Kokes believes in a pi-allyl complex, and to attempt to get a ^{13}C spectrum of adsorbed ethylene.

A sample was prepared by adsorbing propene on a pellet and then pumping it off at room temperature. Such a treatment left .38 std cm^3/gm on the sample. Again the XL-100 failed to produce a spectrum of this sample despite the very high concentration in std cm^3/ml of sample. Four K scans added together from the pulse spectrometer at 15 MHz and subsequently Fourier analyses did produce a spectrum, but the peak was too wide to get a value of its chemical shift or to tell whether it was not in fact partially water formed as before from excess O_2 reacting with the olefin.

The studies on compressed samples served mostly to

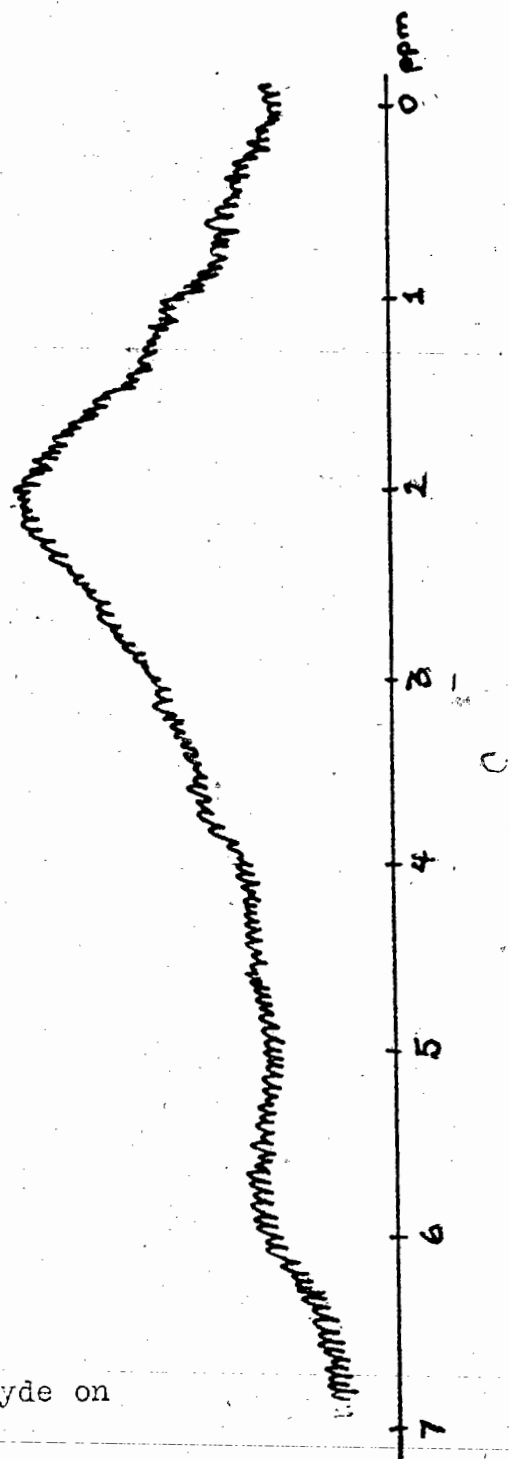


Figure VIII -3

^1H spectrum of acetaldehyde on
a ZnO pellet.

remind one that surface studies are best done on surfaces prepared always in the same way, and on ones which are well characterized.

Chapter IX

Relaxation Studies of Ethylene Adsorbed on Zinc Oxide

There is no inherent reason why relaxation analysis should not be carried out on chemisorbed phases, although for some systems spectrometers that can measure very wide lines and/or pulse NMR spectrometers with fast response times would be necessary.

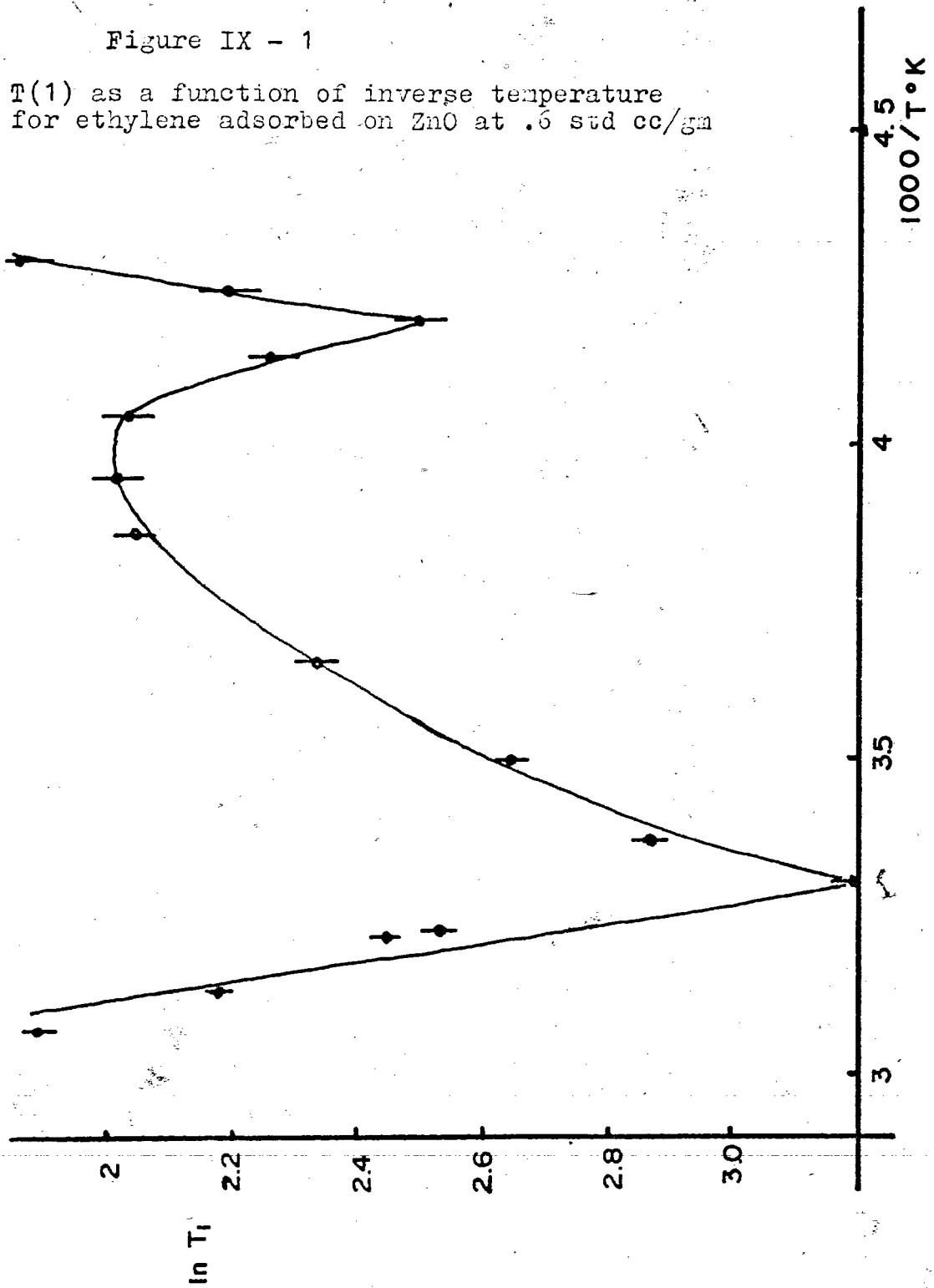
Since the C. W. 100 MHz line widths are not extremely wide, and since it would supply information on the motion of ethylene on the surface, relaxation studies were initiated for the ethylene on ZnO system.

T_1 's were measured at 15 MHz using a 180 degree-tau-90 degree pulse train as described in Chapter III. T_2 's were measured from the line widths of frequency domain spectra at 100 MHz, from 90-tau-180-2tau-180 . . . pulse trains at 15 MHz and from the free induction decays at 15 MHz. Both T_1 's and T_2 's were measured as a function of temperature and of coverage.

Of these measurements the one which supplied the most information is that of T_1 versus temperature at constant coverage. Figure IX-1 shows a plot of $\ln T_1$ versus Temp. for ethylene at a coverage of .6 std cm³/gm on Zinc oxide. Figure IX-2, and IX-3 show plots of T_2 versus temperature at constant coverage and of T_1 and T_2

Figure IX - 1

$T(1)$ as a function of inverse temperature
for ethylene adsorbed on ZnO at .6 std cc/gm



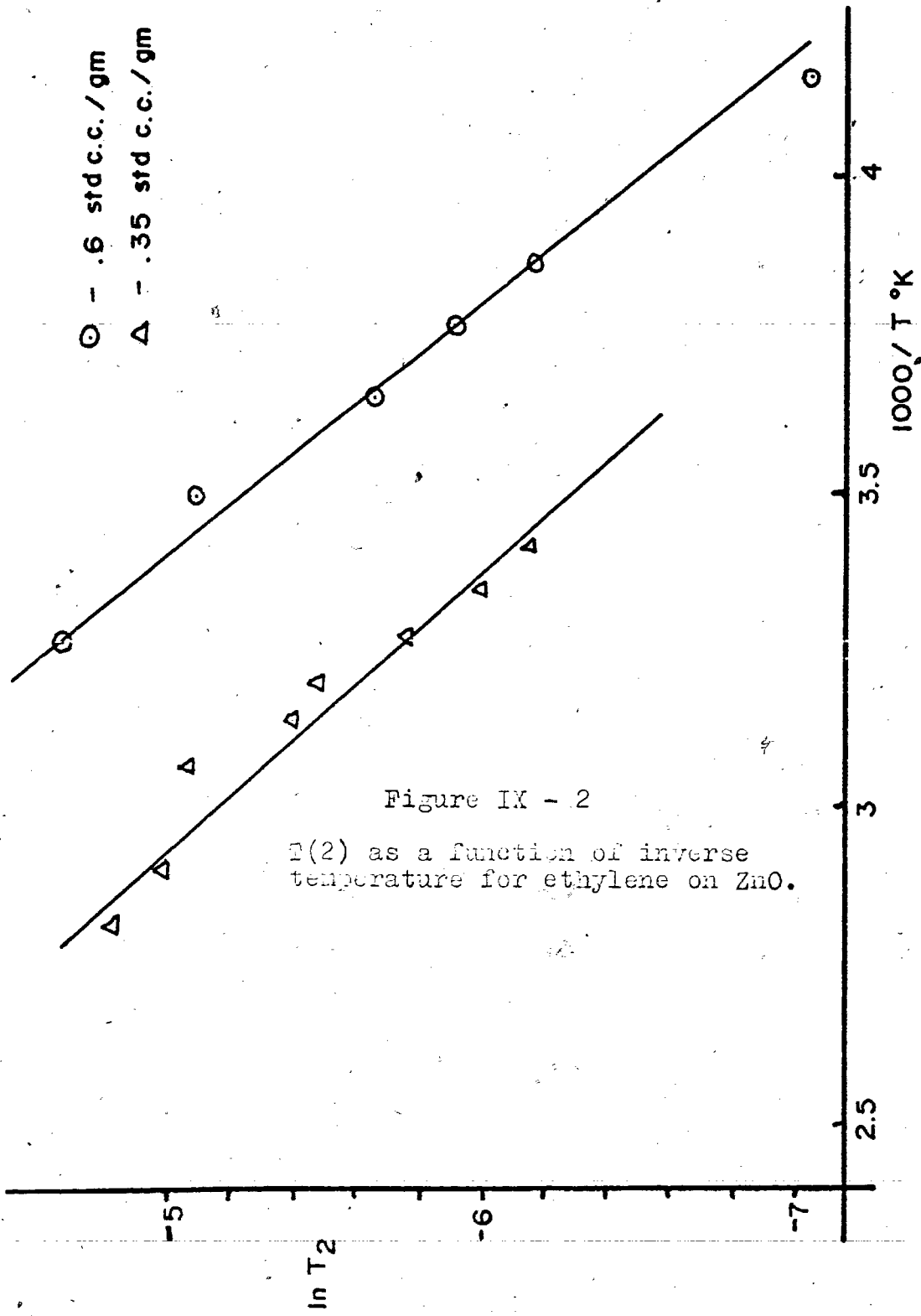
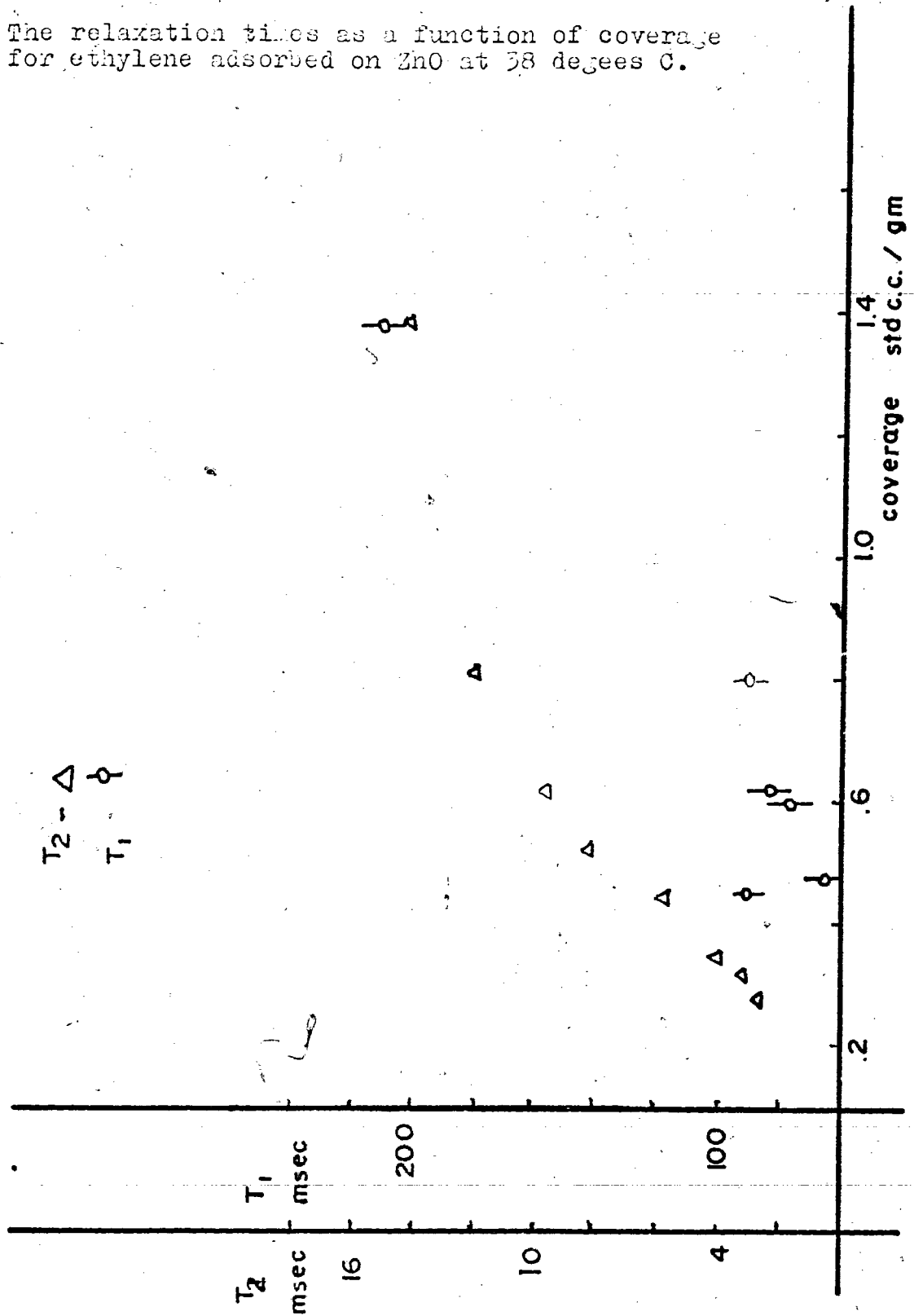


Figure IX - 3

The relaxation times as a function of coverage for ethylene adsorbed on ZnO at 38 degees C.



versus coverage at constant temperature.

Figure IX-1 is typical for a system where there are two correlation times. Each motion is slowed down as the temperature decreases until $\omega_0 \cdot \tau \approx 1$ at which time the contribution of this motion to the spectral density reaches a maximum. At the minimum $\omega_0 \cdot \tau = .616$ (Abragam 1961). This however does not say anything about what motion is represented by that correlation time. Without further information one can only build models and see if they reproduce the data.

There are several possibilities.

One possibility is that the molecules are desorbing, relaxing in the gas phase and then adsorbing. Such a process however should have an activation energy close to the heat of adsorption. Activation energies measured from the two outside slopes of Figure IX-1 are 2.8 kcal/mole and 3.2 kcal/mole. The activation energy for T_2 from Figure IX-2 is 1.35 kcal/mole but this does not give us as much information since T_2 's are induced by both high and low frequencies so the activation energy measured is some weighted average of two or more activation energies (Farrar 1971). The conclusion is that the motion causing T_1 is one which has a lower activation energy than that necessary for desorption.

The next possibility to consider is an intermolecular dipole dipole mechanism brought about by interactions

either with other ethylenes or with surface hydroxyls.

Since dipole dipole relaxation is proportional to γ^2 (spin 1) x γ^2 (spin 2) the relaxation between a proton and a deuteron will not be as effective as between a proton and a proton. (gamma of a deuteron is $< 1/6$ of that of a proton). To test whether protons on C_2H_4 are interacting with protons on the surface (surface hydroxyls), one need compare the relaxation times of such a system with those of ethylene on a surface which has been deuterated. (Of course one must first of all make sure that there is no exchange between the protons of surface hydroxyls and of the ethylene.)

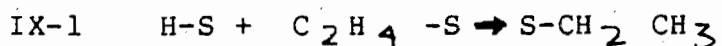
Zinc oxide powder was treated by refluxing in heavy water at 100 degrees C for 48 hours, and subsequently evacuating at 450 degrees C then treating with 20 torr of heavy water vapour at 450 degrees for 2 hours. Such a treatment has been shown to exchange most of the hydroxyls of oxide surfaces. Ethylene exposed to such a surface for up to 24 hours showed no increase in deuterium concentration as determined by mass spectroscopy.

Samples prepared with coverages of $.6 \text{ std cm}^3 / \text{gm}$ of C_2H_4 on the deuterated surface at 31 degrees C and 0 degrees C had relaxation times of 58 msec and 105 msec respectively. From figure 1 comparable samples on an undeuterated surface would have relaxation times of 55 and 100 msec. The difference could easily be attributed to

the variation in temperature caused by the rather poor controller. Were relaxation via an interaction with the surface a significant mechanism one would expect a large increase in the relaxation time.

The next mechanism to explore was relaxation between two ethylene molecules, i.e. intermolecular relaxation. A gas sample was prepared that was 50% C_2H_4 and 50% C_2D_4 . .6 std cm^3/gm of this mixture was adsorbed on ZnO powder and T_1 was measured. The relaxation time was radically different.

Dent and Kokes (1972) had found that C_2H_4 and D_2 reacted over ZnO to form only C_2H_4 D_2 and no products of the form $C_2H_nD(6-n)$, i.e. there was no exchange between ethane species, and if the hydrogenation occurs via:



then such a reaction is not reversible.

Because of this information I did not expect exchange between the C_2H_4 and C_2D_4 . Since T_1 for the 50/50 mixture of C_2H_4 and C_2D_4 differed significantly from that of pure C_2H_4 however the mass spectrum of the sample was checked before any further work was planned.

Mass spectra run on the desorbed gases did however show exchange, i.e. the presence of species C_2H_3D and

C_2D_3H . Figure IX-4 shows the mass spectrum of a 50/50 mixture of C_2H_4 / C_2D_4 which had not been exposed to Zinc oxide, and the spectra of such a mixture after exposure to Zinc oxide at room temperature for 65 minutes and 135 minutes respectively. The ratios of the amplitude of the mass 32 peak to mass 31 peak, and mass 32 to mass 29 is given for each spectrum.

Obviously there is an exchange between the hydrogens and the deuterium. Thus the change in T_1 is as likely due to intramolecular as intermolecular interactions.

Quadrupolar relaxation in ethylene is not a possible relaxation mechanism.

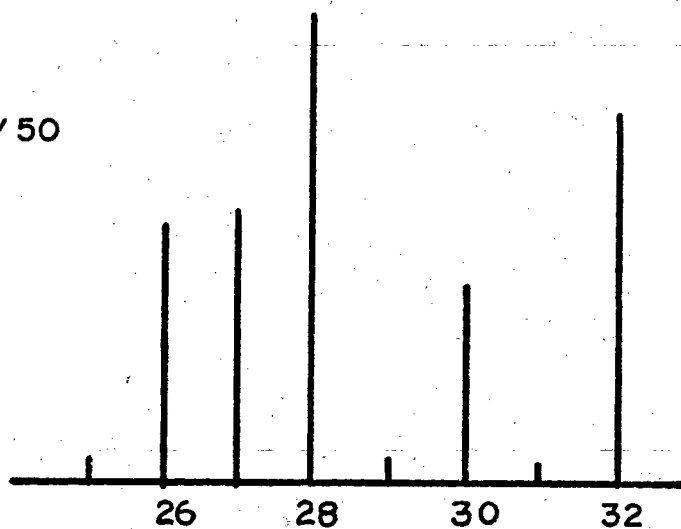
Any large amount of paramagnetic impurities would prove to be a significant relaxation mechanism. There is no proof that small amounts of such impurities are not there. The near agreement between the calculated and the measured relaxation times assuming only dipole-dipole relaxation suggests that the assumption that the levels of such impurities are such that their effect is negligible, is a reasonable one.

Chemical shift anisotropy is a field dependent mechanism; and since T_2 at 100 MHz is the same as T_2 at 15 MHz for several samples, has not been considered. There are two mechanisms as yet unseparated. They are intermolecular and intramolecular relaxation. Intramolecular relaxation depends on rotational diffusion,

C_2H_4 / C_2D_4 50/50

32:31 = 14.5

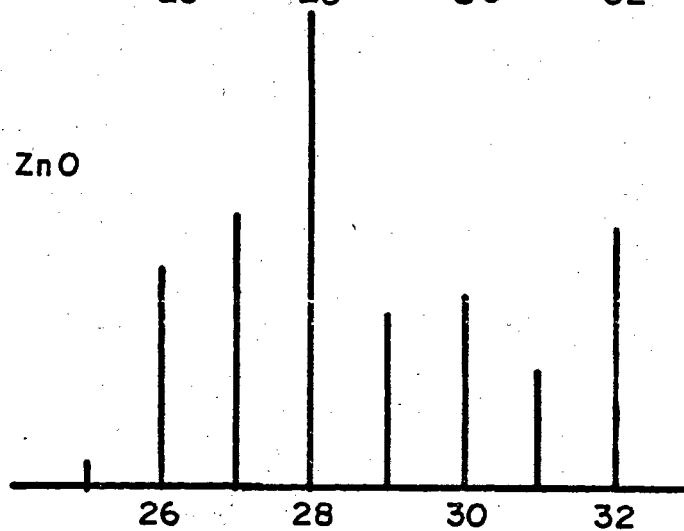
32:29 = 11.1



after 65 min over ZnO

32:31 = 2.2

32:29 = 1.5



after 185 min over ZnO

32:31 = .78

32:29 = .38

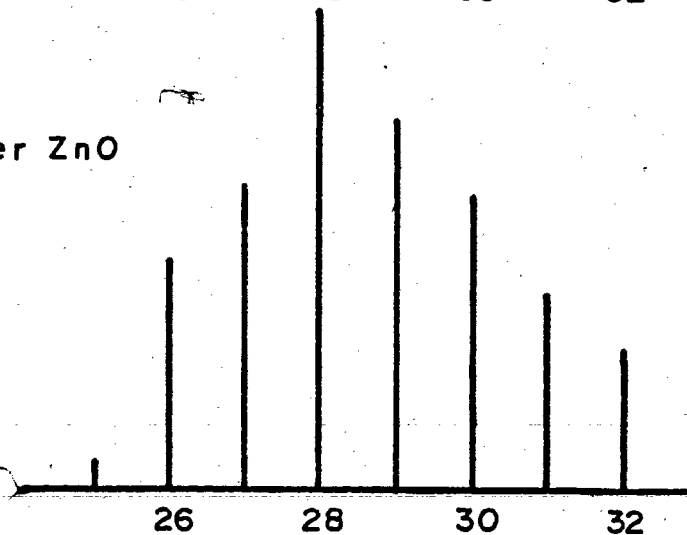


Figure IX -4

The mass spectra of perdeuterated and ordinary ethylene before and after exposure to ZnO.

intermolecular relaxation on translational diffusion.

Figure IX-1 suggests two motions causing the relaxation; one could be diffusion the other rotation, but it is unlikely that the correlation times for the two processes would be so close.

Since the Carr Purcell experiment carried out in a field gradient monitors the spins as they diffuse across the gradient (i.e. the translational diffusion) a series of such experiments were carried out.

The Meiboom Gill variation of the Carr Purcell experiment as described in Chapter 3 was used. However the pulse machine used had no method to create a field gradient in some orthogonal manner nor to get an accurate fix on what gradients were present.

The gradient was established by using the shim coils regularly used to trim the magnet homogeneity. These coils were not considered orthogonal and so the field gradient is a tensor whose diagonal elements differ. Since there were no ways of determining the components of this tensor it was assumed to be a scalar and was evaluated by measuring the T_2^* of a liquid of known T_2 from a free induction decay taken in the inhomogeneous field. The field "width" was determined from:

$$\text{IX-2} \quad 1/T_2 (\text{meas}) = 1/T_2 (\text{act}) + 1/T_2^*$$

where $T_2 (\text{act})$ is the known T_2 of the substance

involved, and

$$\begin{aligned} \text{IX-3} \quad T_2^k &= 1/\pi \Delta\nu \\ &= 2/\gamma \Delta H \end{aligned}$$

The field ΔH was divided by the diameter of the sample to determine the gradient.

T_2 (measured) was calculated from a least squares fit of an off resonance free induction decay of a doped water sample of known T_2 .

The amplitude of the echo produced in a Carr Purcell experiment at time 2τ after the 180° degree pulse is given by Farrar (1971) and Carr (1954).

$$\text{IX-4} \quad A(\text{echo}) = K[\exp(-t/T_2 - 1/3 \gamma^2 G^2 D \tau^2 t)]$$

where G is the field gradient, D the diffusion constant, and T_2 the real T_2 .

A least squares fit of $\ln A$ versus t has a slope m equal to

$$\text{IX-5} \quad m = [-K/T_2 - K/3 \gamma^2 G^2 \tau^2 D]$$

If one measures m as a function of τ (τ is half the time between 180° degree pulses) then a least squares fit of m versus τ^2 has a slope m' equal to

$$\text{IX-6} \quad m' = K/3 \gamma^2 G^2 D$$

and intercept equal to:

IX-7 $-K/ T_2$

Measurements were made on two different samples; a sample of coverage $1.3 \text{ std cm}^3/\text{gm}$ (ca. 1 monolayer) and the other $.6 \text{ std cm}^3/\text{gm}$ (the coverage that was used in making figure IX-1).

For both cases the measurements were made at two different field gradients.

Figure IX-5 shows a plot of the slopes of plots of $\ln A$ (echo at 2τ) versus time; versus the square of the separation time of the 180° degree pulses for the sample of high coverage. Obviously some diffusion is taking place. In figure IX-5 the field gradient is such that T_2^* was .7 msec.

Measurement of D for field gradients represented by T_2^* of .7 and 1.5 msec gave diffusion constants within 10% of each other.

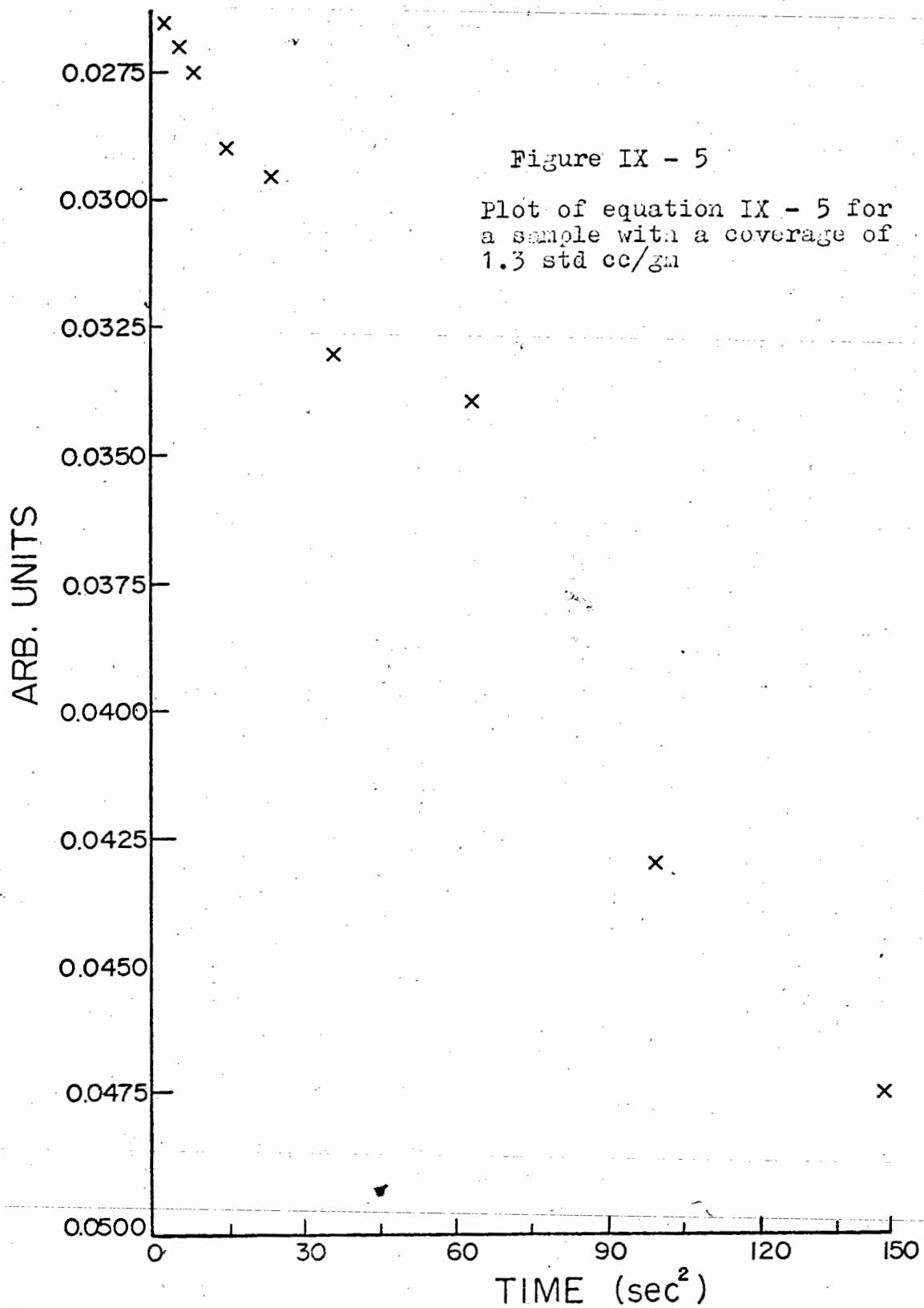
The average value of these D 's is $1.1 \times 10^{-7} \text{ cm}^2/\text{sec}$ which from the relationship:

$$\text{IX-8} \quad \tau(\text{diff}) = d^2/4D$$

(the relationship cited for two dimensional diffusion (Thompson 1965)), or

$$\text{IX-8b} \quad \tau(\text{diff}) = d^2/6D$$

(the relationship for three dimensional diffusion



(Resing 1968).

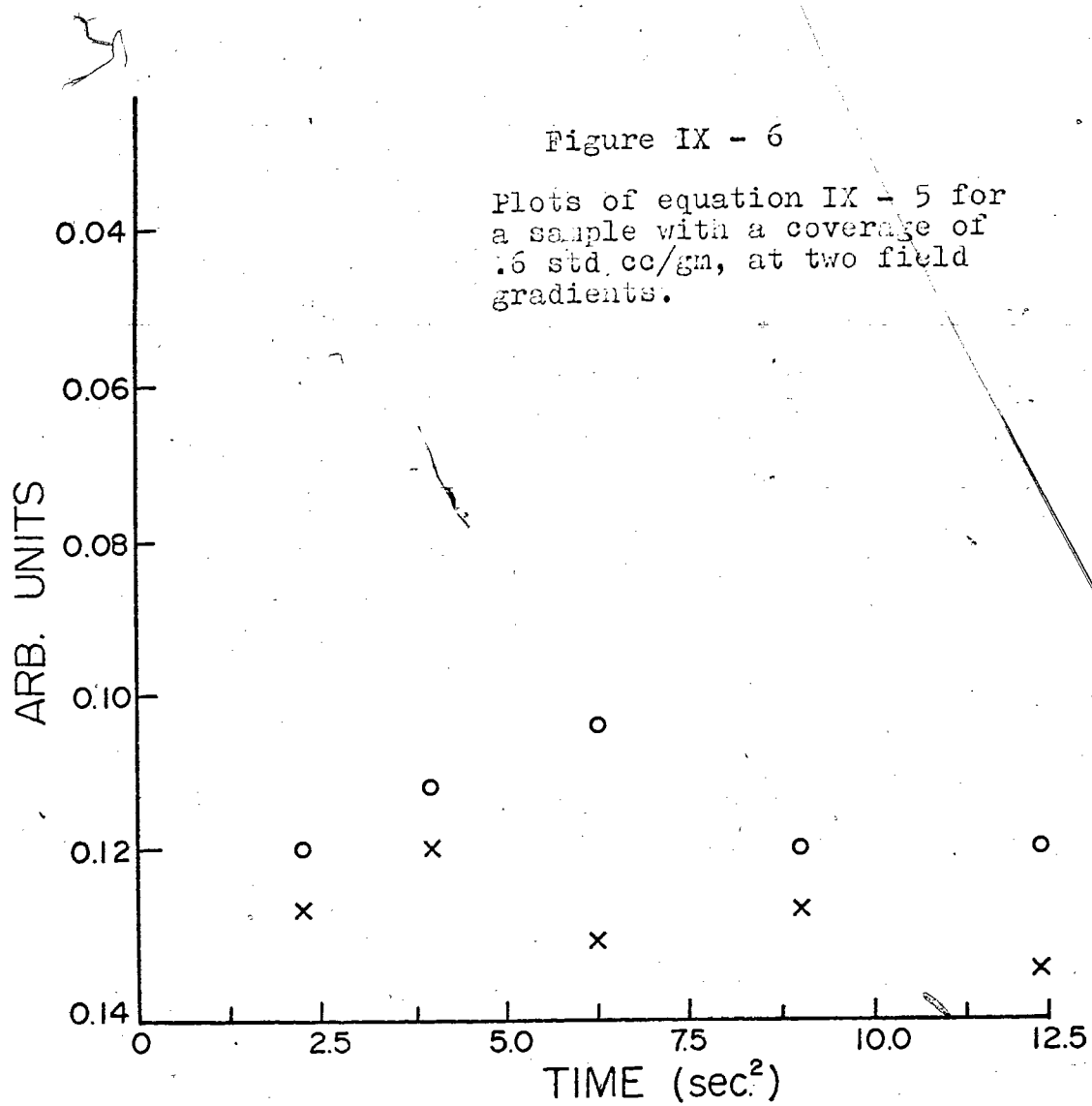
gives a tau diffusion between 1×10^{-8} and 1×10^{-9} if one assumes a jump distance of two angstroms. The standard deviations of the slopes were of the order of 2% and of the intercept 1%. T_2 was known to within 2%. For the high coverage case T_2^* was only known within 5% making G^2 only within 10%. Thus the error in D is of the order of 15%.

The tau diffusion calculated for this sample was near enough to the minima of Figure IX-1 that it was deemed necessary to measure D for the low coverage case.

Figure IX-6 shows the slope for two different field gradients. In both cases the least squares fit slope was positive and small, reflecting only an error in the measurement of T_2 . That is to say no diffusion was measureable across the gradients used ($T_2^* = .59$ and $.73$ msec). A diffusion constant that would produce one of the minima in Figure IX-1 would be easily measureable with the field gradients available, as is shown by the experiment on the high coverage sample.

It becomes appropriate to discuss these results particularly in relationship to Figure IX-3. From the variation of T_1 and T_2 with coverage it is evident that relaxation is more efficient at low coverages, which implies that there is less motion at low coverage.

Intramolecular relaxation is not going to have a



significant coverage dependence at low coverages, but certainly can at higher coverages. Intermolecular relaxation will have a coverage dependence at all coverages.

At low coverages the diffusion correlation time is larger, and as shown such slow motions can effect T_2 without effecting T_1 .

In summary then we have T_1 relaxation dominated by intramolecular relaxation, and T_2 relaxation caused to some extent by both intra and intermolecular relaxation at low coverages.

As the coverage increases there are contributions to both T_1 and T_2 by inter and intramolecular relaxation.

Application of the Model of Intramolecular-Dipole Dipole Relaxation Through Anisotropic Rotation

It is interesting to find out what happens if one supposes that both of the minima in Figure IX-1 are due to motions causing intramolecular dipole dipole relaxations, that is there is anisotropic motion due to the surface interfering with normal rotations.

Figure IX-1 reveals a "freezing out" of motion at 300 degrees C and at 240 degrees C. From the relationship $\omega_0 \tau = .616$ (Abragam 1961), we have a tau values of 6.55×10^{-9} sec for each motion at one of the two temperatures. The relationship (deBoer 1958):

$$\text{IX-9} \quad \tau = \tau_0 \exp(H/RT)$$

gives the values of each tau at the other temperature. Using H as measured from the outside slopes of figure 1 one can calculate the tau(i) at all other temperatures, and thus calculate T_1 and T_2 as a function of temperature so as to compare the model with experimental results. This data was used in Woessner's (1963) model, a model which allows motion parallel to the surface with one correlation time, and motion perpendicular to the surface with another correlation time (see Chap. 5).

By averaging the spherical harmonics involved in these expressions over all space with the limits of $0-2\pi$ for the azimuthal angle (motion parallel to the surface) and with the limits of $\pi/4$ to $\pi/2$ for the longitudinal angle (motion perpendicular to the surface) the calculated T_1 and T_2 were 35 msec and 29 msec respectively, at 300 degrees. The measured relaxation times were 36 msec and 8 msec at 300 degrees.

This model does not allow one to consider motions about any particular rotational axis and thus results in a rather vague picture so it was at this point that the model presented in Chapter 5 was derived.

The chemical shift data and the data of Kokes already mentioned are consistent with ethylene lying on the surface as a π -complex. Consider such a molecule lying flat on

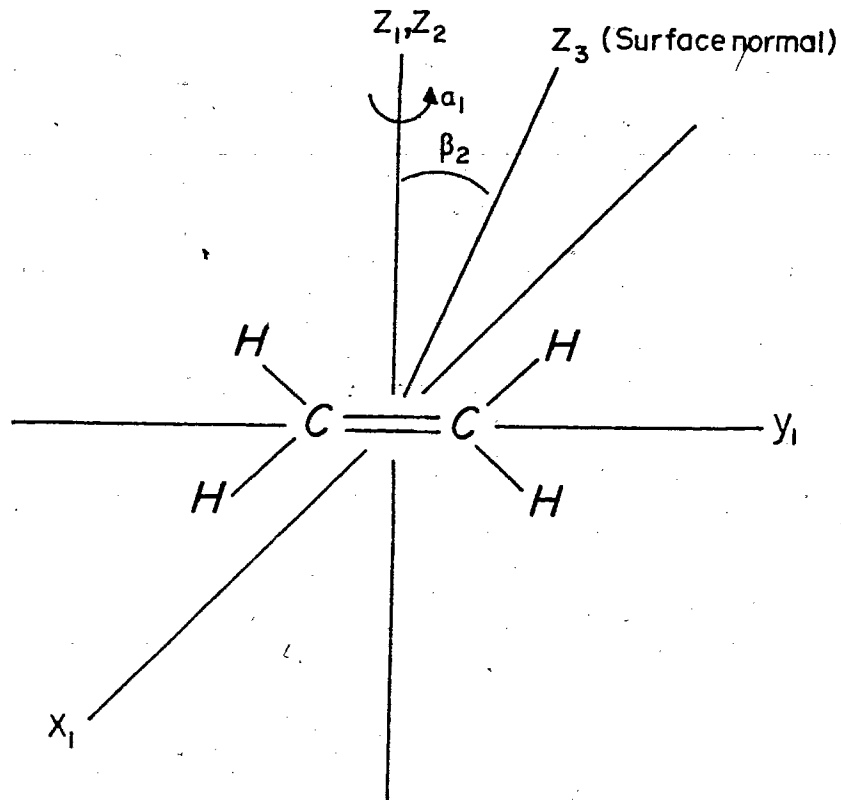


Figure IX - 7

Ethylene lying on a surface plane, rotating about the two fold axis which is perpendicular to the plane, while wobbling, about the surface normal.

the surface rotating about the two fold axis perpendicular to the plane of the molecule while this two fold axis wobbles back and forth in relationship to the surface normal as shown in figure IX-7.

The most convenient molecule fixed frame to use is that w all $\theta_{ij} = \pi/2$ and all $\phi_{ij} = 0$. In this frame using the notation of equation V - 7:

$$\text{IX-10 } \langle Y_{20}(\theta\phi) Y_{20}^*(\theta\phi) \rangle = 1$$

$$\langle Y_{21}(\theta\phi) Y_{21}^*(\theta\phi) \rangle = 0$$

$$\langle Y_{22}(\theta\phi) Y_{22}^*(\theta\phi) \rangle = 1$$

Now we want to allow for motion about the two fold axis. Alpha (1) beta (1) gamma (1) are the Euler angles between the molecule fixed frame and the rotational axis fixed frame. The rotation about the two fold axis is described by letting $\alpha(1) = 0$ 2π , while $\beta(1) = \gamma(1) = 0$. Then:

$$\text{IX-11 } \langle Y_{20}(\theta_2 \phi_2) \cdot Y_{20}^*(\theta_2' \phi_2') \rangle = 1$$

$$\langle Y_{21}(\theta_2 \phi_2) \cdot Y_{21}^*(\theta_2' \phi_2') \rangle = 0$$

$$\langle Y_{22}(\theta_2 \phi_2) \cdot Y_{22}^*(\theta_2' \phi_2') \rangle =$$

$$\exp(-4\tau/\tau_{a_1})$$

To allow for the wobble of the two fold axis in

relation to the surface normal the averages in

$$D_{MM'}^2(\alpha_2 \beta_2 \gamma_2) D_{MM'}^{2*}(\alpha_2' \beta_2' \gamma_2')$$

are taken from $\beta_2(2) = \theta \rightarrow w$ ($w =$ wobble angle) while $\alpha_2(2) = \theta \rightarrow 2\pi$, so that:

$$\begin{aligned} \langle Y_{20}(\theta_3 \phi_3) \cdot Y_{20}(\theta_3' \phi_3') \rangle \\ = 3/4 \langle \sin^4 \beta_2 \exp(-\tau/\tau_{\beta_2}) \\ \cdot \exp(-4\tau/\tau_{\alpha_2}) \cdot \exp(-4\tau/\tau_{\alpha_1}) \\ + 1/4 \langle (3\cos^2 \beta_2 - 1)^2 \exp(-\tau/\tau_{\beta_2}) \rangle \end{aligned}$$

$$\begin{aligned} \langle Y_{21}(\theta_3 \phi_3) Y_{21}(\theta_3' \phi_3') \rangle \\ = [1/4 \langle \sin^2 \beta_2 (1 + \cos \beta_2)^2 \rangle \\ + 1/4 \langle \sin^2 \beta_2 (1 - \cos \beta_2)^2 \rangle] \\ \exp\{-\tau \cdot [1/\tau_{\beta_2} + 4/\tau_{\alpha_2} + 4/\tau_{\alpha_1}]\} \\ + 3/2 \langle \sin^2 \beta_2 \cos^2 \beta_2 \rangle \exp(-\tau/\tau_{\beta_2}) \end{aligned}$$

$$\begin{aligned} \langle Y_{22}(\theta_3 \phi_3) Y_{22}^*(\theta_3' \phi_3') \rangle \\ = [1/16 \langle (1 + \cos \beta_2)^4 \rangle + 1/16 \langle (1 - \cos \beta_2)^4 \rangle] \\ \exp\{-\tau [1/\tau_{\beta_2} + 4/\tau_{\alpha_2} + 4/\tau_{\alpha_1}]\} \\ + 3/8 \langle \sin^4 \beta_2 \rangle \exp(-\tau/\tau_{\beta_2}) \end{aligned}$$

The averages in all cases were performed as follows:

$$\begin{aligned} \langle D_{MM'}^2(\alpha\beta\gamma) D_{MM'}^{2*}(\alpha\beta\gamma) \rangle = \\ 1/\int_0^{2\pi} d\gamma \int_0^{2\pi} d\alpha \int_0^w \sin\beta d\beta \\ \cdot \int_0^{2\pi} d\gamma \int_0^{2\pi} d\alpha \int_0^w F(\alpha\beta\gamma) \sin\beta d\beta \end{aligned}$$

In order to use equations IV-13 and IV-14 we need to evaluate all the $J_i(\omega)$

From the definition of a Fourier transform:

$$IX-13 \quad J_k(\omega) = 2/5 \int_0^{\infty} \langle Y_{2k}(\theta\phi) Y_{2k}^*(\theta\phi) \rangle \exp(i\omega\tau) d\tau$$

where the denominator of the constant comes from the relation given in equation V-4 and the numerator comes from the change of limits from minus infinity to plus infinity, to zero to infinity and the assumption that the correlation function is real and even (Abragam 1961).

Substituting into 13:

$$IX-14 \quad J_k(\omega) = 2/5 \{ (1/4 \langle \sin^2 \beta_2 (1 + \cos \beta_2)^2 \rangle \\ + 1/4 \langle \sin^2 \beta_2 (1 - \cos \beta_2)^2 \rangle) \tau_T / (1 + \omega^2 \tau_T^2) \\ + 3/2 \langle \sin^2 \beta_2 \cos^2 \beta_2 \rangle \tau_{\beta_2} / (1 + \omega^2 \tau_{\beta_2}^2) \}$$

$$J_2(\omega) = 2/5 \{ (1/16 \langle (1 + \cos \beta_2)^4 \rangle \\ + 1/16 \langle (1 - \cos \beta_2)^4 \rangle) \tau_T / (1 + \omega^2 \tau_T^2) \\ + 3/8 \langle \sin^4 \beta_2 \rangle \tau_{\beta_2} / (1 + 4\omega^2 \tau_{\beta_2}^2) \}$$

$$J_0(0) = 2/5 \{ 3/4 \langle \sin^4 \beta_2 \rangle \tau_T \\ + 1/4 \langle (3\cos^2 \beta_2 - 1)^2 \rangle \tau_{\beta_2} \}$$

$$\text{where: } 1/\tau_T = 1/\tau_{\beta_2} + 4/\tau_{d_i}$$

These spectral densities can then be used in the expressions:

$$IX-15 \quad 1/T_1 = 3/2 \delta^4 \chi_n^2 I(I+1) \{ J_1(\omega) + J_2(2\omega) \}$$

$$1/T_2 = \delta^4 \chi_n^2 I(I+1) \{ 3/8 J_0(0) + 15/4 J_1(\omega) + 3/8 J_2(2\omega) \}$$

The expression IX-14 depends on correlation times associated with motions of alpha(1), alpha(2) and beta(2) referred to as tau(alpha1), tau(alpha2) and tau(beta2). In constructing the model one has to almost arbitrarily assign tau values using figure IX-1 to these particular motions. However some intuition also helps.

If the ethylene is pi bonded then motion of alpha(1) (rotation about the pi bond) will be easiest, that is will be the hardest to "freeze out", and in this case could be the low temperature of figure 1.

Thus from IX-9

$$= 1.57 \times 10^{-9} \text{ at } 300 \text{ degrees}$$

$$= 6.55 \times 10^{-9} \text{ at } 240 \text{ degrees}$$

Motion in alpha(2) should be rather hindered by the surface, while motion in beta(2) (a wobble of the rotational axis, with respect to the surface normal) should be more facile.

Assigning the high temperature minimum to motion of beta(2) gives from IX-1

$$= 6.55 \times 10^{-9} \text{ at } 300 \text{ degrees}$$

$$= 2.74 \times 10^{-8} \text{ at } 240 \text{ degrees}$$

Since we have no minimum to assign to tau(alpha2) meaning that it either does not exist, or is outside our limits we can assign it a value of infinity.

Calculations based on such a model are dependent on two parameters. The first and most important is the activation energy of the process, the second is the wobble angle β (2).

In order to examine this model more critically values of T_1 and T_2 were calculated for each temp using equations IX-15 .

Using the activation energy evaluated from the least squares fit slope of the outsides of figure IX-1 one can evaluate each tau as a function of temperature.

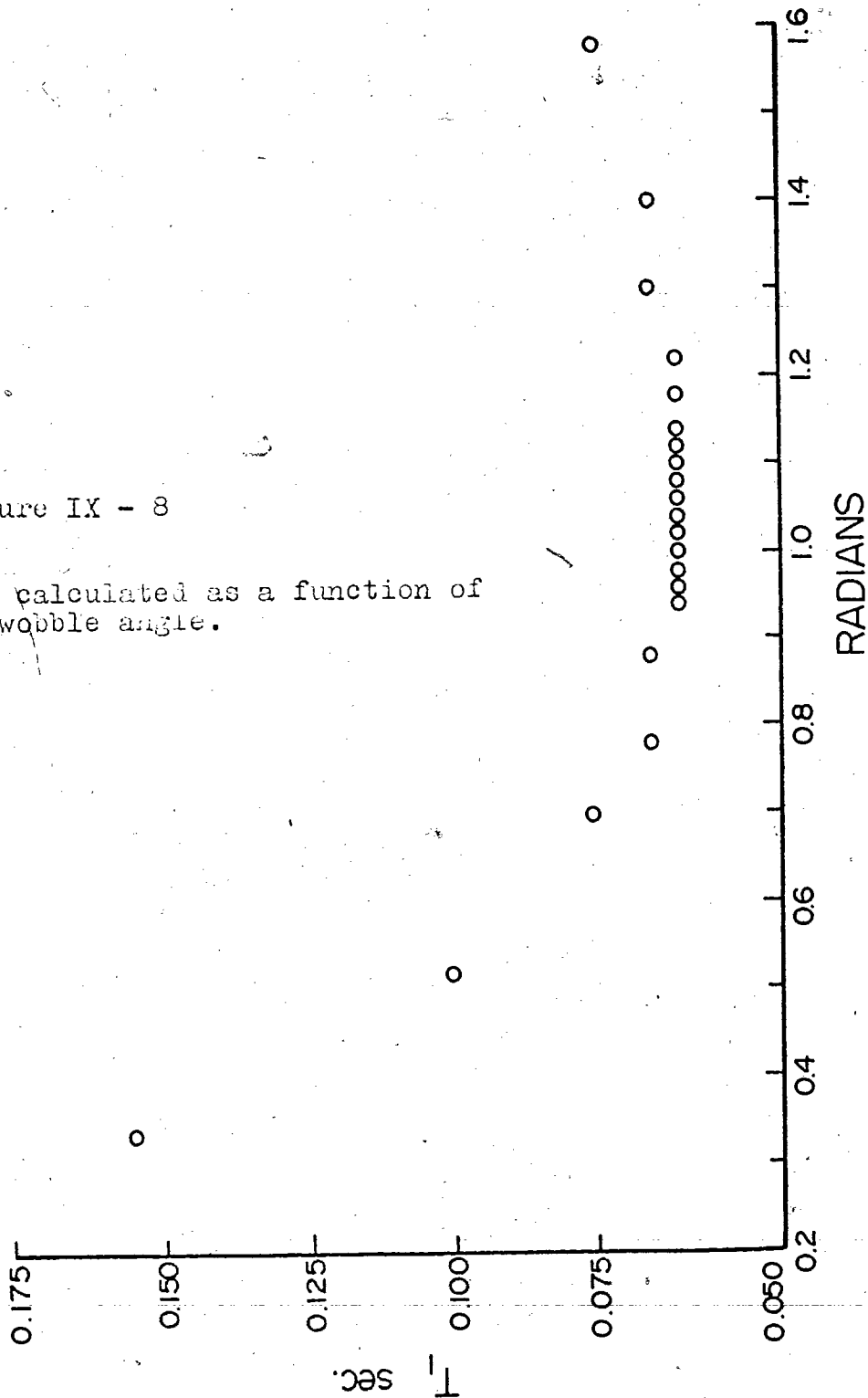
T_1 was also evaluated as a function of the wobble angle w . Figure IX-8 is a plot of T_1 versus the wobble angle. It shows a minimum at approximately 60 degrees, that is a wobble angle of 60 degrees would shorten T_1 the most.

Of course it is possible that w could also be a function of temperature, as well as tau. It is also conceivable to introduce a distribution in w , rather than evaluate the integrals over a single value.

Figure IX-9 shows a plot of T_1 calculated using equation IX-15 versus inverse temperature, calculated using the activation energy for each process as 2800 cal. The slopes of the outsides lines in figure 1 give activation energies of $2.8 \pm .5$ and $3.2 \pm .3$ kcals. The position of the minima from equation IX-7 changes considerably over such a range of activation energies.

Figure IX - 8

$T(1)$ calculated as a function of the wobble angle.



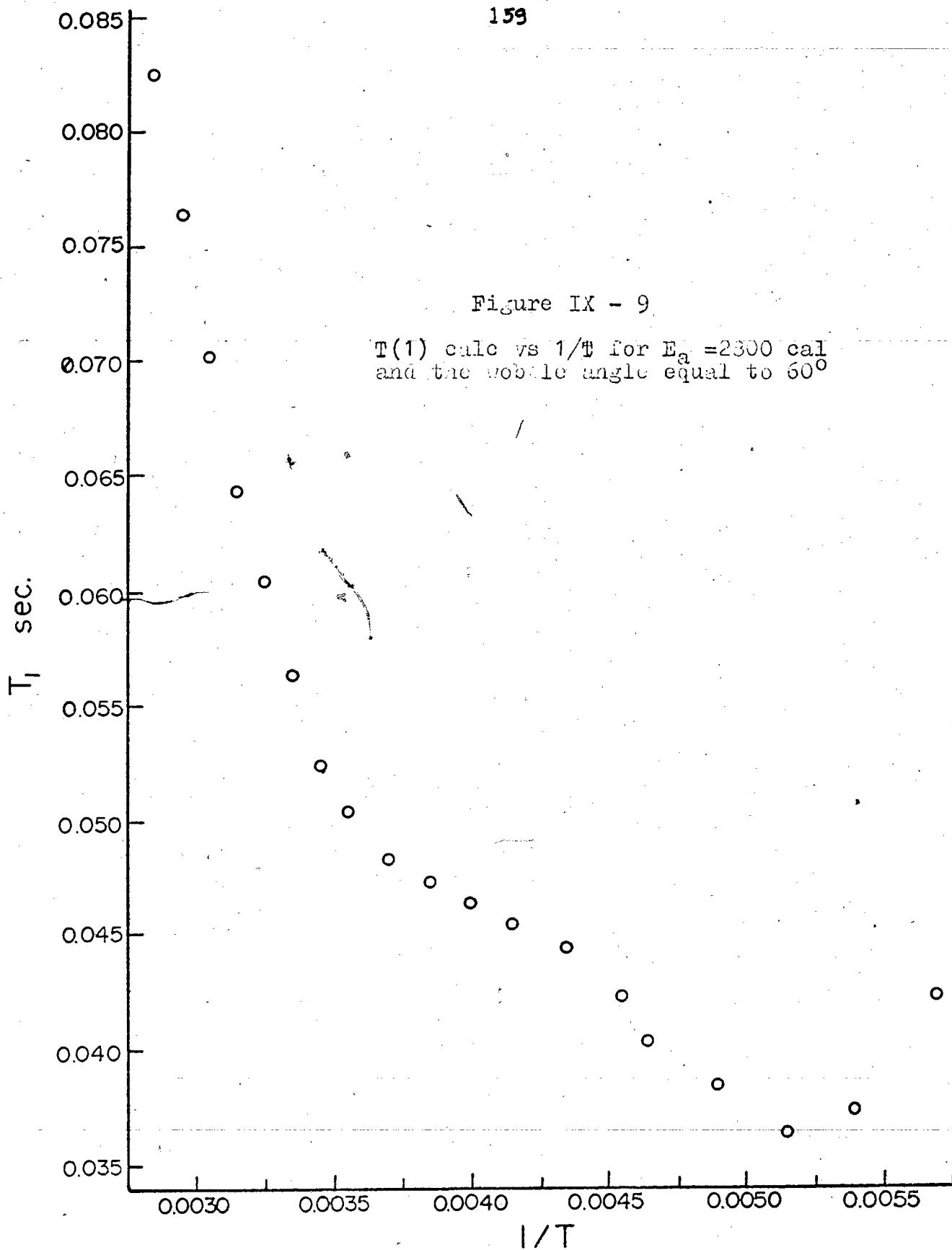


Figure IX-9 shows that the model produces T_1 's which are in the right ballpark even using a fixed wobble angle. The minimum at 300 degrees is not so deep, that at 240 degrees is deeper. This model then predicts T_1 's which are longer than the measured values at high temperatures and shorter than the measured values at low temperature.

Some caution is due in seeking an answer as to why. The points measured in figure one have larger error bars at lower temperatures, but more important as explained in Chapter 7 the temperature controller was of a rather poor quality and temperatures are unlikely to be better than 3 degrees.

An improvement can first be sought by making the angle over which each of the elements of the rotation matrix is integrated a function of temperature. Figure IX-10 shows the calculated values of T_1 using activation energies of 2800 calories but carrying the wobble angle as a function of temperature.

The wobble angles were weighted using the Verhulst equation, which is an S shaped function, an example of which is shown in figure IX-11.

The Verhulst equation is:

$$\text{IX-16} \quad F(T) = F(O) / \{ F(O) + \{1 - F(O)\} \exp -kT \}$$

where $F(O)$ = minimum value/maximum value.

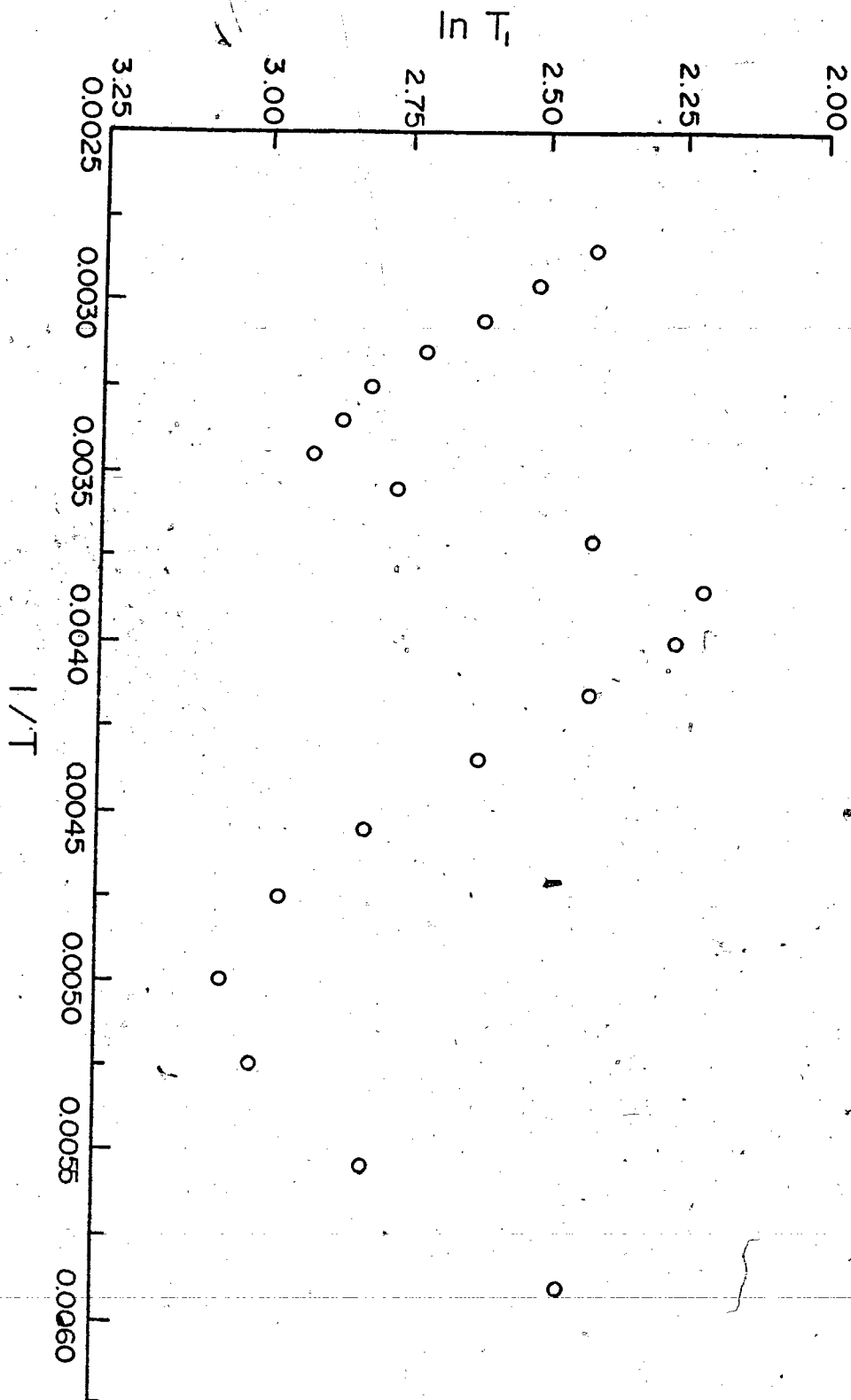
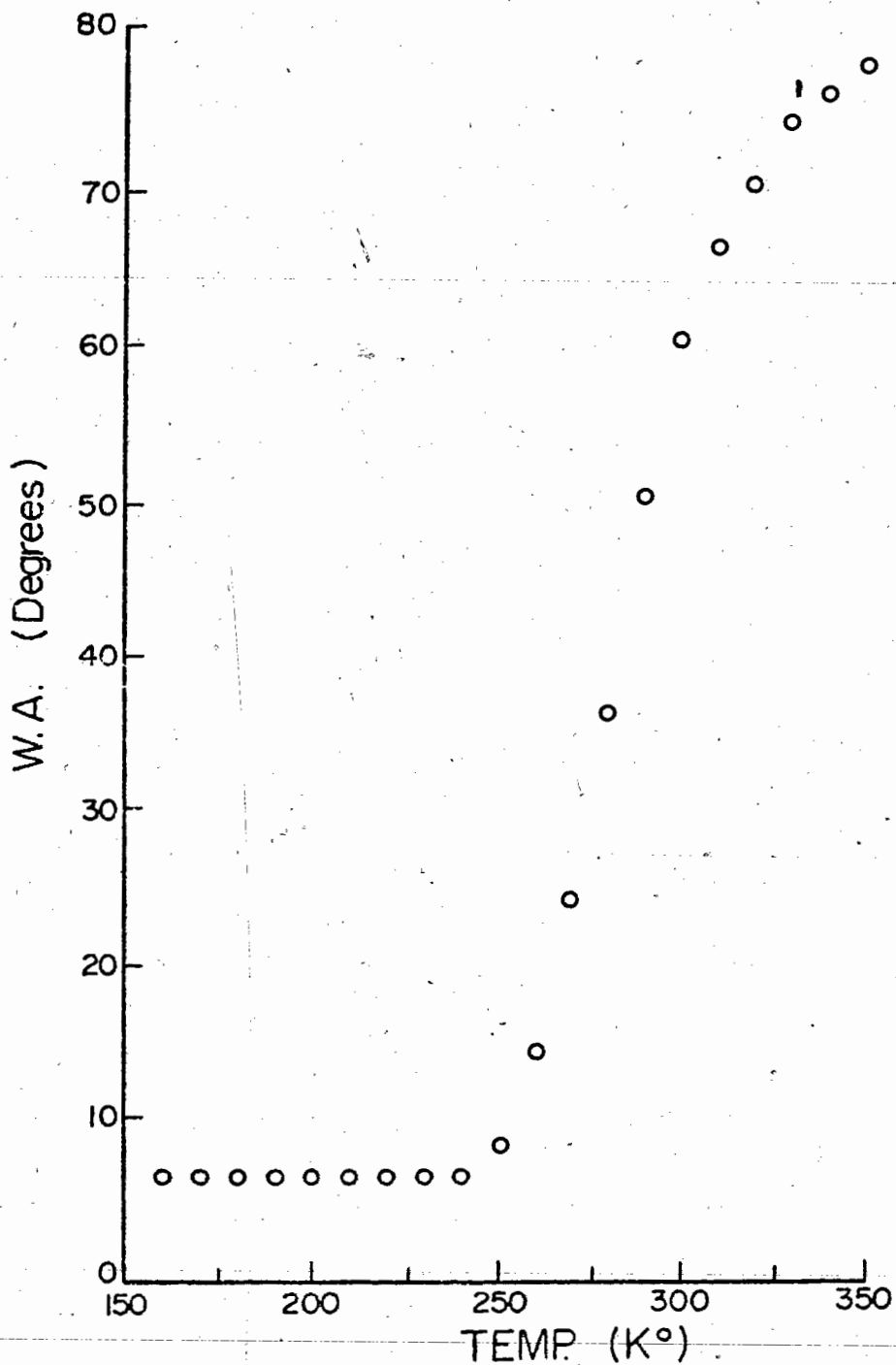


Figure IX -10
 $T(1)$ calculated with a wobble angle which is a function of temperature.

162
Figure IX - 11

The Verhulst Function Times the Wobble Angle Used in Weighing T(1) in Figure IX-10



This equation corresponds to the adsorbed species being able to wobble through some angle which is a function of temperature, but which reaches a maximum value at some temperature.

Again the low temperature minimum is not the same temperature as figure 1, although the calculated values are now closer and the depth of the minima more similar. Figure IX-12 shows T_1 calculated and T_1 measured where T_1 calc. was calculated using an activation energy of 2800 calories for both processes.

The fact that the minimum at low temperature is displaced from the minima for the calculated values raises some important questions about the assumptions one has made to date.

A More Critical Appraisal of this Model

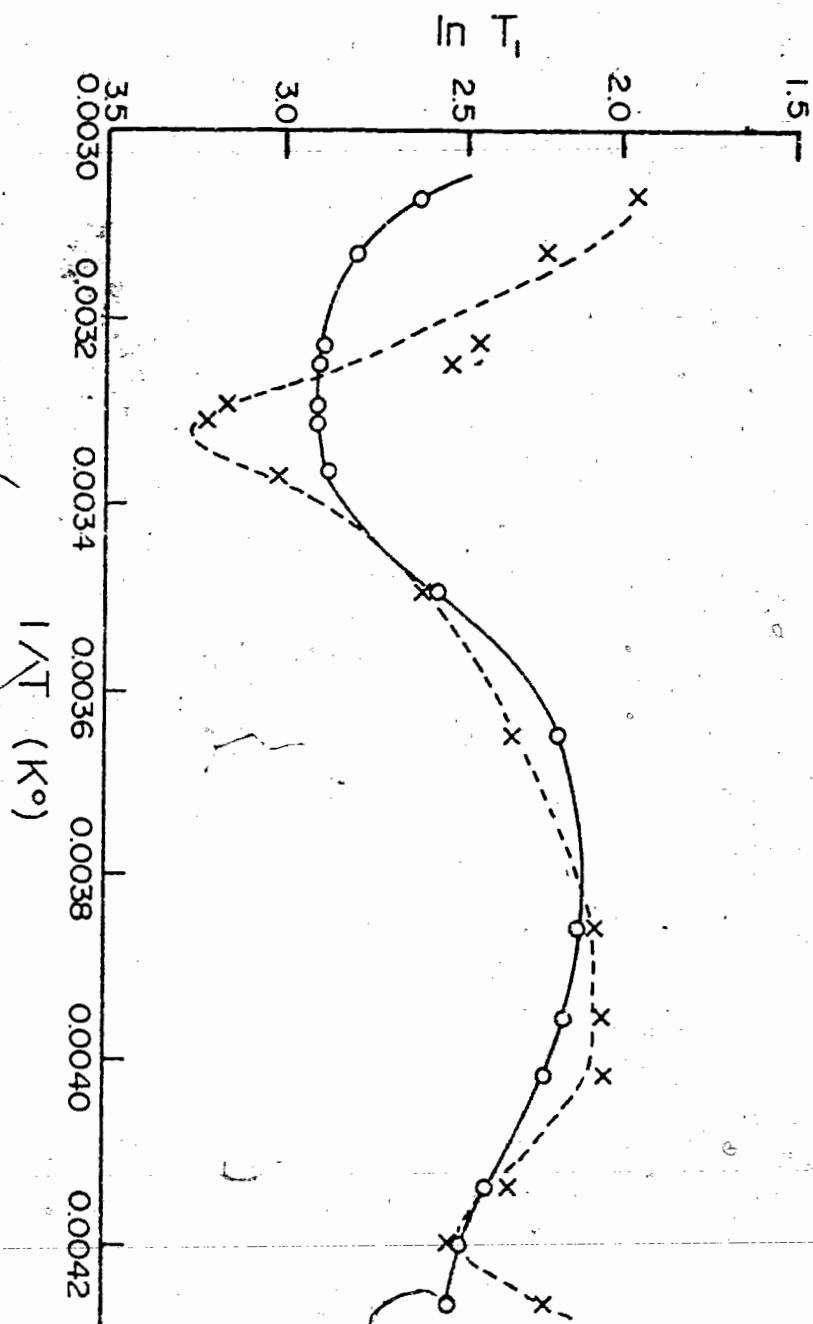
When there is isotropic motion and one correlation time, the sum of $J_1(\omega)$ and $J_2(2\omega)$ have a single maximum (and thus T_1 goes through a minimum) when plotted against tau (Abragam 1961). It is easy to verify that this minima occurs at $\omega\tau = .616$.

When there is no isotropic motion we have seen that multiple correlation times occur, and $J_1(\omega) + J_2(2\omega)$ can have multiple maxima. It is often stated that these maxima will occur at $\omega\tau = .616$ (Woessner 1961, Pfeiffer 1971, Abragam 1961). It can be shown that this

Figure IX - 12

Calculated and measured values of $T(1)$ for ethylene adsorbed on ZnO.

x - measured $T(1)$
o - calculated $T(1)$



is not necessarily true, and in fact will only be true in some very particular situations.

The inverse of T_1 (R_1) depends on the spectral densities $J_1(\omega)$ and $J_2(2\omega)$. In the model presented these can be written as:

$$\text{X-17} \quad R_1 = k \{ A_1 \frac{z}{1+\omega^2 z^2} + A_2 \frac{y}{1+\omega^2 y^2} \\ + A_3 \frac{z}{1+4\omega^2 z^2} + A_4 \frac{y}{1+4\omega^2 y^2} \}$$

where $1/z = 1/y + 4/x$ (τ_T of equation IX-14)

and x, y are the correlation times for rotation and wobbling respectively, and the A_i are the averaged values of the $D_{mm'}^2$.

If one considers z to be only a function of x , (that is y is long c.f. to x) then finding the partial derivatives of R w.r.t. z and y and equating them to zero locates the minima.

Solutions for the resulting two equations were found numerically. The roots of the resulting equations varied between .984 and .999 and between .910 and .966 for the derivative w.r.t. z , and x respectively, depending on the values of the A_i .

Before probing any deeper it is worthwhile to see what these new values of τ at the minima do to the calculated values of T_1 .

The above implies that one correlation time is about 1×10^{-8} at 300 degrees C while the other is about $4 \times$

10^{-8} at 240 degrees or vice versa. This implies that the rotation is now slower than the wobble even if one assigns the minimum at 240 degrees to τ or in this case exclusively to rotation.

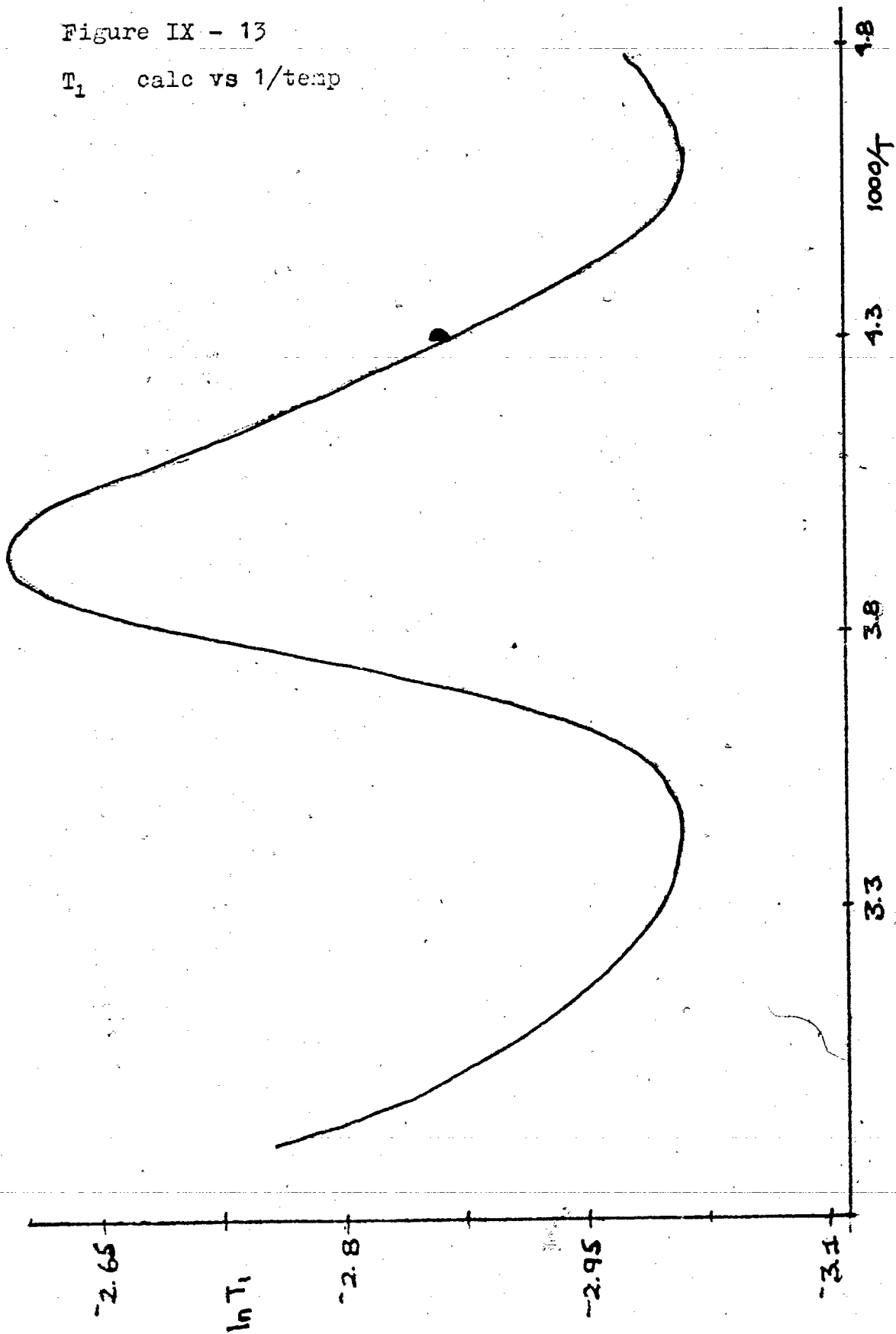
Some attempts in this direction were made, and for example the calculated values for the assignment given above (calculating the average values of the D_{mm}^2 as before), are plotted in Figure IX-13. The low temperature minimum is now much closer to where it is in the measured data. The best fit is obtained using $w_y = .95$ and $w_x = .99$ rather than $w_z = .99$, but a really good fit is not obtained, and it is arbitrary to assume that $\tau(\alpha)$ causes a minimum.

At this point it can be seen that $\tau(\alpha)$ and $\tau(\beta)$ have frequencies that do not differ greatly so that it is unreal to say that z is independent of y .

Differentiation of IX-17 w.r.t. x , and y rather than z and y point out some further problems.

The derivative w.r.t. y is dominated by second and fourth terms in IX-17 and functionally does not behave radically differently than the function derived from assuming that z was independent of y . $(dR_1/dy)_x$ has a root for all values of x and although it is dependent on x this dependence is such that the value of the root changes from .91 to 1.08 as x shifts from 5×10^{-9} to 4×10^{-8} .

Figure IX - 13

 T_1 calc vs $1/\text{temp}$ 

However $(d R_1 / dx)_y$ is highly related to the values of y , and is found to have no real roots for $y < 1.05 \times 10^{-8}$.

It is apparent that when the correlation times are of comparable frequency the model breaks down.

The situation is even more complex from a physical point of view, since if this condition holds then the form of the correlation function chosen is invalid, invalid in fact for two reasons.

The use of the correlation function in the form:

$$1x-18 \quad \langle Y_{2M}(\theta(t)\phi(t)) Y_{2M}^*(\theta(t')\phi(t')) \rangle = \\ \langle Y_{2M}(\theta\phi) Y_{2M}(\theta\phi) \rangle (\exp(-\tau/\tau_c))$$

depends on the process being stochastic and interrupted many times during the period of $1 \tau_c$.

If there is little translational diffusion on the surface then the rotational motion is interrupted by any potential energy barrier to rotation, and by the wobble. Similarly the wobble is interrupted by some potential barrier and by the rotation.

If the frequency for the rotation and wobble is close, then it is possible that neither is getting interrupted often during the period of $1 \tau_c$. Furthermore the process is no longer stochastic. There is some correlation between the two motions.

Attempting to treat this problem correctly has

devastating consequences. Firstly one needs to use some other functional form for the correlation function, since it is likely that one or the other motion will continue coherently for some number of motions. Secondly if the two motions are cross correlated then the the number of terms in the spectral densities goes up immensely. Each of the terms of the form:

$$\text{IX-19} \quad \langle D_{M'}^2(\alpha\beta\gamma) D_{MM'}^2(\alpha\beta\gamma) \rangle$$

now becomes five separate terms. Quite literally a single correlation function would then have some 225 terms in it. Such a mathematical surface would be very complex indeed to handle.

Comparison of Measured and Calculated Values of T_2

One can use the $J_i(\omega)$ to find the values of the intramolecular contribution to T_2 as another check on this model. Substitution of the $J_i(\omega)$ into equation IX-15 yields a T_2 shorter than the T_1 , (i.e. the intramolecular contribution to T_2 is different than T_1) but is approximately a factor 4 longer than the measured T_2 's.

T_2 is shortened beyond the calculated value that assumes intramolecular dipole dipole relaxation only. Figure IX-3 implies a coverage dependent process that at least at low coverages affects T_2 but not T_1 . This

would appear to be an intermolecular contribution. A model consistent with the T_2 measurements taken in a field gradient and with the data of figure IX-3 would be intermolecular dipole-dipole relaxation caused by diffusion, with shorter relaxation times at lower coverages being a result of slower diffusion at lower coverages.

Summary of Conclusions to be Drawn From the Relaxation Analysis

In the temperature and coverage range of these experiments we are able to paint some pictures of what is going on on the surface.

At coverages of about .4 monolayers we have a system where two intramolecular motional processes occur at similar frequencies. These two processes have a much shorter correlation time than that of translational diffusion across the surface. A model consistent with the measured times suggests that these two motions may be the rotation of the ethylene about the C_2 axis perpendicular to the plane of the molecule, and the motion of this axis with respect to the surface normal.

As the coverage increases translational diffusion also increases, and begins to have an effect on relaxation.

Chapter 10

Overall Conclusions and Further Work

My first question was related to the possibility of using conventional NMR spectrometers for doing catalytic research.

The answer to this question while positive needs to be made with severe reservations. In order for studies to be conclusive about reactive species on the surface experiments need to be carried out at low coverages. We are unable to conclude anything about the first fraction of a monolayer that goes on the surface simply because the apparatus available has poor capabilities for measuring broad lines at low concentrations. At the same time the pulse NMR spectrometer available, while more appropriate for the study of a broad line system, does not separate species of only slightly different chemical shift, because of the low field involved for proton work at 15 MHz.

Continuous wave NMR techniques are too costly in expenditure of time to be considered a profitable way of investigating heterogeneous catalysis. It is desirable to be able to measure small quantities of a species which may be relaxing quickly, and for this, time-averaging pulse and Fourier transform techniques at high fields seem able to supply more information much more quickly.

While it is recognized that NMR techniques are costly

also of money, and consequently spectrometers are unlikely to be made available for only one or two research projects, it should be noted that for a research instrument not under the constant care of a technician there is some optimum rather small number of projects that should be carried out at once. Too many workers using the same apparatus leads to scheduling problems of a severe nature, an inordinate amount of down time, the frustration of setting up special experiments several times over, and periods of waiting while fields stabilize after being changed.

Conclusions About Measurements of Olefins on Zinc Oxide

I have been able to study ethylene adsorption on zinc oxide from coverages between .2 and 1 monolayer. While there is no evidence for species other than the ones identified neither is there evidence that they do not exist. However from .2 of a monolayer on up the species on the surface retains olefinic character, and experiences a downfield shift from ethylene in the gas phase, with the greatest shift at the lowest coverage. This shift is most consistent with donation of electrons to the surface; consequently, in contrast to the conclusions of Kokes et al (1972) the adsorption site is likely to be a zinc atom. The carbon spectrum of ethylene on ZnO although at

higher coverages, also supports this conclusion, in that the carbons are shifted downfield.

Studies of propene adsorbed on zinc oxide were also done. Again at low coverages while olefinic character was maintained a downfield shift characteristic of electron donation to the surface was experienced. More evidence for a strongly bound species below coverages of .25 monolayers has been shown, in that the signal becomes too broad to observe.

Other adsorbed species were studied with only a small amount of success. No signal was observed for H_2 on a surface despite knowledge that the concentrations were high. This negative result does suggest a rather tight binding to the surface.

Some ^{19}F substituted ethylenes were studied and were found to behave rather differently on the surface than ethylene. Reasonably large upfield chemical shifts were experienced by the fluorines in all cases.

Some shift measurements were made with physisorbed species, mostly for comparative reasons. The shift in these cases can be explained on the basis of Van der Waals interactions.

The problems on measuring changes of chemical shift on adsorption have been examined, and it was concluded that an empirical correction for magnetic susceptibility was more appropriate than a theoretical correction.

A model has been constructed for the interpretation of nuclear magnetic relaxation experienced by species adsorbed on a surface. This model is much more flexible than those previously developed, since it allows for calculation of all the spectral densities at once, whether or not they are functionally dependent on the frequency. Furthermore it is possible to consider many different possible motions without using a different set of transformations.

Application of this model to ethylene adsorbed on zinc oxide with the assumption that the molecule was relaxing through a rotation about the C_2 axis perpendicular to the double bond, while this axis wobbled with respect to the surface normal, closely reproduced the experimental data.

On closer examination it was found that any model which included a reduced correlation function of the form $\exp(-\tau/\tau_c)$ involved a bad assumption for this particular system. This is so because there are two correlation times that are quite close, and thus the motions involved are unlikely to be stochastic.

Measurement of the translational diffusion coefficient was found to be possible only at higher coverages with the spectrometer available. I was able to measure the diffusional constant at coverages approaching a monolayer, and to show that translational diffusion has

little effect on T_1 at low coverages, and thus is not the cause of one of the minima of the T_1 vs. $1/\text{temp}$ measurements.

Further Work

A large amount of work is available for researchers in this area.

Much useful information about surface interactions would be gained by the tabulation of chemical shifts of adsorbed species on various surfaces as a function of coverage and in relation to the chemical shift of the free species. Such information could undoubtedly be correlated with other surface measurements and models, particularly with surface potential, I.R., and thermal desorption measurements.

Structural studies particularly of species where the symmetry of the adsorbed species is thought to be of importance as in an isomerization or other heterogeneously catalysed reaction would yield valuable information.

N.M.R. will also allow kinetic studies where the concentration of some adsorbed species (or intermediate) could be followed rather than following the concentration of some unbound species.

These and other studies are becoming easier to carry out notably due to improved Fourier Transform techniques. One promising technique masquerading under the dubious

acronym of the PENIS experiment (for proton enhanced nuclear induction spectroscopy) (Pines 1972) promises a gain of the order of 1000 in sensitivity for carbon 13 studies, and has already been used in surface work (Kaplan 1973)

This University is about to convert its XL-100 NMR spectrometer to pulse and Fourier Transform capabilities. This instrument should be much superior for doing catalytic research than the ones available here in the past years. For this reason I will suggest some further catalytic work that could be done.

For some time during this study NMR measurements of cis, trans, and 1 butene adsorbed on ZnO were performed, on the C. W. spectrometer. All of these isomerize over the catalyst, and it was found that they had different characteristic spectra immediately after adsorption and that the final spectrum was the same for all three butenes.

The kinetics of these isomerizations are slow enough to follow on a pulse machine, but proved not slow enough to follow and still get good spectra with a C. W. apparatus. A pulse study of this reaction would not only elucidate the kinetics, but would allow one to determine the intermediate species in the isomerization.

I was able to observe a resonance for ethylene adsorbed on platinum which had been supported on silica.

With good computer backup it would be possible to measure spectra for such a system and for the same coverage of ethylene on the silica and subtract them numerically, enabling one to determine the spectra only of the ethylene on platinum. There are no NMR studies of adsorbed species on metals although there are studies of hydrogen in palladium.

One of the large frustrations in interpreting the data obtained in this work was the knowledge that the system was underdetermined, and that one could only speculate as to the source of minima in the T versus $1/\text{temp}$ curve, then see if calculations based on those speculations were consistent with the measured results. It would be very satisfying to be able to pin the system down.

One method of doing this would be to examine quadrupole relaxation in fully deuterated ethylene adsorbed in the same ZnO.

The perturbation Hamiltonian for quadrupole relaxation is of the same form we have already considered; i.e.: (Abragam 1961)

$$X-1 \text{ Ham} = \sum_{q} F_q(\omega) A_q$$

where the F_q are the same random functions but the A_q are now proportional to the electric field gradient at the nucleus. In this case $r_{ij}(\omega)$ becomes the

C-D axis and it starts with a different angular dependence in the molecule fixed frame. The $F(q)(\Omega)$ would be found in the lab fixed frame in the same fashion as outlined in Chapter 5, and in the most general form would be the same function.

The minimum corresponding to this correlation time would be at a different position on the temperature axis since $\omega(0)$ would now be different. The correlation time would however be the same. One would now have more pieces of information, and hopefully a determinable problem; that is could make an absolute assignment of the motions involved.

Such an experiment involves being able to make pulse measurements of Deuterium. Such an apparatus is not available at this University and is not presently planned, although it is a small enlargement of the present facility.

A more sophisticated experiment for finding the motions on a surface might also be made by using an adsorbate that contained several nuclei with $I > 1/2$. Huntress(1970) outlines the theory necessary for finding the principle elements of the diffusion tensor by utilizing quadrupole relaxation. In the asymmetric top case measurements must be made on three chemically or geometrically different nuclei. Utilizing this work and expanding it by making two more transformations — from the molecule fixed frame, to a rotation axis frame, to a

surface fixed frame, then to the space fixed frame and separating the variables properly, one could make absolute assignments of the surface motions. It should be noted however that one more unknown is added, and thus one more chemically or geometrically different nucleus need be measurable.

Nuclear Magnetic Resonance studies of species adsorbed on surfaces is a field of investigation still in its infancy. It will be interesting to see what future studies of this nature will bring.

180
BIBLIOGRAPHY

- Abragam, A. (1961) *The Principles of Nuclear Magnetism*.
Oxford Press.
- Anderson, P. R. and E. P. Jones. (1972) *J. Chem. Phys.* 57: 3945.
- Banwell, C. N. and N. Sheppard. (1961) *Proc. Royal*
- Baranski, A. and R. J. Cventanivic. (1971) *J. Phys. Chem.* 75: 208.
- Bloom, M., M. Lipsicas, and B. H. Muller. (1961)
Can. J. Phys. 39: 1093.
- Bloombergen, N., E. M. Purcell and R. V. Pound.
(1948) *Phys. Rev.* 73: 679.
- deBoer, J. H. and S. Kruyer. *Proc. Roy. Acad.* (1952)
Amsterdam.
- deBoer, J. H. (1968) *The Dynamical Character of Adsorption*.
Second Edition. Oxford Univ. Press, London.
- Bonardet, S., A. Snobbert, and J. Fraiviard. (1971)
Comp. Rend. Acad. Sci. Paris, 272
- Bonchev, Jordanov, Minkova. (1969) *Nucl. Inst. and Meth.* 70: 36.
- Bond, G. C. (1962) *Catalysis by Metals*. Academic Press, N. Y.
- Bothner-By, A. A. and R. E. Glick. (1957) *J. Chem. Phys.* 26: 1651.
- Bothner-By, A. A. and C. Naar-Colin. (1961) *J. Am. Chem. Soc.* 83: 231.
- Bovey, F. A. (1967) *N. M. R. Data Tables for Organic Compounds*. Vol. I. Wiley Interscience
- Brunauer, S., P. H. Emmett, and E. Teller. (1938) *J. Amer. Chem. Soc.* 60: 309.
- Buckingham, A. D., T. Schaefer, and W. G. Schneider.
(1960) *J. Chem. Phys.* 32: 1227.
- Burger, J. P., N. J. Poulis and W. P. Hass. (1961)

Physica 27: 514.

- Carr, H. Y. and E. M. Purcell. (1954) Phys. Rev. 94: 630.
- Chang, C. C. and R. J. Kokes. (1970) J. Amer. Chem. Soc. 92: 7517.
- Chang, C. C. and R. J. Kokes. (1973) J. Catalysis 28: 92.
- Clark, A. (1970) The Theory of Adsorption and Catalysis. Academic Press, New York.
- Collins, T. R., Z. Starcuk, A. H. Burr, and E. J. Wells. (1973) J. Amer. Chem. Soc. 95: 1649.
- Conard, J. (1970) Bull. Soc. Chim. de France 3291.
- Conner, W. C., R. A. Innes and R. J. Kokes. (1968) J. Amer. Chem. Soc. 90: 6858.
- Conner, W. C. and R. J. Kokes. (1969) J. Phys. Chem. 73: 2436.
- Connick, R. E., and R. E. Poulson. (1959) J. Phys. Chem. 63: 568.
- Dacey, J. R. (1965) Indust. and Eng. Chem. 57: 27.
- Dent, A. L. and R. J. Kokes. (1969a) J. Phys. Chem. 73: 3781.
- Dent, A. L. and R. J. Kokes. (1969b) J. Amer. Chem. Soc. 91: 7207.
- Dent, A. L. and R. J. Kokes. (1970a) J. Amer. Chem. Soc. 92: 1092.
- Dent, A. L. and R. J. Kokes. (1970b) J. Amer. Chem. Soc. 92: 6709, 6718.
- Dent, A. L. and R. J. Kokes. (1970c) J. Phys. Chem. 74; 3653.
- Dent, A. L. and R. J. Kokes. (1971). J. Phys. Chem. 75: 487.
- Dent, A. L. and R. J. Kokes. (1972) Advances in Catalysis. Vol. 22.

- Dowden, D. A. and N. Mackenzie. (1956) *Trapnell J. Chem. Soc.* 237A: 245.
- Duke, C. B. and R. L. Park. (1970) *Physics Today*.
- Edmonds, Pilkethly. (1969) *Surface Science* 17: 450.
- Egerton, T. A. and R. P. Green. (1971) *Trans. Faraday Soc.* 67: 2699.
- Eischens, R. P. and W. A. Pliskin. (1958) *Advances in Catalysis X, I.* Academic Press, N.Y.
- Eischens, R. P., W. A. Pliskin, and M. J. D. Low. (1962) *J. Catalysis* 1: 180.
- Emsley, J. W., J. Feeney and L. H. Sutcliff. (1966) *High Resolution N. M. R. Spectroscopy. Vol I and II.* Pergamon Press, New York.
- Emsley, J. W., J. Feeney and L. H. Sutcliff (eds.) (1971) *Progress in N. M. R.* Vol. 7. Pergamon Press.
- Farrar, J. C. and E. D. Becker. (1971) *Pulse and Fourier Transform N. M. R.* Academic Press, N.Y.
- Fraissard, J., S. Bielikoff and B. Imelik. (1971) *C. R. Acad. Sci. (Paris)* 271, C, 1897
- Fraissard, J., J. L. Bonardet and A. Snobbert. (1971) *C. R. Acad. Sci. (Paris)* 272, C, 1836
- Gay, I. D. (1974) *J. Phys. Chem.* 78: 38.
- Graham, D. and W. D. Phillips. (1957) *Surface Activity*, 2. J. A. Schulman (ed.) Butterworth,
- Goldanski, V. I. and S. P. Suzdalev. (1970) *Russian Chem. Reviews.* 39: 7.
- Goldstein, . (1962) *J. Chem. Phys.* 36: 2644.
- Gordon, S. and B. P. Daily. (1961) *J. Chem. Phys.* 34: 1084.
- Gradsztajn, S., J. Conard and H. Benoit. (1970) *J. Phys. Chem. Solids* 31: 1121.

- Gutowsky, H. S. and C. S. Hoffman. (1951) J. Chem. Phys. 19: 1259.
- Hair, M. L. (1967) I. R. Spectroscopy in Surface Chemistry. M. Dekker, N. Y.
- Hertz, H. G. (1967) Microdynamic Behavior of Liquids Progress in N. M. R. Spectroscopy. Emsley, Feeney and Sutcliffe, editors. Vol. 3.
- Hock, M. J. R. and F. A. Rushworth. (1965) Nuclear Magnetic Resonance and Relaxation in Solids. L. van Gerven, ed. North Holland Co., Amsterdam.
- Huntress, W. T. (1968) J. Chem. Phys. 48: 3524.
- Huntress, W.T. (1970) Advances in Magnetic Resonance.
- Ihrig, A. and L. S. Stanford. (1972) J. Amer. Chem. Soc. 94: 34.
- Jutland, A., D. Vivien, and J. Conard. (1972) Surface Science 32: 258.
- Krylov, O. V. (1970) Catalysis by Non Metals. Academic Press, N. Y.
- Kokes, R. J. and A. L. Dent. (1972) Advances in Catalysis 22: 1.
- Kolboe, S. (1969) J. of Catalysis 13: 208.
- Kubokawa, Y., T. Ono and N. Yano. (1973) J. of Catalysis 28: 471.
- Langmuir, I. (1915) J. Amer. Chem. Soc. 6: 79.
- Langmuir, I. (1916) J. Amer. Chem. Soc. 38: 2267.
- Langmuir, I. (1918) J. Amer. Chem. Soc. 40: 1361.
- Langmuir, I. (1932) J. Amer. Chem. Soc. 54: 1932.
- Little, L. H. (1966) The I. R. Spectra of Adsorbed Molecules. Butterworth, London.
- Lomer, W. M. (1962) Proc. Phys. Soc. 80: 1380.
- Low, M. J. D. (1967) The Solid Gas Interface. E. A. Flood (ed.) Vol. 2. M. Dekker, N.Y.

- Meiboom, Gill D. (1959) Rev. Sci. Instrum. 29: 688.
- Moreland, C. G. and Brey, W. J. (1966) J. Chem. Phys. 45: 803.
- Muha, G. M. and D. J. C. Yates. (1968) J. Chem. Phys. 49: 5073.
- Naryana, D., J. Lal and V. Kesavulu. (1970) J. Phys. Chem. 74: 4150.
- Packer, K. J. (1967) Progresses in N. M. R. Spectroscopy. Vol. 3. Emsley, Feeney, Sutcliffe (ed.). 87.
- Parshall, G. W., and F. N. Jones. (1965) J. Amer. Chem. Soc. 87: 5356.
- Pelman, A. I. (1971) Electron Paramagnetic Studies of Adsorbed Species. Thesis, U.B.C.
- Perrin, F. (1934) J. Phys. Radium 5: 497.
- Pfieffer, H., H. Winkler and D. Freude. (1967) Colloq. Ampere XIV: 1145.
- Pfieffer, H. (1971) Nuclear Magnetic Resonance 7: 53.
- Pickett, J. H. and L. B. Rogers. (1967) Analytical Chem. 39: 1872.
- Pickett, J. H. (1970) High Resolution N. M. R. Spectroscopy of Molecules Adsorbed on Silica. Thesis, Purdue University.
- Pines, A., M.G. Gibby, J.S. Waugh, J. Chem. Phys. 56,1776,(1972)
- Pople, J. A., W. G. Schneider and H. J. Bernstein. (1959) High Resolution Nuclear Magnetic Resonance McGraw-Hill, Toronto.
- Raynes, W. T., A. D. Buckingham and H. J. Bernstein. (1962) J. Chem. Phys. 36: 3481.
- Reddy, G. S. and J. H. Goldstein.(1961)J.Amer. Chem. Soc. 83: 2045.
- Reddy, G. S. (1962) J. Mol. Spec. 8: 475.

- Resing, H. A. (1967-68) *Advances Mol. Relaxation Processes* 1: 109.
- Resing, H.A. *Advances Mol. Relaxation Processes* 3,199 (1972)
- Rideal, E. K. (1938) *Proc. Cambridge Phil. Soc.* 35; 130.
- Riehl, J. W. and K. Koch. (1972) *J. Chem. Phys.* 57: 2199.
- Rose, M. E. (1957) *Elementary Theory of Angular Momentum*: John Wiley and Sons Inc., New York.
- Ross, S. and J. Oliver. (1964) *On Physical Adsorption*. John Wiley and Sons Inc., New York.
- Selwood, P. W. (1956) *Magnetochemistry*. Interscience, New York.
- Shvo, R. Y. and A. Demiel. (1965) *J. Amer. Chem. Soc.* 87: 3995.
- Siegbahn, K. (1967) *ESCA. Atomic Molecular and Solid State Structure Studies by Means of Electron Spectroscopy*. Almquist and Wiksells, Uppsala.
- Slichter, C. P. (1963) *Principle of Magnetic Resonance*. Harper and Row, New York.
- Smith, S. L. and A. M. Ihrig. (1967) *J. Chem. Phys.* 46: 1181.
- Somorjai, G. A. (1972) *Principles of Surface Chemistry*. Prentice-Hall, New Jersey.
- Spiesecke, H. and W. G. Schneider. (1961) *J. Chem. Phys.* 35: 722.
- Steele, W. A. (1963) *J. Chem. Phys.* 38: 2404.
- Steele, W. A. (1963) *J. Chem. Phys.* 38: 2411.
- Steele, W. A., W. B. Moniz, and J. A. Dixon. (1963) *J. Chem. Phys.* 39: 2418.

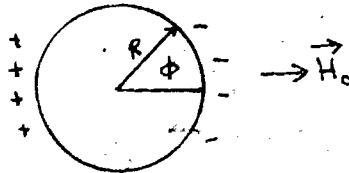
- Stephen, M. J. (1958) Mol. Phys. 1: 223.
- Stothers, J. B. (1972) Carbon-13 -N- M. R. Spectroscopy. Academic Press, New York. Vol. 14 of Organic Chemistry Monographs, Blomquist, A. and Wasserman, H. (ed.).
- Taylor, E. H. and J. A. Wethington. (1954) J. Amer. Chem. Soc. 76: 971.
- Teichner, S. J. and J. Aigueperse. (1963) J. Catalysis 2: 359.
- Teichner, S. J., F. Bozon Verduraz and B. M. Arghirooulos. (1967) Bull. Soc. Chim. Fr. 2854.
- Teichner, S. J. and F. Bozon-Ferduraz. (1968) J. Catalysis 11: 7.
- Thompson, J. K., J. J. Krebs and H. A. Resing. (1965) J. Chem. Phys. 43: 3853.
- Torrey, H. C. (1953) Phys. Rev. 92: 962.
- Whitney, A. G. and I. D. Gay., (1972) J. Catalysis 25: 176.
- Winkler, H. (1961) Proc. 10th Colloq. Ampere, Leipzig 219.
- Woessner, D. E. (1961) J. Chem. Phys. 35: 41.
- Woessner, D. E. (1962a) J. Chem. Phys. 36: 1.
- Woessner, D. E. (1962b) J. Chem. Phys. 37: 647.
- Woessner, D. E. (1963) J. Chem. Phys. 39: 2783.
- Woessner, D.E. and J. R. Zimmerman J.Phys.Chem 67, 1590, (1963b).
- Woessner, D. E. (1965) J. Chem. Phys. 42: 1885.
- Woessner, D. E. (1966) J. Phys. Chem. 70; 1217.
- Woessner, D. E. and J. R. Zimmerman. (1963b) J. Phys. Chem. 67: 1590.
- Woessner, D. E. and B. S. Snowden. (1969a) J. Coll. Interface Science 30: 54.

- Woessner, D. E. (1969b) J. Phys. Chem. 51: 1968.
- Woessner, D. E., B. S. Snowden and Y. C. Chiu.
(1970a) J. Coll. Interface Science
34: 283.
- Woessner, D. E. and B. S. Snowden. (1970b) J.
Coll. Interface Science 34: 290.
- Woodman, J. F., and H. S. Taylor. (1940) J. Amer.
Chem. Soc. 62: 1393.
- Young, P. M. and A. D. Crowell. (1962) Physical
Adsorption of Gases. Butterworth, London.
- Zimmerman, J. R. and M. R. Foster. (1957a) J.
Phys. Chem. 61: 282.
- Zimmerman, J. R. and W. E. Britton. (1957b) J.
Phys. Chem. 61: 1328.

Appendix A. The Correction in Chemical Shift Due to Magnetic Susceptibility

When placing a sample of magnetic susceptibility into a field we must ask what is the real field at a point inside the sample. The field is equal to $H_0 + H_1$ where H_1 equals the demagnetizing fields.

Consider the field to arise from charges where the field goes from + to -. If we want to know the field inside a long column we have a situation as diagrammed below which represents a column of infinite length in the z direction. Maxwell's equation



says that the divergence of $\vec{B} = 0$.

$$(1) \quad \vec{\nabla} \cdot \vec{B} = 0$$

$$\text{where } \vec{B} = \vec{H} + 4\pi \vec{M}.$$

We want to know what the divergence of the field is at the surface of our column. From (1)

$$(2) \quad \vec{\nabla} \cdot \vec{H} = 4\pi (\vec{\nabla} \cdot \vec{M}), \text{ where the } \vec{\nabla} \cdot \vec{M} \text{ term is often called}$$

the volume charge density ρ , and is commonly defined as

$-\vec{\nabla} \cdot \vec{M}$, a sign convention consistent with placing minus signs where the field leaves a surface and + signs where a field enters a surface.

Now we want to evaluate H_1 . We are only concerned with the field due to the surface since everywhere else \vec{M}

is continuous and $\vec{\nabla} \cdot \vec{M} = 0$. A solution of equation (2) is

$$(3) \quad H(\vec{r}) = \int \frac{\sigma dA (\vec{r} - \vec{r}')}{(\vec{r} - \vec{r}')^3}$$

where σ is the charge/unit area. Since the total charge $q = \int \sigma dV$ the total charge on a surface is equal to $\int \sigma dA$. However, Gauss's law says that

$$-\int \nabla \cdot \vec{M} dV = -\int \vec{M} \cdot \hat{n} dA \quad \text{where } \hat{n}$$

is the normal vector to the surface A. From the above it can be seen that

$$(4) \quad \vec{\sigma} = -\vec{M} \cdot \hat{n} = M \cos \theta$$

We want to find H' . From (3) we can see that

$$(5) \quad dH' = \sigma dA \frac{\{ R \cos \phi \hat{x} + R \sin \phi \hat{y} + z \hat{z} \}}{(R^2 + z^2)^{3/2}}$$

$$= M \cos \phi R d\phi dz \cdot R \cos \phi \hat{x} / (R^2 + z^2)^{3/2}$$

since both y and z terms will cancel out due to symmetry.

The field H' is just the integral of (5).

$$(6) \quad H' = \int_0^{2\pi} d\phi \int_{-\infty}^{\infty} dz (R^2 \cos^2 \phi M) / (R^2 + z^2)^{3/2}$$

$$= \pi M R^2 \int_{-\infty}^{\infty} \frac{dz}{(R^2 + z^2)^{3/2}}$$

The integral is solved by letting $z = bR$ then

$$H' = \pi M \int_{-\infty}^{\infty} \frac{db}{(1+b^2)^{3/2}}$$

The integral has a value of 2 so that 6 becomes

$$(7) \quad H' = -2\pi M$$

$$= -2\pi \chi H_0$$

where we are assuming that $M = \chi H_0$, that is the local fields are small compared to H_0 . To ask what is the field at some point it becomes convenient to remove a small sphere and ask what is the field within that hole. It must be equal to $H_0 + H' + H''$ where H'' is the demagnetizing field due to the removal of our small sphere.

H'' is evaluated using equation 3 as before except integrating over a sphere rather than a cylinder and performing the integration in polar coordinates. It proves to be equal to $4/3 \pi M$ in the opposite direction. The total field inside our little sphere is then:

$$(9) \quad H = H_0 - 2\pi\chi H_0 + 4/3\pi\chi H_0 \\ = H_0 - 2/3\pi\chi H_0$$

Now suppose we have two different samples, one a reference sample of overall magnetic susceptibility $\chi(\text{ref})$, the other a sample of susceptibility $\chi(\text{sample})$. We want to find the real difference in the fields at which they resonate without consideration of the difference in magnetic susceptibilities.

The chemical shift is defined as being:

$$(10) \quad \delta = \{H(\text{sample}) - H(\text{ref})\} / H_0$$

where $H(\text{sample})$ and $H(\text{ref})$ are the fields of which the sample and reference resonate

respectively. But the field at the sample is from (9) equal to $H(\text{sample}) - 2\pi/3\chi(\text{sample})H_0$ and the field at the reference sample is $H(\text{ref}) - 2\pi/3\chi(\text{ref})H_0$. So from (10) we have:

$$(11) \delta(\text{real}) = \{H(\text{sample}) - 2\pi/3\chi(\text{sample})H_0 - (H(\text{ref}) - 2\pi/3\chi(\text{ref})H_0)\} / H_0$$

$$\begin{aligned} \delta(\text{real}) &= H(\text{sample}) - H(\text{ref}) + 2\pi/3(\chi(\text{ref}) - \chi(\text{sample})/H_0 \\ &= \delta(\text{observed}) + 2\pi/3(\chi(\text{ref}) - \chi(\text{sample})) \end{aligned}$$

Other expressions are derived in a similar fashion for other shapes of sample tubes.